2013-12-13

In Vivo Imaging of Neutrophil Responses to Localized S. aureus Infection

Harding, Mark

UNIVERSITY OF CALGARY

In Vivo Imaging of Neutrophil Responses to Localized *S. aureus* Infection

by

Mark Geoffrey Harding

A THESIS

SUBMITTED TO THE FACULTY OF GRADUATE STUDIES

IN PARTIAL FULFILMENT OF THE REQUIREMENTS FOR THE

DEGREE OF MASTERS OF SCIENCE

GRADUATE PROGRAM IN IMMUNOLOGY

CALGARY, ALBERTA

NOVEMBER 2013

Abstract

Methicillin-resistant *Staphylococcus aureus* (MRSA) is a highly virulent, multidrug –resistant pathogen responsible for the majority of soft tissue infections. The role of neutrophils in *S. aureus* soft tissue infections is currently unclear. The objective of this thesis was to characterize early neutrophil recruitment to a localized MRSA infection. Using spinning disk confocal microscopy, we developed a mouse model to visualize the behaviour of neutrophils in the skin following the introduction of an agarose bead embedded with GFP-expressing MRSA. We observed significant neutrophil recruitment not only in the venules but also in the capillaries, which we showed to be mediated by the β_2 and α_4 integrins. Blocking these integrins in mouse models increased capillary perfusion, reduced cell death at early time points, and altered lesion size during infection. Understanding the contribution of neutrophils in MRSA soft tissue infection will help to elucidate novel therapeutic targets in these infections.

Acknowledgements

I would like to thank my committee members, Dr. John Conly and Dr. May Ho. Dr. Conly provided valuable clinical insight and excellent advice regarding appropriate bacterial controls. Dr. Ho was critically important in providing feedback that improved my skills as a scientist.

I would also like to thank my co-supervisor, Dr. Kunyan Zhang. Dr. Zhang brought much valuable expertise to the bacterial elements involved in my project.

Special thanks to the past and present members of the Zhang and Kubes laboratories. There were many people who contributed to this thesis, as well as to my own education as a scientist, but in particular I would like to thank Dr. Kaiyu Wu and Dr. Craig Jenne. Dr. Wu provided hands-on help, teaching me about *S. aureus* and the molecular techniques that can be used to manipulate it in the early stages of my project. Dr. Jenne was a constant supporter and mentor within the Kubes lab, who provided me with invaluable feedback and direction throughout my Masters degree.

I would like to especially thank Dr. Paul Kubes, my supervisor. Dr. Kubes was more than a mentor; he provided the education and the insight that has taught me how to think critically. At the same time, Dr. Kubes provided me with the advice and discussion that I needed to hear, not just what I wanted to hear, in order to develop into a better scientist and immunologist.

As a final thank you, I would like to thank my girlfriend, Brienne McKenzie, and my family, for putting up with me throughout this experience and providing me with support. Without them I sincerely doubt I would have completed this degree.

Table of Contents

Abstract ii
Acknowledgements iii
Table of Contents iv
List of Tables vii
List of Figures and Illustrations viii
List of Symbols, Abbreviations and Nomenclature x

CHAPTER ONE: INTRODUCTION 1
1.1 Methicillin resistant *Staphylococcus aureus* 1
1.1.1 Antibiotic resistance and definition 1
1.1.1.1 Resistance to beta-lactam antibiotics 1
1.1.2 Epidemiology 3
1.1.2.1 Resistance to other classes of antibiotics 3
1.1.3 CA-MRSA strain USA300 4
1.2 Host interactions with *S. aureus* 6
1.2.1 Early innate immune response to S. aureus 6
1.2.1.1 Keratinocytes and the passive actions of the skin 6
1.2.1.2 Pattern recognition receptors in response to *S. aureus* 8
1.2.2 S. aureus responses to innate defences prior to neutrophil recruitment 10
1.2.3 Neutrophil recruitment to the site of infection 11
1.2.4 Interactions of neutrophils with S. aureus 17
1.2.4.1 Phagocytosis 17
1.2.4.2 Neutrophil extracellular traps 18
1.2.4.3 Recruitment of additional immunocytes 19
1.2.5 S. aureus responses to neutrophils 19
1.2.6 Detrimental effects of neutrophils during infection 22
1.2.7 Objectives and hypothesis 24

CHAPTER TWO: MATERIALS AND METHODS 25
2.1 Mice 25
2.2 Bacteria 25
2.2.1 Bacterial preparation 25
2.2.1.1 Injection experiments 26
2.2.1.2 Agarose bead experiments 26
2.2.1.3 Plating of PBS/*S. aureus* solution 27
2.2.1.4 Assessment of change in CFUs per bead over time 28
2.3 Imaging of the Murine Skin Tissue 28
2.3.1 Anesthetic for Mice 28
2.3.2 Jugular vein cannulation 28
2.3.3 Superfusion solution preparation 29
2.3.4 Skin preparation of anesthetized mice 29
2.3.5 Spinning disk intravital microscopy 30
2.3.6 Labelling antibodies 31

2.3.7 Subcutaneous injection experiments 32
2.4 Lesion size experiments....32
2.5 Reagents....33
2.5.1 Blocking antibodies....33
2.5.2 FITC albumin experiments....34
2.5.3 Propidium iodide experiments....34
2.6 Analysis 34
2.6.1 Neutrophil recruitment to bead....34
2.6.2 Cell tracking and meandering index measurements....35
2.6.3 Neutrophil recruitment within the capillaries....35
2.6.3.1 3D image generation of neutrophils within the capillaries....36
2.6.3.2 Neutrophil length and width inside the capillaries versus outside of the vasculature 36
2.6.4 Measurement of venule parameters....37
2.6.4.1 Velocity....37
2.6.4.2 Rolling flux....37
2.6.4.3 Adhesion....38
2.6.4.4 Emigration 38
2.6.5 Lesion size experiments 38
2.6.6 FITC albumin experiments....38
2.6.7 Propidium iodide experiments....39
2.6.8 Statistical tests 39

CHAPTER THREE: MODEL DEVELOPMENT....40
3.1 Introduction: mammalian models of *S. aureus* soft tissue infection....40
3.1.1 Spinning disk microscopy 44
3.2 Preliminary observations 45
3.3 Development of agarose bead model....48
3.4 Quantification of neutrophils....51
3.5 Neutrophil recruitment to capillaries 54

CHAPTER FOUR: MOLECULAR MECHANISMS OF NEUTROPHIL RECRUITMENT TO THE CAPILLARIES....70
4.1 Introduction: integrins and their role in neutrophil adhesion and crawling....70
4.1.1 Integrin function: overview 70
4.1.2 Lymphocyte function-associated antigen (LFA-1) 71
4.1.3 Macrophage 1 antigen (Mac-1) 71
4.1.4 Very late antigen-4 (VLA-4)....73
4.2 Blocking recruitment of neutrophils to the capillaries....73
4.2.1 Blocking molecules on the neutrophil....73
4.2.2 Blocking molecules on the endothelium 84
4.3 Effect of blocking antibodies on recruitment in the venules 92

CHAPTER FIVE: FUNCTIONAL EFFECTS OF NEUTROPHIL RECRUITMENT ..101
5.1 Introduction: local consequences of *S. aureus* infections....101

5.2 Microvasculature perfusion 102
5.3 Cell death 105
5.4 Lesion size 112

CHAPTER SIX: DISCUSSION 116
6.1 Summary and significance of this study 116
6.2 Analysis of model development 117
6.3 Analysis of the molecular components of capillary recruitment 125
6.4 Functional consequences of infection analysis 129
6.5 Limitations 134
6.6 Significance and final Conclusions.....138

List of Tables

Table 1 : Models of *S. aureus* infection targeting different layers of the skin 43

List of Figures and Illustrations

Figure 1: Response to *S. aureus* by innate immune cells in the skin. 7

Figure 2: The neutrophil recruitment cascade in post-capillary venules. 13

Figure 3: Changes in neutrophil parameters following subcutaneous injection of *S. aureus* 46

Figure 4: Parameters for *S. aureus* infection 49

Figure 5: Neutrophil recruitment towards *S. aureus* beads 53

Figure 6: Directional motion and recruitment of neutrophils 56

Figure 7: Neutrophil recruitment to capillaries during *S. aureus* infection 58

Figure 8: Comparison of the recruitment of cells labelled by the anti-Ly6g antibody clones RB6 8C5 and 1A8. 60

Figure 9: Differences in neutrophil shape when in capillaries 63

Figure 10: Behaviours of neutrophils within the capillaries 65

Figure 11: Recruitment of neutrophils to a bead containing *S. aureus* of either the strain, USA300 or the strain ATCC25923 67

Figure 12: The role of CD18 in mediating neutrophil recruitment in the capillaries 75

Figure 13: Neutrophil behaviour following treatment of mice with anti-CD11b blocking antibodies 77

Figure 14: Neutrophil behaviour following treatment of mice with anti-CD11a blocking antibodies 80

Figure 15: Neutrophil behaviour following treatment of mice with anti-α_4 blocking antibodies. 82

Figure 16: Neutrophil behaviour following treatment of mice with anti CD18 and anti-α_4 blocking antibodies 85

Figure 17: Expression of VCAM-1 in the microvasculature 2-3 hours post bead infection 88

Figure 18: Expression of ICAM-1 in the microvasculature 2-3 hours post bead infection 91

Figure 19: Neutrophil behaviour following treatment of mice with ICAM-1 blocking antibodies 93

Figure 20: Neutrophil behaviour following treatment of mice with VCAM-1 blocking antibodies. 95

Figure 21: Neutrophil behaviour following treatment of mice with VCAM-1 and ICAM-1 blocking antibodies 97

Figure 22: Effect of CD18 and α_4 blocking antibodies on venular recruitment 99

Figure 23: Occlusion of the capillary microvasculature following insertion of *S. aureus* bead. 104

Figure 24: Effect of *S. aureus* bead on cell death 107

Figure 25: Quantification of cell death induced by beads 109

Figure 26: 10x magnification of propidium iodide positive cells and Ly6g positive cells..... 111

Figure 27: Effect of blocking antibodies on lesion formation 48 hours after bead injection. 114

List of Symbols, Abbreviations and Nomenclature

Symbol	Definition
ACME	Arginine Catabolic Mobile Element
AMPs	Anti-Microbial Peptides
ANOVA	Analysis of Variance
BHI	Bacto Brain Heart Infusion
CA	Community-Associated
CA-MRSA	Community-Associated Methicillin-Resistant *Staphylococcus aureus*
CCY	Casein Hydrosylate and Yeast Extract
CHIPS	Chemotaxis Inhibitory Protein of *Staphylococcus aureus*
Clfa	Clumping Factor a
CFU	Colony Forming Units
DAMPs	Danger Associated Molecular Patterns
EGFR	Epidermal Growth Factor Receptor
ESAM	Endothelial cell Selective Adhesion Molecules
FOV	Field of View
Gent	Gentamycin
GFP	Green Fluorescent Protein
GTP	Guanine Triphosphate
HA	Hospital-Associated
HA-MRSA	Hospital-Associated Methicillin Resistant *Staphylococcus aureus*
HBD3	Human Beta-Defensin 3
HK	Heat Killed
Hla	Alpha hemolysin (also known as alpha toxin)
ICAM-1	Intracellular Adhesion Molecule 1
ICAM-2	Intracellular Adhesion Molecule 2
JAM	Junctional Adhesion Proteins
IL-1β	Interleukin-1β
IL-8	Interleukin 8
LFA-1	Lymphocyte Function Associated Antigen 1
LAD 1	Leukocyte Adhesion Deficiency Type 1
LTB4	Leukotriene B4
LSP1	Leukocyte Specific Protein 1
Mac-1	Macrophage 1 antigen
Mg	Milligram
Ml	Millilitre
Mm	Millimetre
MRSA	Methicillin-Resistant *Staphylococcus aureus*

MPO	Myeloperoxidase
NETs	Neutrophil Extracellular Traps
NLRP3	Nod-Like Receptor Pyd 3
P. aeruginosa	*Pseudomonas aeruginosa*
PAMPs	Pattern Associated Molecular Patterns
PBPs	Penicillin Binding Proteins
PBS	Phosphate Buffered Saline
PCR	Polymerase Chain Reaction
PECAM-1	Platelet/Endothelial Cell Adhesion Molecule (also known as CD31)
PIP_2	Phosphointidonositol 4,5, Bisphosphate
PRRs	Pattern Recognition Receptors
PSGL-1	P-Selectin Glycoprotein Ligand-1
PSMs	Phenol Soluble Modulins
PTEN	Phosphatase and Tensin Homologue
PVL	Panton-Valentine Leukocidin
ROS	Reactive Oxygen Species
TLR	Toll-Like Receptors
µg	Microgram
µl	Microliter
µm	Micrometre
S. aureus	*Staphylococcus aureus*
SC	Subcutaneous
S. epidermis	*Staphylococcus epidermis*
SHIP	SH2 Containing Inositol Phosphatase
VCAM-1	Vascular Adhesion Molecule 1
VLA-4	Very Late Antigen 4

Chapter One: Introduction

1.1 Methicillin resistant *Staphylococcus aureus*

Staphylococcus aureus is a Gram-positive, facultative anaerobic bacterium that poses considerable challenges to human health, as a re-emerging pathogen in both hospital and community settings. As a commensal bacterium, approximately 50% of the general population carry *S. aureus* in the anterior nares (1). Despite its commensal status, *S. aureus* has been associated with a wide variety of human diseases, from mild to severe. It is responsible for approximately 18,500 deaths per year in the United States, more than all deaths caused by AIDS, influenza, or viral hepatitis (2). *S. aureus* infections have been increasing in frequency in recent years, and now account for the majority of all clinical skin infections (3). Importantly, these infections can cause serious complications, such as necrotizing fasciitis, necrotizing pneumonia, and sepsis (4).

1.1.1 Antibiotic resistance and definition

1.1.1.1 Resistance to beta-lactam antibiotics

Historically, *S. aureus* is associated with the discovery of penicillin, the first successful antibiotic against many serious diseases. Penicillin contains a β-lactam ring in its molecular structure, similar to the D-Ala-D-Ala, a component involved in peptidoglycan cross-linking during cell wall synthesis. Penicillin can bind transpeptidases, named as penicillin binding proteins (PBPs), blocking the binding of D-Ala-D-Ala to PBPs, resulting in inhibition of the cell wall synthesis and bacterial growth. However, penicillin-resistant *S. aureus* emerged soon after

penicillin was widely used in clinics (5), because they produced β-lactamase that hydrolyzes the β-lactam ring of the penicillin molecule.

Methicillin, a semisynthetic β-lactamase resistant β-lactam derivative, was introduced in 1959 to treat infections caused by penicillin-resistant *S. aureus*, but the first case of methicillin resistant *S. aureus* (MRSA) infection was reported in 1961 (6). The resistance was mediated by *mecA* gene, encoding the low-affinity penicillin-binding protein PBP2a, which fails to bind methicillin and other β-lactam antibiotics allowing bacterial growth in the presence of β-lactam (7, 8). This altered protein is encoded within the staphylococcal cassette chromosome *mec* (SCC*mec*), SCC*mec* is a mobile genetic element which integrates into the *orfX* gene on the *S. aureus* chromosome, characterized by the presence of terminal inverted and direct repeats, two essential genetic components (the *mec* gene complex and the *ccr* gene complex), and three joining (J) regions. The *mec* gene complex includes *mecA* gene and its regulator genes, *mecR1* and *mecI*. The *ccr* gene complex encodes recombinases of the invertase/resolvase family responsible for the integration and excision of SCC*mec*. The J regions (J1, J2 and J3) are located between and around the *mec* and *ccr* complexes, encoding additional virulence factors and resistance to other antibiotics (9). To date, according to the organization of the *mec* complex and the *ccr* complex, 11 different SCC*mec* types with several subtypes have been identified (8, 9). SCC*mec* I-III are relatively large (34-67 kb), commonly found in HA-MRSA strains. SCC*mec* IV-V are relatively small (21-28 kb) and are associated with CA-MRSA infections. The other SCC*mec* types are uncommon.

1.1.2 Epidemiology

Epidemiologists differentiate between hospital-associated (HA) and community-associated (CA) *S. aureus* strains. HA-MRSA typically infects hospital patients whose immune systems are already compromised, whereas CA-MRSA is capable of infecting both hospital patients and healthy individuals outside of the hospital setting, generally through skin-to-skin contact. CA-MRSA strains are typically more virulent than HA-MRSA strains (4). Recent emergent CA-MRSA strains (including USA300) have been shown to possess a short SCC*mec* element (10). Some have speculated that while the longer SCC*mec* elements found in HA-MRSA may allow for resistance to antibiotics other than the beta lactams, they also induce a fitness cost, resulting in reduced virulence factor expression and slower replication rates (11, 12). Thus, the shorter SCCm*ec* found in CA-MRSA may confer a fitness benefit, possibly explaining CA-MRSA's shorter replication time and increased virulence (10, 12).

1.1.2.1 Resistance to other classes of antibiotics

A more recent development is *S. aureus* resistance to vancomycin (13). Vancomycin is an antibiotic used as a drug of last resort to combat drug resistant Gram-positive infections. The function of vancomycin is similar to that of beta-lactam antibiotics: to prevent appropriate peptidoglycan formation and thus cell wall synthesis. However, this occurs by a different mechanism, as vancomycin binds to the glycan precursor that would be incorporated into the cell wall. As the vancomycin-glycan precursor complex cannot penetrate the cytoplasmic membrane, the glycan precursor is effectively stranded inside the cell and cannot be incorporated in the cell wall (14). While resistance to vancomycin is not yet common, it is becoming more

prevalent (13). Mutations that are associated with increased vancomycin resistance have been identified, but the mechanism by which *S. aureus* can protect itself from vancomycin is not known (15). If vancomycin resistance is found, daptomicin is used as an alternative; however, there are a number of reports that indicate that vancomycin treatment may increase resistance to daptomicin in *S. aureus* strains (15).

CA-MRSA clones have also shown resistance to other antibiotics, such as erythromycin and mupirocin, reducing the available treatment options for this infection (16). Although recent studies have begun to address the use of combination therapies to restore the efficacy of antibiotics against *S. aureus* (17), there is no clinically available therapy for treating *S. aureus*, should it prove resistant to these cocktails of currently available antibiotics. The development of novel antibiotics capable of targeting *S. aureus* has been hindered by the capacity of this pathogen to adapt and develop resistance. As pharmaceutical companies shy away from further investment in new antibiotics, the search for new therapeutic approaches is critical. One area of research that has emerged is the examination of the interactions between *S. aureus* and the host immune system. Understanding these complex interactions may help to elucidate key therapeutic pathways, and thus could eventually lead to effective strategies to bypass the antibiotic resistance of this problematic pathogen and yield novel approaches for treatment.

1.1.3 CA-MRSA strain USA300

A single CA-MRSA strain, USA300, is responsible for a substantial proportion of the disease burden in North America. USA300 (known in Canada as CMRSA10) is the dominant CA-MRSA strain, and causes the majority of *S. aureus* infections in the USA (16, 18). This

strain is also responsible for the majority of new MRSA infections in multiple Canadian communities (19, 20), and is now the predominant MRSA strain in western Canada (21, 22).

Reasons for this strain's dominance are not yet clear. USA300 does express many genes that have been associated with virulence, such as the Arginine Catabolic Mobile Element (ACME) (23) and Panton-Valentine Leukocidin (PVL) (24, 25). A recent study on ACME has shown that it may be associated with increased capacity to colonize the skin, by conferring additional protection against the skin's natural acidity (23). Data on PVL is controversial, with no clear consensus on whether it plays an important role in soft tissue infections (24-27). This putative virulence factor is difficult to study *in vivo*, as murine leukocytes are resistant to PVL, due to the fact that PVL targets human but not murine C5a receptors (26, 28). Additionally, rabbit studies have recently demonstrated conflicting data on the effect of PVL in soft tissue infections. When PVL-deficient mutants were used to induce skin infections, they yielded either no effect (24) or a large reduction in lesion size (25). This may be due to differences in culturing the bacteria. Lipinska et al. use casein hydrosylate and yeast extract (CCY) media, which greatly enhances the production of bacterial PVL prior to infection (25, 29). This increase in the amount of PVL might be the reason why PVL played an important role in the study of Lipinska et al. (25). Additionally, these studies used different strains of rabbits (24, 25), which could result in different immunological responses, yielding these divergent results.

Another hypothesis is that USA300 hypervirulence is due to increased expression of core virulence factors, such as α-hemolysin, and phenol-soluble modulins (PSMs), due to changes in regulatory genes such as *agr* (27, 30, 31). A complete understanding of the genetic factors that induce hypervirulence in USA300 has not yet been attained. Despite understanding much about this strain of *S. aureus*, USA300's prevalence as the dominant strain of *S. aureus* in North

America make it an important strain to study, in order to more effectively combat *S. aureus* infections.

1.2 Host interactions with *S. aureus*

1.2.1 *Early innate immune response to S. aureus*

1.2.1.1 Keratinocytes and the passive actions of the skin

During a *S. aureus* infection, bacteria must interact with a multitude of cell types, and modulate the responses of those cells, in order to generate a successful infection (Figure 1). The first barrier to infection is the skin, which has several functions to prevent effective pathogen invasion. The outermost layer of the skin consists of dead keratinocytes, which provide a physical barrier and slough off the skin to deny pathogenic microbes a foothold (2). In addition to acting as a physical barrier to infection, live keratinocytes have potent anti-microbial properties. Keratinocytes express the toll-like receptors (TLRs) such as TLR1, 2 and 6 (32) and can induce pro-inflammatory signalling when exposed to pathogens (2). They also divide faster in response to sub-lytic concentrations of the *S. aureus* toxin, alpha hemolysin (Hla), due to increased activation of the epidermal growth factor receptor (EGFR) (32, 33).
Keratinocytes can also secrete a wide range of anti-microbial peptides (AMPs), such as the cathelicidin LL37 and beta defensins (34) in response to pathogens or inflammatory cues. LL37 is microbicidal to a wide range of bacteria, and is also broadly chemotactic, attracting neutrophils, monocytes, and T-cells via the formyl peptide receptor like-1 (35). The beta defensins are small molecules that can also be broadly antimicrobial. Human beta-defensin 3

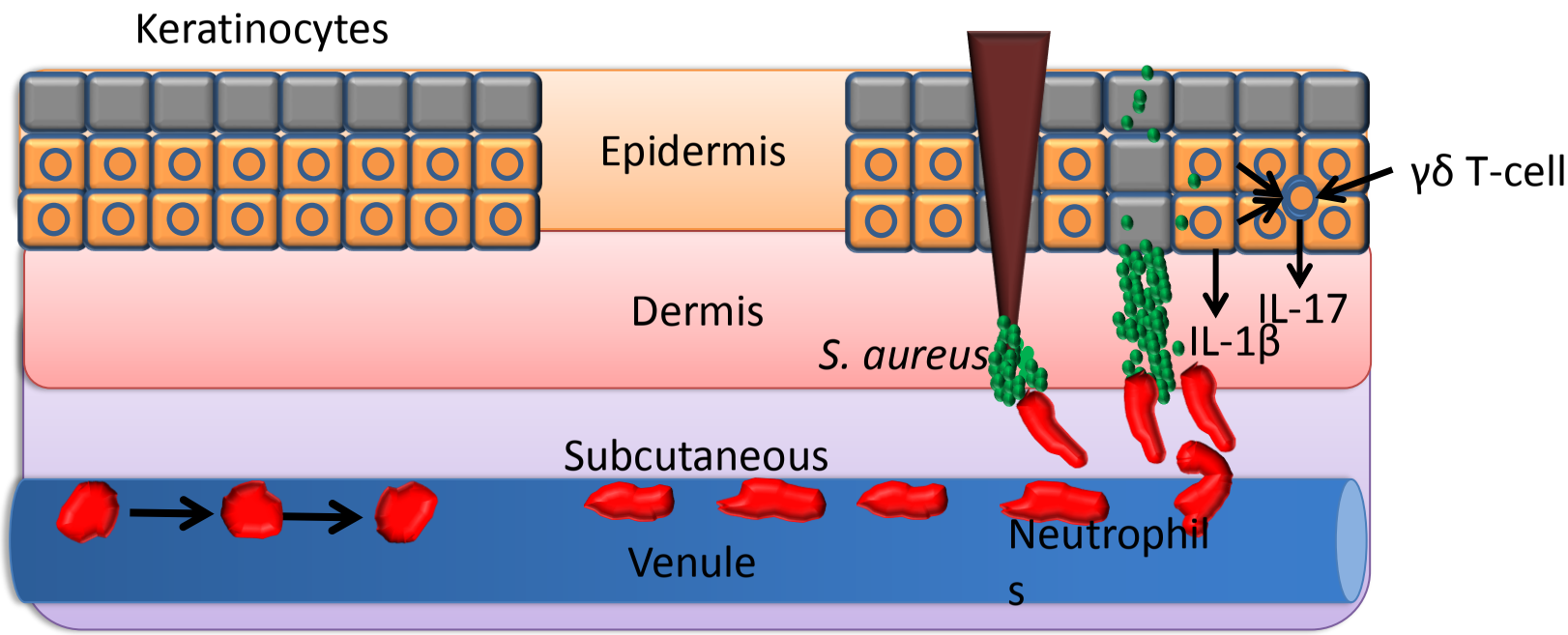

Figure 1:Response to *S. aureus* by innate immune cells in the skin.

In order for *S. aureus* to successfully cause a soft tissue infection, it must pass through the epidermis, either by destroying keratinocytes (via molecules such as alpha hemolysin) or through introduction by a foreign body causing abrasions in the skin. Keratinocytes, and other cells in the skin, can release IL-1β in response to *S. aureus*, which is highly pro-inflammatory and induces IL-17 production by γδ T-cells, leading to the production of chemokines which recruit neutrophils to the site of infection.

(HBD3) in particular can kill *S. aureus* via cell-cell interactions between keratinocytes and bacteria (36). A clinical study by Zanger et al. showed that low HBD3 expression in patients can be associated with severe skin infections induced by *S. aureus* (37). Keratinocytes can be stimulated to produce these molecules by commensals such as *Staphylococcus epidermis* on the skin, generating an inhospitable environment for pathogens (38). Keratinocyte AMPs have synergistic effects when combined with the antimicrobial peptides of skin commensals such as *S. epidermis* (39). These molecules have multiple purposes, including killing microbes, promoting proinflammatory cytokine and chemokine production, and inducing recruitment of innate and adaptive immune cells (34).

There are several ways that bacteria may breach the keratinocyte layer and be introduced to the layers below the epidermis. For example, *S. aureus* may successfully colonize the skin by counteracting the preventative measures of other skin microbiota and the host, through virulence factors such as ACME (23). Skin abrasions or damage to the epidermis by a foreign body can also provide an environment in which *S. aureus* can proliferate (Figure 1). This mechanism of infection is often used to induce reproducible tissue damage in animal models (40, 41), and has been identified as a mechanism by which MRSA can effectively induce infection during some outbreaks (42).

1.2.1.2 Pattern recognition receptors in response to *S. aureus*

As *S. aureus* penetrates the keratinocyte barrier, a series of innate defenses against infection will respond to signals indicating infection. The skin possesses innate immune cells, such as macrophages, dendritic cells, γδ T-cells and keratinocytes, all of which possess pathogen recognition receptors (PRRs) and can sense multiple antigens produced by *S. aureus* (2). Some

of these PRRs become activated when toxins secreted by *S. aureus* damage the host membrane and induce intracellular activation of the cytoplasmic PRR, NOD2, leading to inflammasome activation (43). This leads to the production of interleukin-1β (IL-1β), which is critical for a robust inflammatory response against this infection (44). IL-1β is typically released by resident cells such as keratinocytes, macrophages, and dendritic cells (44, 45)**,** where it acts in an autocrine/paracrine fashion through its receptor IL-1R and results in robust downstream activation of the adapter protein MyD88. IL-1β also induces IL-17 release from γδ T-cells (46). IL-17 acts to promote increased production of AMPs by resident keratinocytes and enhance neutrophil recruitment (2). Together, these cytokines induce a strong neutrophil response (2, 44, 46), through chemokine production and activation of endothelial cells. IL-1 receptors, which can bind IL-1β, are not required to be present on neutrophils for a strong immune response against *S. aureus* (47). Furthermore, wild type neutrophils transferred to IL-$1^{-/-}$ mice are sufficient to decrease the size of *S. aureus*-induced abscesses to similar sizes as those induced in wild type mice (48), suggesting that IL-1β production by neutrophils is important for responses to *S. aureus*-induced soft tissue infection. The influx of neutrophils to the site of infection appears in some cases to confer protection against *S. aureus* (49). The complex relationship between neutrophils and *S. aureus* will be discussed in further detail in Section 1.2.5 and Section 1.3.

Another PRR involved in *S. aureus* infection is TLR2, which forms heterodimers with TLR1 and TLR6 on the surface of many immune cells. TLR2 is expressed on a wide range of cells that are found in the skin, such as keratinocytes, Langerhans cells, and macrophages (2). TLR2 recognizes *S. aureus* by binding to lipotechoic acid and peptidoglycan (2, 50, 51). This induces proinflammatory signalling through MyD88, leading to NF-κB mediated activation of

pro-inflammatory genes (45). TLR2 is thought to be one of the most important TLRs in *S. aureus* infections. It is important both *in vitro* and in systemic infection for neutrophil activation and bacterial killing of *S. aureus* (52, 53) but its importance in skin infection *in vivo* is not entirely clear (45), (54). In subcutaneous infection models, TLR2-deficient animals have been shown to possess a delayed neutrophil response, but resolve tissue damage in approximately the same amount of time as healthy mice (45). TLR2 also plays a role in the generation of antimicrobial neutrophil extracellular traps (NETs) during subcutaneous infection with *S. aureus* (54). Together, these studies show that TLR2's role in soft tissue infections may be multifaceted: during early stages of cutaneous infection, it appears less important than IL-1β, but its role in NET production suggests an important secondary role in preventing bacterial dissemination from the initial infection site.

1.2.2 S. aureus responses to innate defences prior to neutrophil recruitment

S. aureus is adept at overcoming various anti-microbial defenses through secreted and surface-expressed virulence factors, as well as other responses to antimicrobial peptides. Many molecules produced by *S. aureus* act in tandem, targeting separate parts of the innate immune system to circumvent targeted killing and prevent immune surveillance. Virulence factors, such as iron surface determinant and aureolysin, can act on the AMPs produced by the skin (55, 56). Iron surface determinant A, a *S. aureus* surface protein, increases the resistance of *S. aureus* to lysis by the beta-defensin hBD2 and the cathelicidin LL37 (55) through decreased cellular hydrophobicity. Staphyloxanthin, the protein that gives *S. aureus* its typical gold colony colour, protects against host AMPs (57). Another protein, aureolysin, can cleave LL37, rendering it

non-functional (56). *S. aureus* can also make changes to its cell wall, further reducing its susceptibility to antimicrobial proteins. For instance, *S. aureus* incorporates D-alanine into techoic acids, resulting in reduced *S. aureus* susceptibility to AMPs from the beta defensin family (58). These studies demonstrate that *S. aureus* is exquisitely adapted to survive and evade the innate immune killing functions at this stage of the infection.

To counteract keratinocyte functions, *S. aureus* produces virulence factors that induce cell death and increase its ability to penetrate this layer of the skin. For example, alpha hemolysin can increase keratinocyte growth via EGFR signalling, but is also capable of inducing pyroptosis (a caspase-1-dependent form of programmed cell death) in skin keratinocytes, by inducing calpain and caspase activity (59). Alpha hemolysin is a general cell death inducer, capable of targeting cells such as endothelial cells, keratinocytes and T-cell (though not neutrophils) by forming a beta barrel pore in the cell surface (60). This function is also reproduced in other *S. aureus* toxins, such as phenol-soluble modulins (PSMs). The range of toxins produced by *S. aureus* can quickly and efficiently induce cell death in many cell types, such as neutrophils, erythrocytes and monocytes (31).

1.2.3 Neutrophil recruitment to the site of infection

The downstream effect of signalling cascades induced in the host cells in response to *S. aureus* infection is the recruitment of neutrophils to the site of infection. These cells are critical for abscess formation and clearance of the bacteria (49). Individuals with deficiencies in neutrophil function, such as defective leukocyte recruitment (leukocyte adhesion deficiency, or LAD type 1) are at greatly increased risk of *S. aureus* infection (44). Further evidence for the

importance of neutrophils comes from murine studies, in which depletion of neutrophils before intradermal infection of *S. aureus* resulted in impaired healing, and increased likelihood of sepsis (61).

Neutrophil recruitment is mediated via the leukocyte recruitment cascade in response to infection (Figure 2). This is a series of sequential steps that allow neutrophils to leave the circulation and interact with localized sites of inflammation. In the skin, this process is thought to occur exclusively in the post-capillary venules, where the shear stress is much lower than found in the arterioles. The first step of the cascade in the skin is tethering and rolling, mediated largely by P- and E-selectin on endothelial cells binding with P-selectin glycoprotein ligand-1 (PSGL-1) on neutrophils (62). Other molecules on the neutrophil, such as CD44 and E-selectin ligand, as well as integrins such as LFA-1, Mac-1 and VLA-4, have been reported to play minor roles during rolling (62-64). The selectins are carbohydrate-binding proteins found on endothelial cells and platelets. In the skin, E-selectin is constitutively expressed (unlike in other organs), whereas preformed P-selectin, contained in structures known as Weibal Palade bodies, is rapidly mobilized to the endothelial cell surface through fusion of the Weibal Palade bodies with the cell membrane in response to pro-inflammatory mediators (62, 65, 66). Selectins bind via "catch-bonds". These catch-bonds respond to increases in tension with a concomitant increase in binding force, allowing neutrophils to roll effectively while the shear stress typical of blood flow is being applied to the selectins. In fact, removal of shear stress reduces selectin-mediated rolling of neutrophils (64).

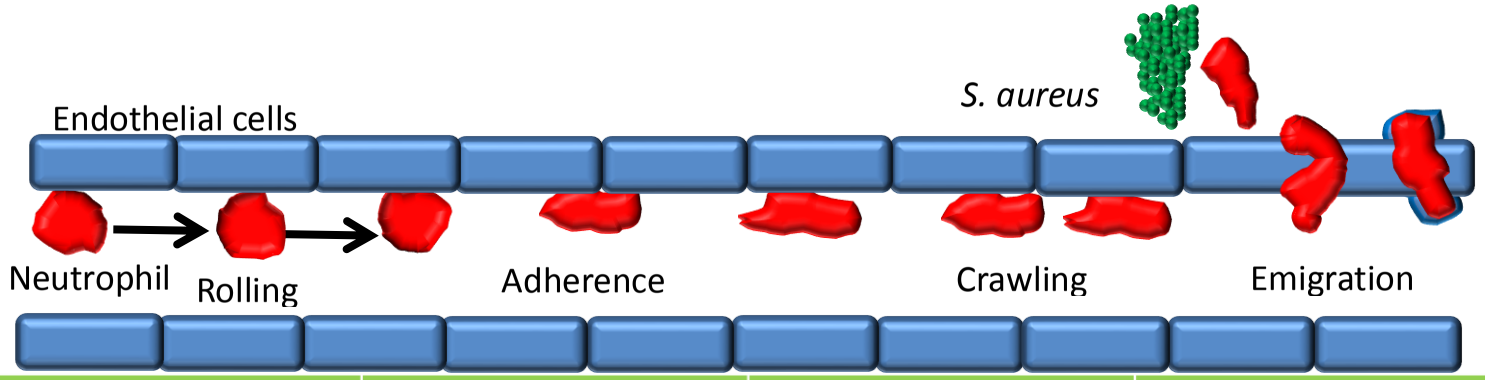

1. Rolling		2. Adherence		3. Crawling		4. Emigration	
Molecules on Neutrophil	Molecules on Endothelium	Molecules on Neutrophil	Molecules on Endothelium	Molecules on Neutrophil	Molecules on Endothelium	Molecules on Neutrophil	Molecules on Endothelium
PSGL-1, E-selectin Ligand	E-selectin, P-selectin	LFA-1	ICAM-1, ICAM-2	Mac1	ICAM-1	LFA-1, Mac1	ICAM-1, ICAM-2
LFA-1/Mac1	ICAM-1	VLA_4	VCAM-1			VLA_4	VCAM-1
VLA_4	VCAM-1					PECAM-1	PECAM-1
							ESAMs, JAMs,

Figure 2: The neutrophil recruitment cascade in post-capillary venules.

In response to *S. aureus*, neutrophils undergo a sequential series of interactions with endothelial cells leading to recruitment out of the post-capillary venules to sites of infection. Neutrophils adhere, crawl, and then transmigrate, either paracellularly at endothelial cell junctions or transcellullarly encompassed by endothelial cell "domes"

Following transient selectin-mediated contact with endothelial cells, neutrophils become activated. This process is mediated both by intracellular changes induced by selectin binding, and by chemokine-induced changes. Selectin-induced activation of the integrin LFA-1 induces an intermediate form of this molecule, but does not fully activate it. In contrast, chemokines appear critically important for the full extension of this integrin, and in subsequent activation (67). Chemokines, such as CXCL1 (also known as KC, found in mice) (62) and IL-8 (68) have both been shown to interact with neutrophils to promote signalling pathways that activate G-protein coupled receptors, leading to the production of diacylglycerol and inositol triphosphate from phosphointidonositol 4,5-bisphosphate (PIP_2). Both the formation of these substrates and the binding of PSGL-1 to the selectins results in guanine exchange factors activating Rap1 via guanine triphosphate (GTP) cycling. Rap1 signalling mediates the redistribution of the β_2 integrins LFA1 (67) and Mac1 (69), and enhances clustering of integrins in lipid rafts on the neutrophil surface. Rap1 also recruits active Talin1. Talin1 acts upon integrins, cleaving clasp structures found between the α and β subunits of these molecules (70). This allows the integrin to switch from an inactive to intermediate activity position, by extending the extracellular region and exposing the previously hidden binding portion of the molecule. During this process, kindlin-3 is also recruited. Signalling via this molecule promotes an influx of intracellular Ca^{2+} into the neutrophil cytoplasm (62), which (in the case of LFA-1) is critical for multiple integrins clustering together to promote firm adhesion (68). Kindlin-3 also appears important in the transition from an intermediate state to a fully activated or high affinity state (67). The clustering, as well as conformational changes of the integrin to its active configuration, allows for stable integrin-ligand receptor interactions. These interactions are critical for neutrophil firm adherence to the endothelium.

Neutrophil firm adhesion in post-capillary venules is typically mediated by the integrin LFA-1, whereas crawling is mediated by Mac-1. Crawling is a distinct process, where neutrophils migrate along the vessel walls and can move against blood flow (71). It is thought that this process allows neutrophils to find optimal regions for emigration out of the vasculature. Other molecules play a role in neutrophil recruitment in some organs. $\alpha_4\beta_1$ or VLA-4 may play a role in neutrophil recruitment into the lung (72), and may be involved in neutrophil recruitment during specific infections or conditions, such as sepsis (73). However, in the periphery, LFA-1 and Mac1 are believed to be the primary integrins involved in neutrophil post-capillary venular recruitment.

Following adhesion and crawling, neutrophils emigrate either via transcellular or paracellular pathways. Neutrophils emigrate using predominantly the paracellular pathway, but can also perform transcellular emigration. However, transcellular migration is slow, and therefore perhaps less efficient compared to paracellular migration (64, 74). Both paracellular and transcellular emigration are mediated by integrin interactions with intracellular adhesion molecules (ICAMs). In addition, platelet/endothelial cell adhesion molecule (PECAM-1, also known as CD31), junctional adhesion proteins (JAMs), and endothelial cell selective adhesion molecules (ESAM) also play important roles in neutrophil emigration from the vasculature (66, 75). Paracellular neutrophil emigration involves disruption of junctional adhesion proteins such as cadherin. Recent studies suggest that neutrophils may preferentially emigrate paracellularly via tricellular endothelial cell junctions, possibly as these regions have lower expression of junctional proteins (76). Both paracellular and transcellular emigration involves the formation of endothelial transmigratory cell cups which transition into “domes”, structures that effectively separate the neutrophil from intravascular space, reducing permeability and preventing loss of

endothelial barrier integrity during emigration. These structures contain high concentrations of ICAM-1, and are largely mediated by leukocyte specific protein 1 (LSP1) on the endothelium (74, 77). Without LSP1, dome structure formation during emigration is impaired, while vascular permeability is increased (66). Emigration, whether by transcellular or paracellular processes, is crucial for neutrophils to exit the vasculature and be recruited to inflammatory stimuli.

A recent paper has identified another potential step in neutrophil recruitment that occurs outside the vasculature. Following emigration, neutrophils can be primed by capillary and arteriolar but not venular NG2+ pericytes. These are cells located outside of the vasculature in the basement membrane which can alter vessel diameter. This priming process can improve the lifespan and motility of neutrophils (78).

Following emigration (and perhaps subsequent priming by pericytes), neutrophils migrate through chemotaxis towards the stimulus along gradients of molecules such as chemokines, but also pathogen associated molecular patterns (PAMPs), and danger associated molecular patterns (DAMPs). For example, formylated peptides released from bacteria (as PAMPs) or from mitochondria (as DAMPs) are potent chemoattractants. There is evidence that neutrophils respond to chemotactic signals in a hierarchical fashion, favouring end target attractants such as DAMPs or PAMPs over chemokine signals such as LTB4 or IL-8 (79, 80). Chemotaxis is a complex process involving multiple signals, with different signalling cascades occurring within the uropod and the pseudopod of the cell, to mediate movement along a gradient. The pseudopod of the cell is the site of actin polymerization, which results in the leading edge pushing forward. Integrins and some associated molecules such as talin are critical in mediating adherence of this leading edge. In the uropod, by contrast, actin forms large bundles that can be

used to retract the cell, in a process that appears to be mediated by heat shock protein 27 and LSP1 (81). These processes are typically mediated by the phosphorylation of phosphoinositol 3,4 biphosphate (PIP_2) to phosphoinositol 3,4,5, triphosphate (PIP_3) at the pseudopod of the cell. Simultaneously, molecules such as phosphatase and tensin homologue (PTEN) or SH2 containing inositol phosphatase (SHIP) dephosphorylate PIP_3 to PIP_2 in parts of the cell other than the pseudopod, inducing the structural changes that lead to chemotaxis (82).

1.2.4 Interactions of neutrophils with S. aureus

1.2.4.1 Phagocytosis

Upon recruitment to sites of *S. aureus* infection, neutrophils utilize multiple mechanisms to interact with the bacteria. Classically, neutrophils interact with *S. aureus* via phagocytosis, engulfing the pathogen through the extension of pseudopods. This process is initiated when pathogens display "eat me" signals. These can be bacterially-derived PAMPs such as peptidoglycan (PGN) and lipotechoic acid (LTA), which enhance bacterial recognition via activation of PRRs, or can be molecules generated by components of the immune system such as complement receptors or antibodies, which appear to have more direct roles in inducing phagocytosis (83). Neutrophil receptors interact with these molecules, promoting the formation and internalization of a membrane-bound vacuole containing the pathogen. Phagocytosis allows neutrophils to sequester infectious organisms or dead cellular components within a vacuole (the phagosome) for subsequent destruction (84). Following phagocytosis, other vacuoles (such as endosomes and lysosomes) and granules will fuse with the phagosome, resulting in the destruction of bacteria. This is achieved by reactive oxygen species (ROS) and antimicrobial molecules, including AMPs. Antimicrobial molecules are mostly pre-stored in granules within

the neutrophil cytoplasm. A wide range of different antimicrobial molecules are involved in this process, such as defensins, cathelicidins, azurocidin, cathepsin, lactoferrin, and elastase (83). These molecules can kill bacteria independently of ROS (83). In the bacterially-occupied phagosome, the role of antimicrobial molecules is to act in concert with ROS, generated by NADPH oxidase and myeloperoxidase, to kill the pathogen. Myeloperoxidase (MPO) is an enzyme that produces ROS, such as hypochlorous acid, which is a potent antimicrobial molecule, and is believed to enhance neutrophil killing of bacteria (83). ROS, such as hydrogen peroxidase, are also produced by NADPH oxidase within the cell. As a result of these antimicrobial molecules, neutrophils are efficient at phagocytosing and killing bacteria.

1.2.4.2 Neutrophil extracellular traps

Neutrophils can also secrete antimicrobial proteins through the release of neutrophil extracellular traps (NETs) in response to *S. aureus*. NETs are produced in response to pathogenic stimuli, including both bacteria (85) and viruses (86). Structurally, NETs are composed of deoxyribonucleic acid (DNA), decondensed chromatin, and proteases, which can act to trap and possibly kill bacteria, although a recent paper has disputed the latter outcome (87). NETs are not entirely beneficial for the host; many of the molecules contained in NETs are equally capable of damaging host cells and therefore NET release also induces significant host tissue damage (88). *S. aureus* is a potent activator of NETs (85); incubation with *S. aureus* supernatant can induce neutrophils to release NETs within one hour (89).

1.2.4.3 Recruitment of additional immunocytes

Finally, neutrophils can also release proinflammatory cytokines, such as IL-1β (48), and chemokines (90), such as LTB_4, which are capable of attracting other neutrophils and pro-inflammatory macrophages (91). IL-1β is a potent pro-inflammatory cytokine, which can induce a wide variety of reactions in other cells, such as endothelial cells. It is important to note that the production of IL-1β by neutrophils is a matter of some controversy. Some reports have suggested that neutrophils do not use the inflammasome to produce IL-1β (92). A more recent report has suggested that neutrophils indeed use the inflammasome to produce IL-1β (93). Regardless, IL-1β production from neutrophils has been reported to play a critical role in the context of *S. aureus* infections (48). Neutrophils are also capable of producing many cytokines, including IL-1α, IL-6, and IL-17 (94).

Neutrophils also release chemoattractants such as leukotriene B_4 in response to inflammatory or infectious stimuli, which can attract other pro-inflammatory immunocytes such as monocytes and other neutrophils (95). Neutrophils thus propagate further recruitment of other neutrophils during the responses to infection. Leukotriene B_4 and other chemokines, including MIP-2 and MCP-1, can attract other cells, such as pro-inflammatory monocytes (94). In *S. aureus* infections, myeloid progenitor cells may differentiate into neutrophil-like cells at the site of a lesion (96).

1.2.5 S. aureus responses to neutrophils

The complex responses and adaptations of *S. aureus* to the presence of neutrophils further demonstrate the difficulty in determining the beneficial or detrimental nature of the neutrophil in

S. aureus infection. Many virulence factors that *S. aureus* produces have important effects on the recruitment of neutrophils and their behaviour. Others allow the bacteria to escape neutrophil killing mechanisms and thus survive when phagocytized.

During chemotaxis, molecules such as the chemotaxis inhibitory protein of *S. aureus* (CHIPS) bind to the formylated peptide receptor, interrupting neutrophil recruitment and disrupting this chemotactic signalling pathway (97, 98). Another example is the virulence factor clumping factor a (Clfa), which can alter neutrophil phagocytosis by binding to fibrinogen, a ligand receptor of the β_2 integrins (99). However, not all behaviour-altering *S. aureus* virulence factors act as antagonists for neutrophils. Some virulence factors, such as alpha hemolysin (Hla), can induce the production of chemoattractants for these cells (100).

Some *S. aureus* strains alter neutrophil functions in another way: by removing signals and molecules that can induce neutrophil-mediated cell killing. Aureolysin can protect the bacteria from neutrophil killing mechanisms by inactivating the complement molecule C3, thereby reducing phagocytosis by removing an important "eat me" signal.

Other molecules can both enhance neutrophil recruitment and induce neutrophil death. Phenol soluble modulins have potent pro-inflammatory effects, recruiting neutrophils and inducing interleukin-8 (IL-8) production (31). However, these molecules induce neutrophil lysis at high concentrations (31), and can furthermore enhance secondary necrosis of apoptotic neutrophils (101).

Another virulence factor known to influence *S. aureus* infection is alpha toxin. Alpha toxin can form beta barrel pores, which induce cell death in many different cell types (60), though not in neutrophils. It is, however, expressed at higher levels following neutrophil phagocytosis of *S. aureus* (102). This toxin is also capable of inducing cell death in association

with other bacterial proteins through the nod-like receptor pyd 3 (NLRP3) activation of the inflammasome in monocytes (103, 104). Alpha toxin stimulation can induce neutrophil recruitment (100), stimulate neutrophil leukotriene B4 (LTB4) production (105) and increase inflammatory responses (43).

When *S. aureus* is phagocytosed by neutrophils, the bacteria do not die immediately, and can mount a response from within the neutrophil. Within one hour of being phagocytosed, bacteria rapidly increase expression of virulence factors (102). This is thought to be mediated by the *agr* quorum system; when in a small compartment such as the phagosome, *agr* becomes activated and upregulates virulence factor production (106). Some of these virulence factors, such as catalase and superoxide dismutase, can disrupt the production of ROS inside the phagosome (83). Other virulence factors can disrupt the neutrophil's antimicrobial molecules. Aureolysin can degrade antimicrobial molecules such as LL37, disrupting neutrophil-mediated killing of bacteria (56). *S. aureus* can also sense and respond to antimicrobial molecules, modifying its cell wall to increase its ability to survive within the phagosome (83). *S. aureus* thus has methods to successfully mitigate the challenge of being phagocytized by an activated neutrophil.

In addition to releasing toxins that can interrupt and alter neutrophil recruitment and activation, *S. aureus* can interfere with the immune system by secreting anti-inflammatory signalling molecules recognized by the host. *S. aureus* is known to secrete adenosine, via adenosine synthase A (107). Adenosine is well known to suppress neutrophil recruitment by reducing selectin and integrin binding to associated ligand receptors, as well as reducing ROS production and inhibiting phagocytosis (108).

To summarize, neutrophils are an important component in the host response to *S. aureus* soft tissue infections. Neutrophil depletion or deficiency both increases the likelihood of *S. aureus* infections and increases the severity of those infections (83). The role of neutrophils is further illustrated by the wide variety of different *S. aureus* toxins that interact with neutrophils, although whether these interactions are to the benefit of the host or the pathogen appears to be toxin-specific and in many cases is unclear. Thus, improving our understanding of neutrophil recruitment may better elucidate the mechanisms at work in *S. aureus* soft tissue infections.

1.2.6 Detrimental effects of neutrophils during infection

The importance of neutrophils in *S. aureus* infections cannot be understated; neutrophils make up much of the lesion that develops during *S. aureus* infection (47). Additionally, neutrophil deficiencies (either genetic, or due to treatments such as chemotherapy or corticosteroids) make individuals highly susceptible to infection with *S. aureus* (83). Finally, live animal models have demonstrated that neutrophil depletion prior to infection enhances tissue damage and reduces resolution of disease (40, 109).

However, while neutrophils are critically important in protecting the host against bacterial infections (83), they are also capable of causing bystander tissue damage, as demonstrated in multiple distinct models (88, 110, 111). Many of the molecules released by neutrophils to kill bacteria also have detrimental effects on host cells. For example, NETs, while effective in capturing bacteria in flow chamber assays (88) and in the liver (112), can also induce bystander tissue damage to the host. Molecules such as LL37 and other cathelicidins, while effective AMPs, can cause bystander tissue damage, and appear to be involved in autoimmune diseases such as arthritis (110).

Additionally, studies concerning neutrophil-*S. aureus* interactions have demonstrated that neutrophil recruitment is not always beneficial for the host, particularly because *S. aureus* can survive when phagocytized by neutrophils (113). Gresham et al. further demonstrated that reduced neutrophil recruitment to *S. aureus* infections in a mouse model of peritonitis was beneficial for the host and enhanced host survival (113). Neutrophils may act as a "Trojan horse", allowing the bacteria to disseminate from the point of infection and cause additional damage to the host (114). The above studies may aid in understanding the observation made by Kim et al, described below (96). In this study, the authors showed that neutrophil depletion 24 hours after *S. aureus* infection led to decreased lesion size and increased wound healing in a mouse model. Thus, neutrophil recruitment to *S. aureus*, may play a dual role. Early on, neutrophil recruitment is critical to protect the host from the bacterial infection, but later the neutrophil recruitment leads to additional bystander tissue damage, and may actually be a mechanism by which *S. aureus* enhances its virulence.

Neutrophils are therefore a double-edged sword: capable both of bacterial killing (via mechanisms such as phagocytosis and NET production) and host tissue damage (via NET production and the release of toxic molecules to both bacteria and host). These dual functions are heavily intertwined, with many molecules that play important antimicrobial functions also injuring host tissue. *S. aureus* may actively manipulate these functions, by altering neutrophil signalling and surviving phagocytosis, in order to promote pathogenesis and tissue damage. Elucidating the complex interactions between these two roles may aid in modulating neutrophils so as to minimize detrimental aspects of neutrophil behaviour.

1.2.7 Objectives and hypothesis

In this thesis, we sought to address the question: how are neutrophils recruited to the site of *S. aureus* infection in the skin? We hypothesized that a localized *S. aureus* skin infection would cause neutrophil recruitment and that this recruitment would have detrimental physiological effects on the surrounding tissue.

To test this hypothesis, three specific objectives were identified:

1) To develop and validate a model of localized *S. aureus* skin infection, in which neutrophil recruitment and behaviour could be visualized and quantified using *in vivo* spinning disk confocal microscopy
2) To use this model to quantify neutrophil recruitment and behaviour at the site of *S. aureus* infection
3) To determine whether inhibition of neutrophil recruitment results in physiological changes in the surrounding tissue, and whether these changes affect the formation of *S. aureus*-induced lesions

Chapter Two: Materials and Methods

2.1 Mice

C57BL6 male mice (Jackson, Bar Harbour), aged 6-8 weeks were used for all experiments. Mice had access to tap water and food *ad libitum* prior to experiments, and during lesion size experiments. All animal protocols were approved by the animal care committee of the University of Calgary (protocol number AC12-0222).

2.2 Bacteria

Green fluorescent protein (GFP)-expressing *S. aureus* was made by Dr. Kaiyu Wu in Dr. Kunyan Zhang's lab from the previously isolated clinical strain USA300-2406 (PVL positive, SCC*mec* type IV, described previously (54)). The strain ATCC25923 (ATCC, Manassas, VA) was also used for several experiments (PVL positive, SCC*mec* negative).

2.2.1 Bacterial preparation

Bacteria were grown in 5ml of Bacto^{TM} Brain Heart Infusion (BHI) media (Becton and Dickenson, Sparks, MD) in a 17x100mm nylon tube (WVR, Radnor), and were incubated overnight in a shaker (Thermo Scientific, Waltham, MA) at 37^{o}C and 200 rotations per minute (rpm). GFP-expressing *S. aureus* (strain USA300, type number: 2406) was grown in 20 µg chloramphenicol per ml of media (EMD Biosciences, La Jolla, CA). The ATCC strain 25923 was grown in kanamycin sulfate (Merck, Darmstadt, Hessen) at 20 µg per ml of media.

2.2.1.1 Injection experiments

For preliminary experiments involving injection of bacteria in saline, the bacteria were subcultured with 250µl of the overnight culture being added to 5ml of fresh BHI (Becton and Dickenson, Sparks, MD) with antibiotics (chloramphenicol). The bacteria were then measured for optical density 660 (OD). An optimal OD of between 0.4 and 0.6 was used. If the OD exceeded 0.6, the bacteria were re-cultured as above and then the OD measurements were repeated. The following equation was then used to identify the number of colony forming units (CFU) in the media:

$$\frac{\text{OD measurement}}{x\ \text{CFU}} = \frac{0.5}{3\text{x}10^8\ \text{CFU}/ml}$$

This was used to identify the number of ml required for $1\text{x}10^8$ CFU. The bacteria were then spun at 4000 rpm for 10 minutes in a centrifuge and resuspended in 100µl saline. This equation was determined to be accurate previous to this project.

2.2.1.2 Agarose bead experiments

After overnight incubation, 5ml of overnight media was mixed with 45ml of fresh BHI with 20µg/ml chloramphenicol, and grown for a further two hours. This media was then centrifuged in a 50ml conical tube (BD, Franklin Lakes, NJ) at 2000 rpm for 10 minutes. The supernatant was removed, and 250µl of 1x phosphate buffered saline (PBS, 137mM NaCl; 2.68mM KCl; 8.1mM Na_2HPO_4; 1.47mM KH_2PO_4; pH 7.5) was added to the *S. aureus,* which was then vortexed at maximum speed to resuspend the bacteria in the PBS. For sterile beads without bacteria (control beads), 250µl of 1x PBS alone was used. For strains that did not express GFP and sterile control beads, 2µl of Fluoresbrite plan yg 1.0 micron microspheres (Polysciences,

Warrington, PA) were added to the solution. 10µl from all solutions containing bacteria were taken and serially diluted with 1x PBS, to identify CFUs. All solutions were then added to 2.25 ml of liquid 1.5% TSA agar. This media was prepared by mixing 750µg of TSA agar to 50ml of double distilled water, then autoclaved, and microwaved to return it to fluid state 30 minutes prior to use, then maintained before experiments in a hot water bath at approximately 37^{o}C. The TSA/PBS/*S. aureus* solution was slowly injected via a 3ml syringe (BD, Franklin Lakes, NJ) attached to a 16½ gauge needle (BD, Franklin Lakes, NJ) into a mixture of 40 ml of mineral oil (Sigma-Aldrich, St Louis, MO) and 400µl of Tween 20 (Sigma-Aldrich, St Louis, MO), which was stirred gently (at the lowest stir setting possible to get uniform stirring) by a magnetic stir bar. This solution was maintained at 4^{o}C on ice. The mixture was stirred for 15 minutes, and then spun at 2000rpm for 10 minutes to isolate the beads. The mineral oil layer was then removed. Beads were further washed with 5 ml of PBS and resuspended, then spun again at 2000rpm. The removal of the mineral oil, washing with PBS, and spinning was repeated three times. Beads were then filtered by a 100µl filter twice, and resuspended with PBS. Following this procedure, beads were stored at 4^{o}C for up to 6 days for use.

2.2.1.3 Plating of PBS/*S. aureus* solution

10µl of the 250ul PBS/*S. aureus* solution was added to 990µl of PBS, and then serially diluted. These dilutions were then plated onto BHI agar (Becton and Dickenson, Sparks, MD) plates, in three 10ml aliquots per dilution. These plates had chloramphenicol (Calbiochem, La Jolla, CA) added at a concentration of 20µg per ml for the GFP USA300, and kanamycin added at 20µg/ml for ATCC25923. Plates were incubated overnight, and were examined the following day for

CFUs. Total CFU was determined by the number of CFU present in each of the three aliquots at the lowest dilution at which CFU could be identified (typically 10^{-10} dilutions) and were then divided by 4 to determine the total CFU being used to produce *S. aureus* beads.

2.2.1.4 Assessment of change in CFUs per bead over time

10µl of the PBS/*S. aureus* bead solution was serially diluted on chloramphenicol plates and grown overnight in an incubator. This process was repeated at two, four, six and eight days following construction of *S. aureus* beads.

2.3 Imaging of the Murine Skin Tissue

2.3.1 Anesthetic for Mice

Male C57B6 mice were anesthetised with 200mg/kg ketamine (Rogar/STB, London, ON) and 10mg/kg xylosine chloride (MTC Pharmaceuticals, Cambridge, ON) injected intra-peritoneally 20 minutes prior to surgery. After 20 minutes, and throughout the experiment, mice were tested via squeezing of either footpad to determine degree of consciousness. If the mouse responded to footpad squeezing, mice were given approximately 50µl of the ketamine/xylosine chloride mixture immediately, and retested in five minutes.

2.3.2 Jugular vein cannulation

Following anesthesia, surgical tape was used to immobilize both forelimbs. 4.0 silk (Look, Reading, PA) was inserted underneath the teeth, and was secured with surgical tape, to expose the neck. The neck between the skull and the shoulder was coated with mineral oil, and then a

small incision was made, exposing the jugular vein. The tissue surrounding the jugular vein was cleared using surgical tweezers, and then 1 line of 4.0 silk was threaded underneath the jugular vein. This was secured with tape. The region around the jugular vein was further cleared, and two more silk lines were threaded underneath the jugular vein. A 1 ml syringe (BD, Franklin Lakes, NJ) was filled with heparinized saline to approximately 600ul. The heparinized saline was created by diluting heparin (Sandoz, Boucherville, QC) to 100unit/ml with saline. This syringe was then connected to PE10 surgical tubing (Becton Dickinson, Sparks**,** NV), via insertion of a 30 gauge needle into one side of the PE10 surgical tubing. A 30 gauge needle (BD, Franklin Lakes, NJ) was bent at 45° and then inserted and removed from the jugular. The tubing was then inserted into the jugular vein at the site of the 30 gauge needle insertion. To test for proper insertion, the syringe plunger was withdrawn 50µl and the tubing was monitored to ensure that tubing was inside the vessel and blood could be withdrawn.

2.3.3 Superfusion solution preparation

Approximately 150 ml of superfusion solution (NaCl 7.70g/L, KCl 0.350g/L, $CaCl_2$ 0.222g/L, $MgSO_4$ 0.144 g/L, $NaHCO_3$ 1.68g/L) was stirred at room temperature. The pH was then measured by a pH probe (Fischer Scientific, Ottawa, ON). Hydrocloric acid (HCl) and sodium hydroxide were used to achieve a pH of 7.4 ($\pm$ 0.10).

2.3.4 Skin preparation of anesthetized mice

During skin preparation and imaging, mice were maintained on a heat pad (Fine Science Tools, Foster City, CA), on a plastic board made in house. The dorsal flank on the right side of the

mouse was painted with mineral oil, and then the hair was parted along the spinal cord. The skin was then cut along the spinal cord and exteriorized on the right flank. A 4-0 suture (Ethicon, Markham, ON) was used to pierce and thread through the skin tissue 3-4 times at the edge of the exteriorized skin tissue, with threads corresponding to the region closest to the tail, the region closest to the skull and the region in between those two. The sutures were attached to the board via surgical tape. 3 bead clusters, of a diameter between 250 and 350µm were selected and inserted into the exteriorized skin tissue at different locations, and inserted to a depth of approximately 50µm underneath the exterorized tissue surface. Each bead cluster was located a minimum of 5 mm away from the edge of the skin tissue. Following insertion of a bead cluster, the tissue was then rinsed with superfusion solution to displace any beads that were not firmly inserted into the exteriorized tissue. The skin was then covered with a cover slip (VWR, Radnor, PA), which was connected to the plastic board with high vacuum grease (Dow Corning, Midland, MI). A pump (Mandel, Guelph, ON) was connected to the plastic board (constructed in house), connecting the superfusion buffer (above, section 2.3.3) to the region of exteriorized skin tissue, and allowing for the fluid to be perfused over the mouse skin tissue. Mice were imaged for up to 4 hours after anesthetization with 10mg/kg xylosine chloride/ketamine.

2.3.5 Spinning disk intravital microscopy

Spinning disk confocal microscopy was performed using an Olympus BX51 (Olympus, Center Valley, PA) upright microscope. The microscope used a confocal light path (WaveFx, Quorum) based on a modified Yokogawa CSU-10 head (Yokogawa Electric Corporation). Laser excitation at 488, 561 and 647 was used in rapid succession and fluorescence in green, red and

far red channels was visualized with long pass filters (Semrock). Exposure time and sensitivity setting were uniformly maintained for each set of experiments. For imaging, velocity acquisition software (Improvision Inc. Lexington, KY) was used to drive the microscope. A 512x512 pixel back thinned EMCCD camera (C9100-13 Hamamatsu) was used for fluorescence detection. Mice were imaged using a 4x/0.16 (approximately $1mm^2$ field of view FOV) air objective (Olympus, Center Valley, PA) for approximately two hours following introduction of the *S. aureus* bead cluster. Data on neutrophil numbers was collected at the 30, 60, 90 and 120 minute timepoints. Images were collected once every 15 seconds. Some mice were also imaged as required following 2 hours of infection with a 10x/0.30 (approximately $500\mu m^2$ FOV) numerical aperture air objective (Olympus, Center Valley, PA). Mice were imaged for 10 minutes per video at maximum speed using this objective, approximately 18-19 images per minute. Some experiments also collected individual images using a 20x/0.45 (approximately $250\mu m^2$ FOV) numerical aperture air objective.

2.3.6 Labelling antibodies

Mice were injected with 10µl of anti-Ly6G (clone RB6-8C5) conjugated with PE (Ebioscience, San Diego, CA), at a concentration of 0.2 mg/ml. In experiments where propidium iodide was used, mice were injected alternatively with 10µl anti-Ly6g (clone RB6-8C5) conjugated with Alexa680 (Ebioscience, San Diego, CA) at a concentration of 0.2 mg/ml, or 10µl of anti-Ly6g (clone 1A8) conjugated with PE (BioLegend, San Diego, CA)at a concentration of 0.2mg/ml. Mice were also labelled with 10µl of CD31 (Clone 390, Ebioscience, San Diego, CA) conjugated to Alexa647 (Molecular Probes, Eugene, OR), at 1.0 mg/ml. CD31 was conjugated in house to Alexa647 with Alexa Fluor ® labeling kit (Molecular Probes, Eugene, OR). For experiments

where ICAM-1 expression was measured, mice were injected with 10µl 1.0mg/ml anti-ICAM-1 antibodies conjugated to PE (EbioKAT-1, Ebioscience, San Diego, CA) or 20µl 1.0mg/ml anti-VCAM-1 antibodies conjugated to FITC (Clone 429, Ebioscience, San Diego, CA).

2.3.7 Subcutaneous injection experiments

Mice were injected with ketamine/xylosine chloride, and the right dorsal flank was shaved. Bacteria were injected subcutaneously in the right dorsal flank in 100µl of saline. The skin prep was then performed as described above, without any beads being inserted. Mice were imaged for up to two hours following infection. Mice were imaged for 5 minute videos at the 1 hour timepoint up to the 2 hour timepoint.

2.4 Lesion size experiments

Individual beads were selected and isolated in 100µl of saline. 2-3 beads from every group were vortexed for approximately 60 seconds and then serially plated on BHI agarose (Becton and Dickenson, Sparks, MD) plates with 20µg/ml chloramphenicol. The remaining beads were placed in 1ml syringes (BD, Franklin Lakes, NJ). Mice were temporarily anesthetized by isoflouride and the right dorsal region of the mouse between the shoulder and thigh was shaved. A single bead per mouse was then injected using a 16 gauge needle (BD, Franklin Lakes, NJ) subcutaneously. Mice were then returned to their cages. Mice were sacrificed 48 hours after infection, and skin (epidermis to subcutaneous) was harvested around the area of the bead injection (up to $2x2cm^2$.) The tissue was photographed and measured with a ruler and then placed in 10% neutrophil buffered formalin (EMD Chemicals, Gibbstown, NJ) for storage.

2.5 Reagents

2.5.1 Blocking antibodies

Blocking antibodies were administered intravenously in saline in most imaging experiments two hours following introduction of the bacteria into the host. Video recordings for quantifying the effect of blocking antibodies were performed 20 minutes after antibody injection. In experiments using propidium iodide, blocking antibodies were administered 5 minutes before the introduction of *S. aureus*. In lesion studies, blocking antibodies were administered two hours before or after introduction of bacteria into the host as indicated. Isotype control antibodies were: IgG2b at 100µl and 50µl volumes at a concentration of 1.0 mg/ml (Pharmigen, San Diego, CA), IgG2a, at 100µl and 30 µl, at a concentration of 1.0 mg/ml, (Pharmigen, San Diego, CA) and IgG1, at 30µl at a concentration of 1.0mg/ml (Pharmigen, San Diego, CA). For blocking the β_2 integrins, 30µl of the monoclonal anti-CD18 antibody clone game46 was used at a concentration of 1.0g/ml (Pharmigen, San Diego, CA). For blocking LFA1, 20µl of the monoclonal anti-CD11a antibody clone M17/4 was used at a concentration of 1.0 mg/ml (Ebioscience, San Diego, CA). For blocking Mac1, 20µl of the monoclonal anti-CD11b clone M1/70 at a concentration of 1.0 mg/ml (Ebioscience, San Diego, CA). For blocking VLA-4, 50µl of the anti-α_4 integrin antibody clone r1-2 was used at 1.0mg/ml (Pharmigen, San Diego, CA). For blocking ICAM-1, 100 µl of the monoclonal anti-ICAM-1 antibody YN1/1.7.4 at a concentration of 1.0mg/ml was used (Ebioscience, San Diego CA). For blocking VCAM-1, 50µl of the monoclonal and anti VCAM-1 antibody clone 429 at 1.0mg/ml was used (Ebioscience, San Diego CA).

2.5.2 FITC albumin experiments

FITC albumin was prepared in house. Bovine fluorescein isothyiocyanate albumin (Sigma-Aldrich, St Louis, MO) was diluted to 5mg/ml. Approximately 50µl of this solution was injected IV with saline into anesthetized mice, with exteriorized skin tissue. Mice skin preps were imaged as the FITC albumin was being injected.

2.5.3 Propidium iodide experiments

50µl of 2µM propidium iodide was superfused over the skin. Cell death was measured by counting the number of PI positive cells present. Mice were anesthetized with ketamine/xylosine and the skin tissue was exteriorized. Mice were then injected with CD31 and Ly6g labelling antibodies, as well as isotype controls or dual blocking antibodies intravenously at approximately the same time as the bead was inserted. Mice were treated with propidium iodide at the 2 hour timepoint. Propidium iodide was superfused across the tissue for 30 seconds, and then rinsed off with superfusion buffer. Images were then collected for up to 5 minutes after the superfusion of propidium iodide.

2.6 Analysis

2.6.1 Neutrophil recruitment to bead

Images at 4x Magnification of were analyzed by removing light collected from the 488 and 561 and 649 nanometer channels of the spinning disc confocal microscope. The contrast and brightness used to analyze data was held constant for analysis of each set of experiments. The number of neutrophils at 30, 60, 90, and 120 minutes was counted by using the point tool function of Volocity (Perkin-Elemer, Waltham, MA). For analysis of location of neutrophils,

the 649 channel was used to examine the vasculature. Neutrophils that co-localized with CD31 labelled vessels were considered to be inside capillaries if the vessels did not exceed 10μm in width. Neutrophils both inside and outside the capillaries were counted using the point tool function of Volocity.

2.6.2 Cell tracking and meandering index measurements

Cell tracking was performed as previously described (80), with several modifications. During the last 15 minutes of a 2 hour 4x magnification video, 20 red cells were characterized at particles using the Volocity trackng function. These 20 particles (or all particles if <20 present) outside of the microvasculature (as determined by not colocalizing with CD31 expressing cells) were randomly selected and tracked. Tracking and chemotaxis parameters (tracking plots and meandering index) were measured using Volocity software. Tracking plots were normalized to place the bead above the neutrophil, resulting in a Cartesian plane with all neutrophils starting at the 0, 0 point. The meandering index is quantified by the following equation:

$$Meandering\ index = \frac{Total\ Displacement\ of\ Particle}{Total\ Distance\ traveled}$$

This equation generates a number between 1.0 and 0. A high meandering index implies that the cell is moving in a uniform direction, whereas a low meandering index implies that a cell is moving randomly.

2.6.3 Neutrophil recruitment within the capillaries

Videos were used to quantify the number of neutrophils in the capillaries using 10xmagnification. The image was focused on the capillaries in the proximity (within 500μm) of

the *S. aureus* bead. The number of neutrophils that were adherent or crawling within the microvasculature in 10 minutes was quantified. Neutrophils were classified as adherent if they remained stationary within the FOV for thirty or more seconds. Neutrophils were classified as crawling if they remained within the FOV for thirty or more seconds, and moved at time of data collection. If a neutrophil crawled it was not counted as adherent. The definitions for these parameters were based on measuring adhesion and crawling in the post-capillary venules, as described previously (71). The number of neutrophils overall (crawling + adherent) and the individual parameters of crawling and adhering neutrophils were then normalized by dividing the total number of neutrophils by the total number of capillaries, then multiplying by 10 to get the normalized number of neutrophils per 10 capillaries. To quantify behaviour, multiple videos (at minimum four) were analyzed, and then averaged per mouse to generate the data.

2.6.3.1 3D image generation of neutrophils within the capillaries

For some experiments, Z-stacks were taken during imaging of the skin at 10x magnification. Z-stacks were taken after two hours of imaging. Z-stacks consisted of 10 slices, taken 2 µm apart. Z-stacks were imaged for 10 minutes. The images were then processed using Volocity software (Perkin-Elmer, Waltham, MA).

2.6.3.2 Neutrophil length and width inside the capillaries versus outside of the vasculature

The length of individual neutrophils was measured in terms of length using Volocity line tool. Neutrophils were selected randomly, and were measured every two minutes for a ten minute video, with the lengths and widths over those timeframes being averaged. Neutrophils were determined as inside a capillary if they entirely co-localized with any CD31 expressing vessels

that were ≤10um in width. Neutrophils were defined as extravascular if they did not entirely co-localize with CD31 expressing cells.

2.6.4 Measurement of venule parameters

During subcutaneous injection experiments, venules within 500µm of the injection site which were 20-40µm were quantified for the velocity, rolling flux, adhesion and emigration of neutrophils. The parameters of adhesion and emigration were also measured in some bead experiments. In this case, venules were measured which were within 500µm of the bead.

2.6.4.1 Velocity

Neutrophil rolling velocity was determined by quantifying the time it took the first 20 neutrophils imaged to pass through a 100 µm length of the venule being examined. This length of the vessel was chosen randomly before the video was analyzed, to avoid the possibility of bias.

2.6.4.2 Rolling flux

Rolling flux was determined as the number of neutrophils passing through the same 100µm length of the venule over one minute (the first minute of the video). This was repeated for the second minute, and the third minute of the video, and then averaged to achieve the rolling flux per minute.

2.6.4.3 Adhesion

The number of adherent neutrophils within the 100µm section of the venule was quantified over 5minutes of the video. Neutrophils were defined as adherent if they remained stationary for 30 or more seconds.

2.6.4.4 Emigration

The number of neutrophils per FOV external to any vascular bed at the 5 minute timepoint of the video in question was defined as the number of emigrated neutrophils.

2.6.5 Lesion size experiments

Photographs were analyzed using imageJ (National Institutes of Health, USA) to quantify the size of the lesion. The lesion was traced and the size in pixels was determined. This was then divided by the number of pixels required for single millimeter squared, to determine the overall area of the lesion.

2.6.6 FITC albumin experiments

The image was analyzed 30 seconds after FITC albumin became visible within the vasculature. The number of capillaries were quantified and then scored as either perfused (green) or not perfused (not green) at the 30 second timepoint. This number was then converted into a percentage of the total capillaries quantified.

2.6.7 Propidium iodide experiments

Greater than four images per mouse were quantified for propidium iodide, at 10x magnification. The number of red cells was quantified per FOV. Images were selected randomly in the region surrounding the bead (within 500μm). The total numbers of propidium iodide positive cells were averaged over the FOVs per mouse.

2.6.8 Statistical tests

Data was analyzed using unpaired Students t-tests to compare the number of recruited neutrophils under different conditions. When more than one comparison was made in the same graph, a bonferroni correction was used to correct for false positives. When three variables were all compared with one another in the same graph, a one-way analysis of variance (ANOVA) with a Bonferroni correction was used. All statistical analysis was performed using the statistical software GraphPad prism 4, version 4.03 (GraphPad Software Inc., La Jolla, CA).

Chapter Three: Model Development

3.1 Introduction: mammalian models of *S. aureus* soft tissue infection

Many models have been designed to examine tissue damage induced by *S. aureus* during soft tissue infections. The variety of infections that *S. aureus* can cause has resulted in many different experimental protocols, even when focusing exclusively on soft tissue infections (Table 1). The simplest method of examining *S. aureus* soft tissue infection involves using a needle to inject *S. aureus* in saline into a mammalian host. Injections are often performed intradermally (25) or subcutaneously (24, 45, 115) into tissue, resulting in different responses depending on which level of the skin or soft tissue is infected. There are a variety of animal models available to study *S. aureus*. Many studies use mice, but when studying some virulence factors, such as PVL, rabbits are used instead (24, 25), due to the resistance of mouse neutrophils to this virulence factor (26). The intradermal or subcutaneous injection method is used in examining the effect of different numbers of CFUs in soft tissue infections without much bystander tissue damage due to the delivery. It has been used to examine the importance of specific virulence factors when targeted to specific regions of the skin (31, 116, 117). These methods can also be used to compare the virulence of different strains of *S. aureus*. However, the injection of *S. aureus* in a fluid does not generally mimic clinical types of infection. Rare *S. aureus* cases may involve *S. aureus* infection via contaminated IV lines, but even then, this infection is intravascular, rather than in the surrounding tissue.

An alternate model involves damaging the skin of a mammalian host and applying *S. aureus* into these open wounds. Methods vary widely but all result in removal or disruption of various levels of the skin to generate easily reproducible infections. The tools to achieve this

vary: one can induce a mechanical injury using dermal punches (118), surgical scalpels (119, 120), large bore needles (40), or even tape (41). These tools cause superficial damage to the host, resulting in exposure of layers of the skin to the external environment. The tools used allow measurement of the depth of penetration into the skin, which thus determines the type of soft tissue infection being modelled. In all of these models, the original wound is colonized by *S. aureus* (either by infecting immediately following injury or by placing *S. aureus* on the mechanical device used to induce injury). Generally, the result of these experiments is the formation of lesions and generation of secondary complications of infection. These models may also resemble soft tissue infections resulting from poor aseptic technique during surgery.

Others methods involve altering the suspension used to infect the host. As early as 1965, W.C. Noble injected *S. aureus* mixed with cotton dust to mimic a contaminated wound (121). He used this model because the number of CFUs required to successfully induce a reproducible *S. aureus* soft tissue lesion without cotton was orders of magnitude higher, suggesting that the addition of foreign particles could enhance the pathogenicity of the bacteria (121, 122). More recently, researchers have replaced cotton dust with microparticles. The overall effect is similar: abscess formation occurs at lower CFUs compared with *S. aureus* injected with saline alone (approximately $2x10^3$ to $3x10^3$ versus $1x10^6$) (123, 124).

These models create a penetrating injury to the skin, resulting in a mixture of both the bacteria and the other foreign particles being deposited in the wound. This method of infection may have contributed to a college outbreak of MRSA when both the particles and tissue damage caused from artificial turf burns and body hair shaving are believed to have enhanced infection rates in football players in the USA (42). While foreign body/*S. aureus* mixtures are capable of

inducing much greater tissue damage to the host relative to the CFU introduced (121, 123, 124), the mechanism involved is not entirely clear.

Based on these observations, we developed a model introducing bacteria on a foreign particle. A number of additional issues were considered, including the reproducibility of the size of the foreign particle, as well as an experimental design that would allow for state of the art imaging using spinning disk microscopy. This permitted us to examine the entire process of immune cell recruitment into the infected site, allowing for effective localization of the pathogen, and clear visualization of changes in neutrophil behaviour and motility.

Skin Tissue	**Infection Models**	**Type of *S. aureus* infection being modeled**	**References**
Epidermis	Tape Stripping followed by *S. aureus* application	Impetigo	(41)
Dermis	Injection (with foreign particles or in fluid), Mechanical injury (via needle)	Furunculosis, folliculitis	(40, 123)
Subcutaneous	Injection (with foreign particles or in fluid), Mechanical injury (scalpel, punch biopsy, needle)	Cellulitis	(118, 119, 121, 124)

Table 1 : Models of *S. aureus* infection targeting different layers of the skin and soft tissue

Different models are used to target different depths of the skin, resulting in different soft tissue models of infection, dependent on the goal of the study and the type of *S. aureus* infection being mimicked.

3.1.1 Spinning disk microscopy

Spinning disk confocal microscopy is a recent innovation in the development of microscopes capable of providing high quality resolution with high frame rate, resulting in a powerful tool for examining not just the location of cells, but also their identities and behaviour in real time.

To understand the benefits of using a spinning disk, we must first describe the benefits of a confocal microscope over that of a bright field microscope. A confocal microscope works by excluding light originating from areas other than that of the focal region being imaged via a pinhole, which reduces the light from out of focus regions that can be collected from the specimen (125). Altering the size of the pinhole alters the amount of light being collected, with smaller pinholes decreasing the amount of light being collected and larger ones increasing it. This allows us to focus on a single section of the sample, and collect the light from only that section, resulting in a clear image with less background light from other sections of the sample compared to a bright field microscope.

Confocal microscopy provides major benefits over bright field microscopy by providing improved image clarity (greater resolution), but has some limitations. The use of a single pinhole means that the pinhole must scan across the entire FOV to collect a complete image, resulting in a low frame rate. This allows for collection of high-resolution pictures, but not for effective imaging of real time cellular activity. A spinning disk system resolves this problem by the introduction of a nipkow disk (125). This is a disk that rotates at high speed (faster than 1800 rotations per minute), and contains multiple pinholes, which each collect images from the FOV in parallel. The pinholes are spaced on the disk to allow every location to be imaged as the disk is rotated (125). These multiple pinholes can collect images at a much higher rate than that of

single pinhole scanning confocal microscope, thus yielding both a high frame rate and high resolution.

A major limitation of this tool is the depth that it can penetrate host tissue (to a maximum of 50μm). While providing high quality images, spinning disk microscopy has poor penetrance; it is difficult to image thick tissue (125, 126). As a result, any imaging of a specimen needs to be of thin tissue, or must be imaged on the surface of this tissue in order to collect usable information. Thus, the model needed to image *S. aureus* infections in soft tissue must utilize a relatively thin tissue. To achieve this, our imaging set up makes use of exteriorized skin tissue. The model also perfuses fluid over the exteriorized skin tissue to keep it warm and moist, in order to better resemble physiologically normal conditions. Thus, we identified further parameters that we required for our model: we needed a model that localized the *S. aureus* in an easily viewable tissue bed, as well as effectively anchoring the bacteria in order to prevent the perfused superfusion buffer from washing away the bacteria applied to the tissue.

3.2 Preliminary observations

Preliminary data were collected to examine the recruitment of neutrophils to *S. aureus* induced by injecting $1x10^8$ CFU of *S. aureus* in 100μl of saline subcutaneously, then exteriorizing the skin tissue 1 hour after infection. Neutrophils were quantified in terms of the number of cells rolling within a 100μm length of a venule during 60 seconds (rolling flux), the speed with which the neutrophils were rolling (velocity), as well as the number of adherent and crawling neutrophils. This demonstrated increased neutrophil adhesion within

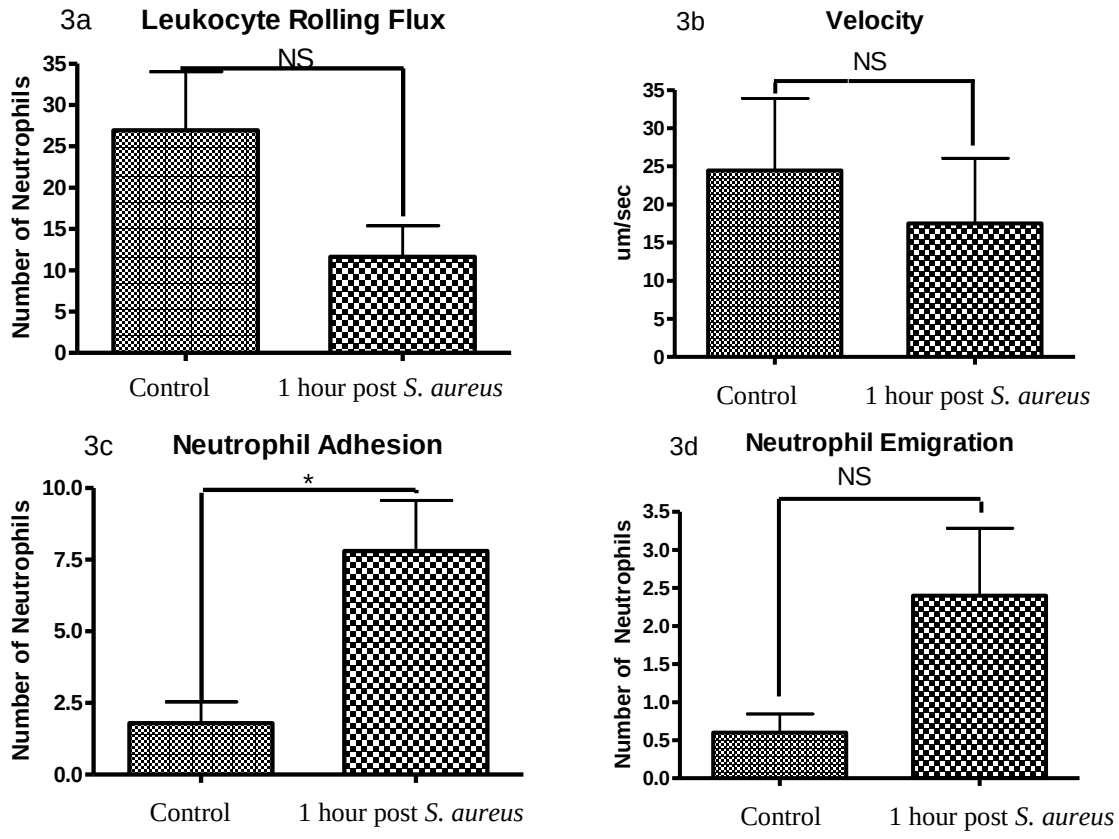

Figure 3: Changes in neutrophil parameters following subcutaneous injection of *S. aureus*

S. aureus was grown overnight and then recultured for 2 hours prior to infection. The OD_{660} of the subcultured sample was then taken, and provided the optical density at 660nm (OD_{660}) was between 0.4 and 0.6, the volume required for $1x10^8$ CFU was determined. This quantity was centrifuged for 10 minutes at 5000 rpm, and then resuspended in 100µl of saline. Mice were injected subcutaneously. The venules (the width of which was between 20µm and 40µm) were examined near the *S. aureus* injection and the neutrophil behaviours were quantified. 3a: Rolling flux - the number of neutrophils rolling in a 100µm length of venule was measured over 60 seconds. This process was repeated 3 times per venule. 3b: Velocity - the speed of the first 20

neutrophils to travel through the 100μm length of the venule was quantified. 3c: Adherence - the number of adhering neutrophils (neutrophils which remained in the same location for 30 seconds) was determined in 100μm of venule. Adhering neutrophils were measured over 5 minutes. 3d: Emigration - the number of neutrophils outside of the vasculature in the FOV was quantified. N=5 independent experiments for both *S. aureus* and control conditions, with 2-3 venules examined and averaged per experiment. * $p<0.05$

the venular vasculature at one hour after infection (Figure 3), allowing us to conduct some preliminary experiments to interrogate neutrophil responses to *S. aureus*. However, this model had significant limitations and did not achieve the desired objectives for our project. It was difficult to determine the proximity of these venules to the infection and to confirm whether we had similar concentrations of bacteria in different FOVs. This model also did not include a foreign body, which can increase the pathogenicity of *S. aureus* and may have been important in community-associated outbreaks of *S. aureus* (42).

3.3 Development of agarose bead model

Given the limitations of subcutaneous injection, we developed a model that used a solid agarose bead as a vehicle for delivering pathogen into the skin (Figure 4a). Agarose beads have previously been used to induce a long lasting *Pseudomonas aeruginosa* infection in mouse lungs to model cystic fibrosis (127, 128). This model had the benefit of providing an immobile nidus of infection, allowing us to focus on the dynamics of immune cells in response to the *S. aureus* insult. Most importantly, the placement of agarose beads subcutaneously meant that the tissue could be exteriorized and imaged *in vivo* in real time (Figure 4d). The beads were inserted below the superficial fascia, within the subcutaneous tissue (Figure 4e). An added benefit was that *S. aureus*, when mixed with foreign particles, is more pathogenic (121, 123, 124), thus requiring fewer CFUs to induce an infection, and better modelling some CA-MRSA outbreaks (42).

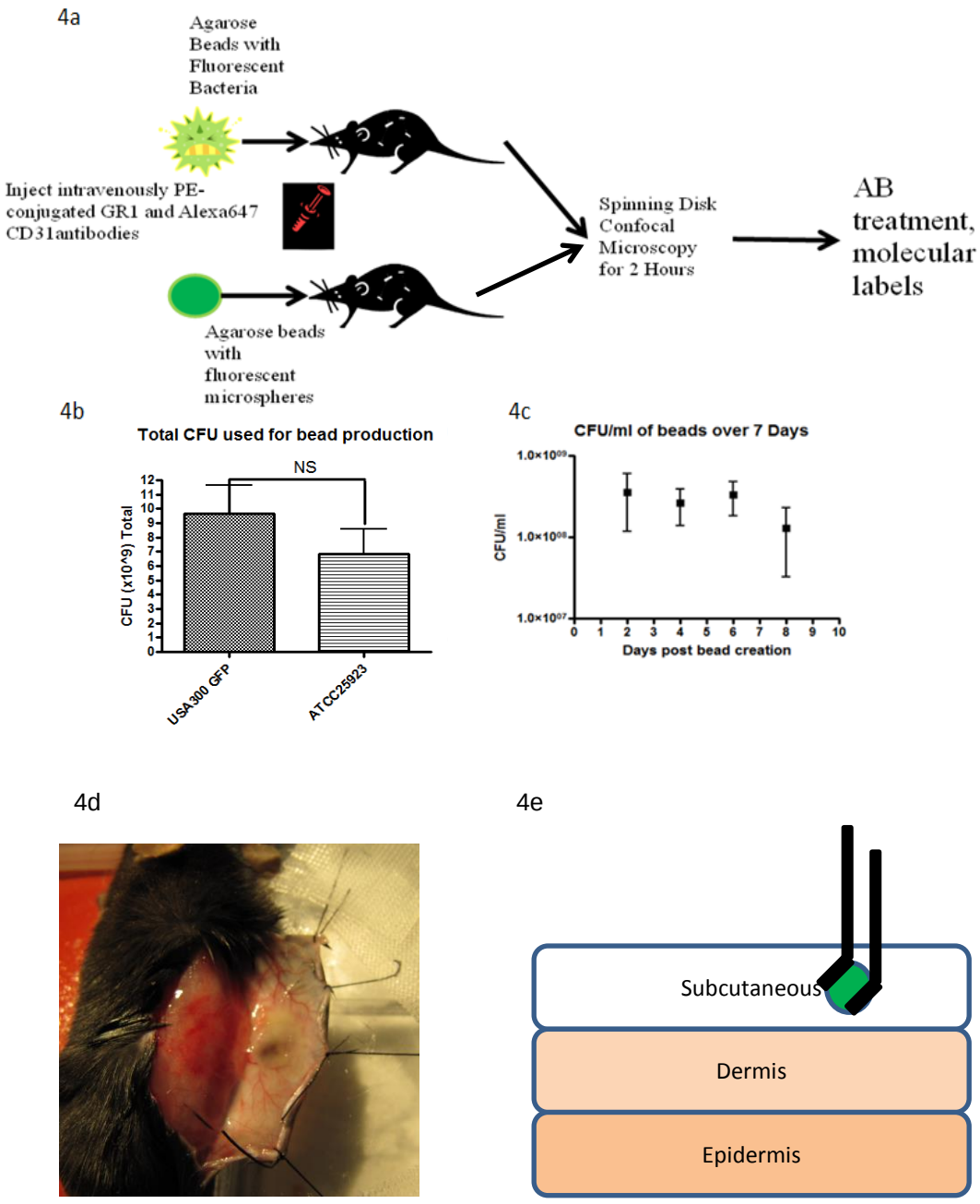

Figure 4: Parameters for *S. aureus* infection

4a: Flow chart of experimental model. Mice were anesthetized, and then either an agarose bead with GFP-expressing *S. aureus* or an agarose bead with GFP fluorescent microspheres was inserted into the subcutaneous tissue below the superficial fascia**.** The mice were then treated IV

with 10µl at 0.2 g/ml anti-GR1 antibodies conjugated to PE (to enable neutrophil detection) and 10µl at 1 g/ml of anti-PECAM-1 antibodies conjugated to alexa-647 (blood vessel detection). Mice were then imaged for 2 hours at 4x magnification, and then treated with blocking antibodies or molecular treatments to interrogate different aspects of the model system. 4b: CFU used for bead preparation. 5ml of BHI and chloramphenicol (20µg/ml) containing an overnight *S. aureus* culture was subcultured with 45ml of BHI and chloramphenicol (20µg/ml) over 2 hours. The bacteria were spun down, and then resuspended in 250µl of PBS. 10µl of the 250µl resuspension was then serially diluted and plated to determine the total CFU being used to make the beads. N=10 independent experiments for the GFP expressing USA300strain and 4 independent experiments for strain ATCC25923. Each independent experiment consisted serially diluting and plating a 10µl volume of *S. aureus*/PBS prior to the addition of agarose. 4c: CFU of beads over time. Following bead construction, the GFP-expressing USA300 strain beads were resuspended in 5ml of PBS. 10µl of the bead/PBS mixture was vortexed, then serially diluted and plated on BHI plates with 20µg/ml chloramphenicol. The CFU was measured via serial dilution of 10µl every two days up to 8 days post bead construction. N=4 independent experiments. 4d: Image of mouse skin prep. Mice were anesthetized, and then an incision was made on the dorsal region above the spine. The skin tissue was then exteriorized, and sutures were used to attach it to a board by surgical tape, as shown. 4e: Schematic depicting physical insertion of agarose beads into the subcutaneous tissue. The skin prep results in the exteriorization of subcutaneous, dermis and epidermis. Beads were then physically embedded into the exteriorized skin tissue in the subcutaneous layer.

As shown in Figure 4b, the bead process resulted in approximately $1x10^{10}$ CFU's in 2.5 ml of agarose/PBS mixture. CFUs did not vary significantly between different strains of *S. aureus* used (p=0.4242). Individual beads produced a CFU of between 10^5 and 10^7 depending on the size of the bead, with larger beads producing a commensurately larger CFU. We therefore controlled for bead variability by imaging only smaller beads (250-350μm in diameter), which produced CFUs of ~10^5. Bead CFU (as measured by plating the PBS-CFU mixture produced by generating the beads) remained relatively stable up until approximately day 8, when variation in recoverable CFUs began to increase (Figure 4c). Due to this observation, beads were used up to 6 days after being produced.

As a control, we used beads that contained fluorescent nanoparticles, with no bacteria, to represent the surgery without the infection. These sterile microspheres were highly fluorescent, allowing the beads to be clearly imaged (Figure 5a). Additionally, they do not appear to leave the beads following insertion, allowing us a clear view of the agarose bead. We also tested heat-killed bacteria (Figure 5d) as a further control and saw low levels of neutrophil recruitment, similar to the recruitment seen with sterile microspheres.

3.4 Quantification of neutrophils

We inserted three clusters of beads, with a diameter of approximately 250-350μm, 5mm apart from one another into the subcutaneous tissue of the mouse, and then quantified the number of neutrophils being recruited to one of those beads over two hours. There were significantly more neutrophils (p=0.0311) recruited to the infected beads when comparing sterile beads with those containing USA300 *S. aureus* (Figure 5). There were no significant (p=0.1527) differences in neutrophil recruitment to *S. aureus* beads used 1-2 days

5a

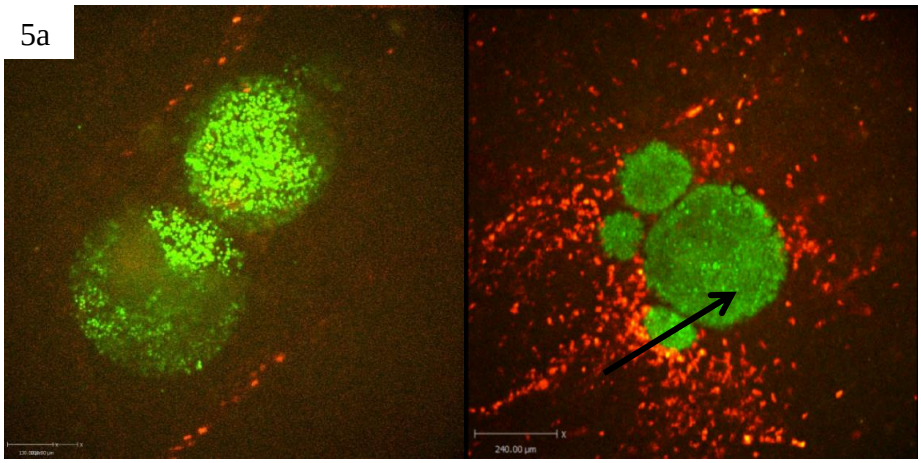

5b

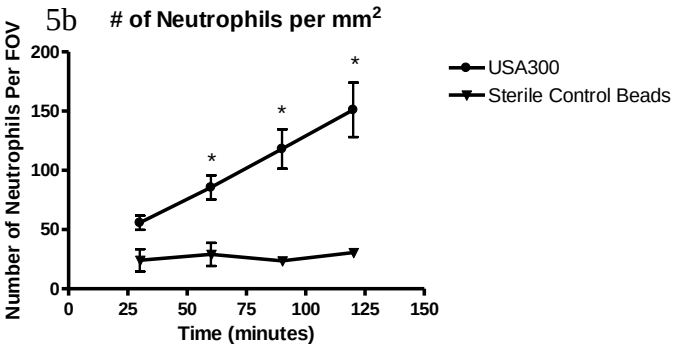
# of Neutrophils per mm2
Number of Neutrophils Per FOV
Time (minutes)
USA300
Sterile Control Beads
0
25
50
75
100
125
150
200
*

5c

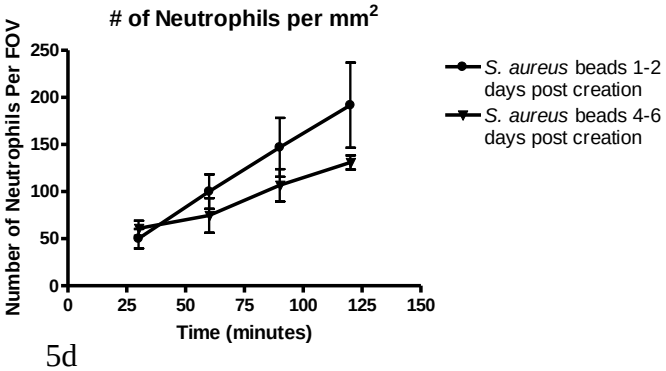
# of Neutrophils per mm2
Number of Neutrophils Per FOV
Time (minutes)
S. aureus beads 1-2 days post creation
S. aureus beads 4-6 days post creation
0
25
50
75
100
125
150
200
250

5d

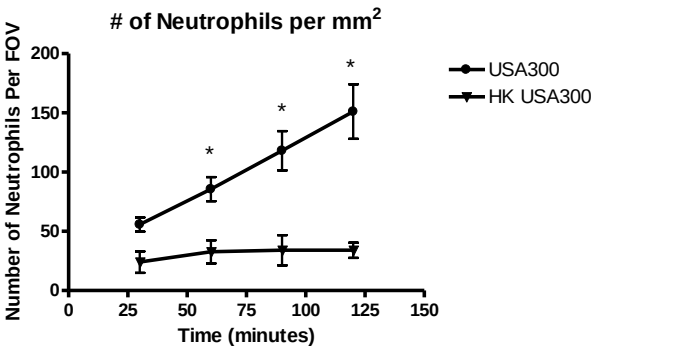
# of Neutrophils per mm2
Number of Neutrophils Per FOV
Time (minutes)
USA300
HK USA300
0
25
50
75
100
125
150
200
*

Figure 5: Neutrophil recruitment towards *S. aureus* beads

5a: Representative images of neutrophil recruitment to a bead with microspheres (left) and a bead with GFP-expressing *S. aureus* (right). Images were taken 2 hours after insertion of the bead into the subcutaneous skin tissue. The neutrophils are shown in red, labelled with anti-Ly6g. In green (on the left) is the bead with sterile microspheres. On the right, the green is the bead with GFP-expressing *S. aureus*. 5b: The number of neutrophils being recruited to a *S. aureus* bead over two hours. The number of neutrophils was quantified at 30, 60, 90 and 120 minutes post-insertion of the bead into the skin tissue. The 0 timepoint was not quantified as the amount of time needed to place the prep on the scope varied from one experiment to the next. N=4 for control beads, and N=11 for *S. aureus* beads. * $p<0.05$. 5c: The recruitment patterns of neutrophils to *S. aureus* beads either 1-2 days old or 4-6 days old. Experiments were divided based on the age of the beads in order to determine whether there were any differences in the number of neutrophils recruited to the beads depending on their age. N=5 for 1-2 days old, and N=3 for 4-6 days old. 5d: Comparison between beads containing live *S. aureus* and beads containing *S. aureus* that had been heat killed (HK) prior to bead construction. Bacteria were killed at 90^{o}C for 30 minutes prior to being used in bead construction. Beads with GFP-expressing USA300 *S. aureus* were compared to beads with heat-killed GFP-expressing USA300 *S. aureus*. N=3 independent experiments for heat killed *S. aureus* beads, and 11 independent experiments for USA300 beads. The data from a single 4x FOV around a bead over 2 hours made up a single independent experiment.

after bead generation as compared to 4-6 days after bead generation, further demonstrating that the beads remain viable and induce the same neutrophil response throughout the period that the beads were used.

Examination of neutrophil behaviour revealed that neutrophils crawled directionally towards the site of the infection. Comparisons between sterile beads and beads containing *S. aureus* indicated that neutrophils were not just being recruited to the area proximal (within approximately 500 μm) to the bead, but would actively crawl towards the site of infection (Figure 6a and 6b). Furthermore, neutrophils imaged from infected mice crawled in a more linear fashion than those from mice with sterile agarose beads (Figure 6c), as determined by the meandering index.

3.5 Neutrophil recruitment to capillaries

During directional crawling studies, a subset of neutrophils did not appear to be crawling in a directional fashion, but instead crawled back and forth in a linear fashion proximal to the bead insertion site. These observed neutrophils were extremely elongated and moved in a linear fashion. To better examine this cell subset, labelling of the vasculature with PECAM-1 was performed. This allowed for labelling of venules, capillaries, and arterioles in the skin, and revealed that the linear movement occurred in the smallest vessels, the capillaries. When the location of neutrophils in sterile or *S. aureus* bead conditions was compared, there were significant differences in the number of neutrophils both external to the vasculature, as well as in the capillaries (Figure 7a and 7b). In particular, there were approximately eight times more neutrophils per FOV in the capillaries in the mice with *S. aureus* beads, when compared with

FOV from mice with sterile beads inserted into the skin (p=0.0172). For these experiments, we had used the RB6-8C5 anti-Ly6g antibody, which can label Ly6c (a molecule found on monocytes as well as neutrophils) as well as Ly6g. To test whether these cells were neutrophils, or a combination of neutrophils and monocytes, we compared the anti-Ly6g RB6-8C5 clone with the anti Ly6g antibody clone 1A8, which is known to only label Ly6g (and thus is neutrophil specific)(129). Labelling with the anti-Ly6g antibody 1A8 revealed similar levels of Ly6g positive cell recruitment as that seen when using the anti-Ly6g antibody RB6-8C5. This was seen both in terms of overall recruitment to the bead (Figure 8a, p=0.5433) and in the capillaries (Figure 8b, p=0.7248).

To further provide evidence that neutrophil recruitment occurred within the capillaries, z-stack imaging was performed and 3D images were reconstructed from this technique. Z-stack imaging allows for multiple images to be taken at varying depths of the tissue, which can then be reconstructed into a 3D image to better examine where the cells are located. This technique clearly demonstrates that neutrophils were being recruited within the capillary microvasculature (Figure 7d). Further observation also determined that neutrophils within the capillaries were shaped differently from those found outside the capillaries. The maximum lengths and width of the neutrophils either inside the capillaries or outside of the vasculature were determined every 2 minutes over a 10 minute period. Neutrophils inside the capillaries appear to be both longer (p =0.0094) and thinner (p=0.005), when comparing length and width with neutrophils outside the capillaries (Figure 9).

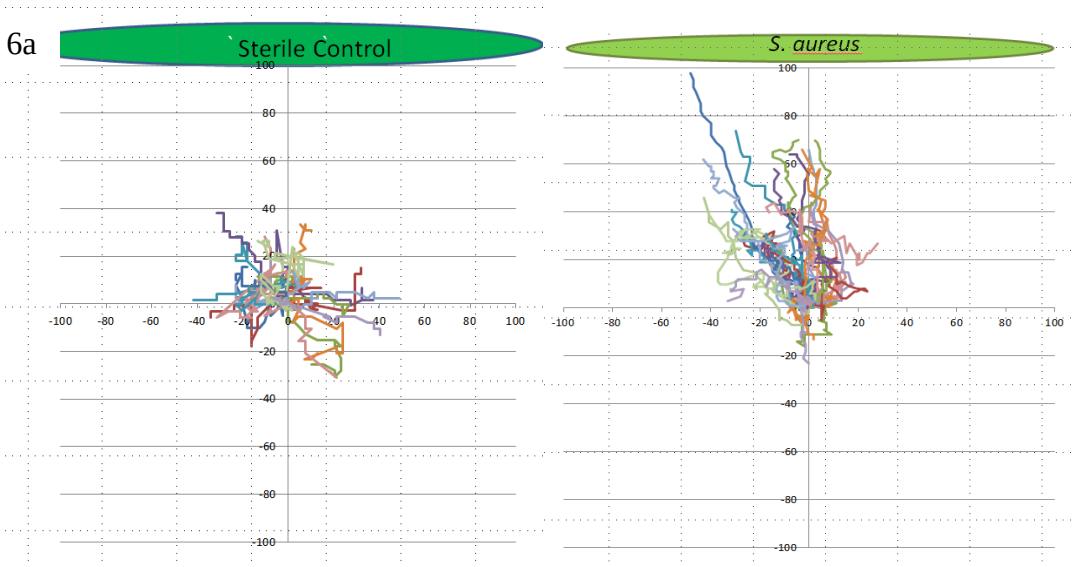

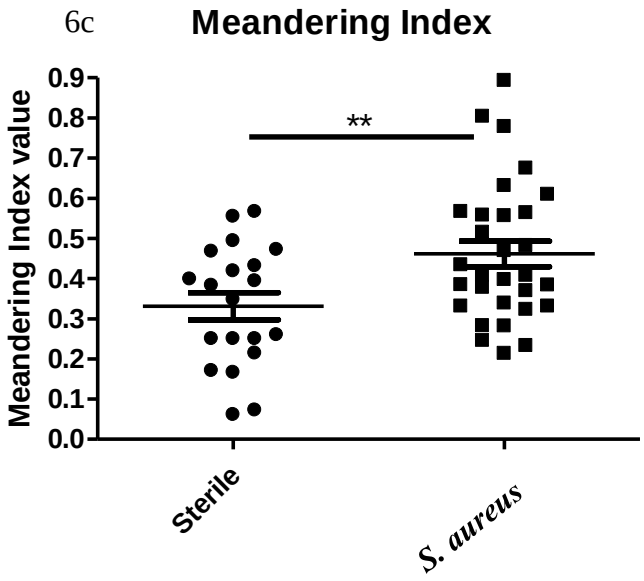

Figure 6: Directional motion and recruitment of neutrophils

Figure 6a: Directional crawling of neutrophils. The path of individual neutrophils over 10 minutes was quantified using the "track objects" tool in the Volocity analysis program. The pathways of the neutrophils were then placed on a Cartesian plane with track start point placed at x=0 and y=0. The location of the bead (with either *S. aureus* or sterile microspheres) was

normalized to be in the positive y-axis. 6b: The absolute distance (the change in the x and y coordinates) that neutrophil travelled was divided by the total distance the neutrophil travelled (the length of the neutrophil path), yielding the meandering index. N=3 independent experiments for both sterile and *S. aureus* conditions. In each independent experiment, 10 neutrophils (or fewer if there were less than 10 neutrophil visible outside of the vasculature) from a single 4x FOV over 10 minutes were quantified. $^{**}p<0.01$

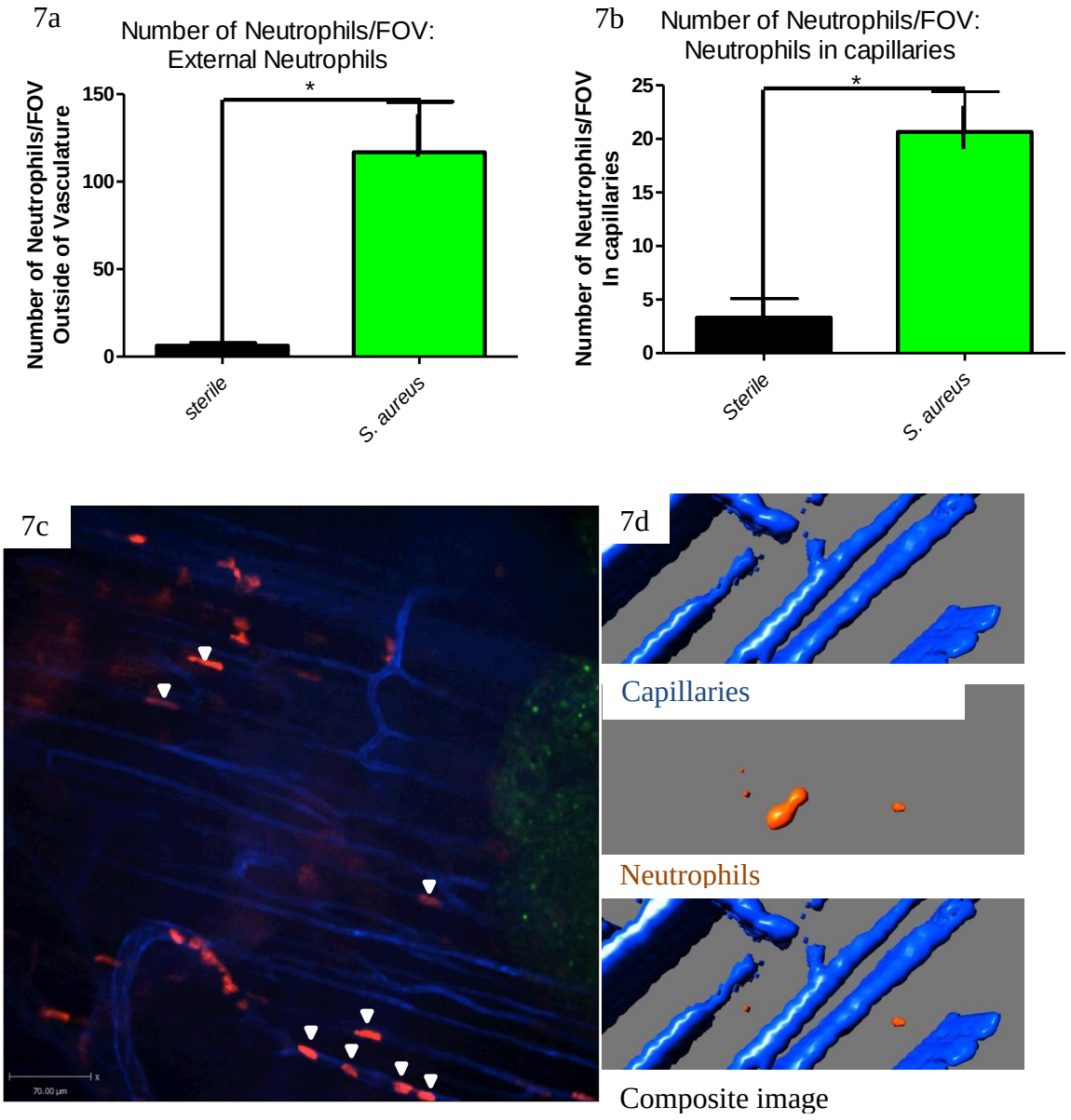

Figure 7: Neutrophil recruitment to capillaries during *S. aureus* infection

7a: The numbers of neutrophils external to any vascular bed were quantified per FOV at 4x magnification, 2 hours after insertion of the bead into skin tissue. N=3 independent experiments for sterile beads, and 4 independent experiments for *S. aureus*. Each independent experiment

consisted of neutrophils numbers from a single 4x FOV around an agarose bead. 7b: The number of neutrophils in the capillaries was quantified per FOV, at 4x magnification after insertion of the bead into the skin tissue. 7c: Image of neutrophil recruitment to the capillary microvasculature, taken at 10x magnification. In red are the neutrophils, in green is the *S. aureus* bead, and in blue is the vasculature. White arrows indicate the location of neutrophils in the capillary microvasculature. 7d: 3D reconstruction of a capillary with a neutrophil inside it. Neutrophils are in orange, the capillaries in blue. The upper panel shows the capillaries alone, without any neutrophils. The middle panel shows a neutrophil without any capillaries. The bottom panel shows the overlap of the red and blue channels, with the orange neutrophil inside the blue capillary, and thus not visible. $*p<0.05$

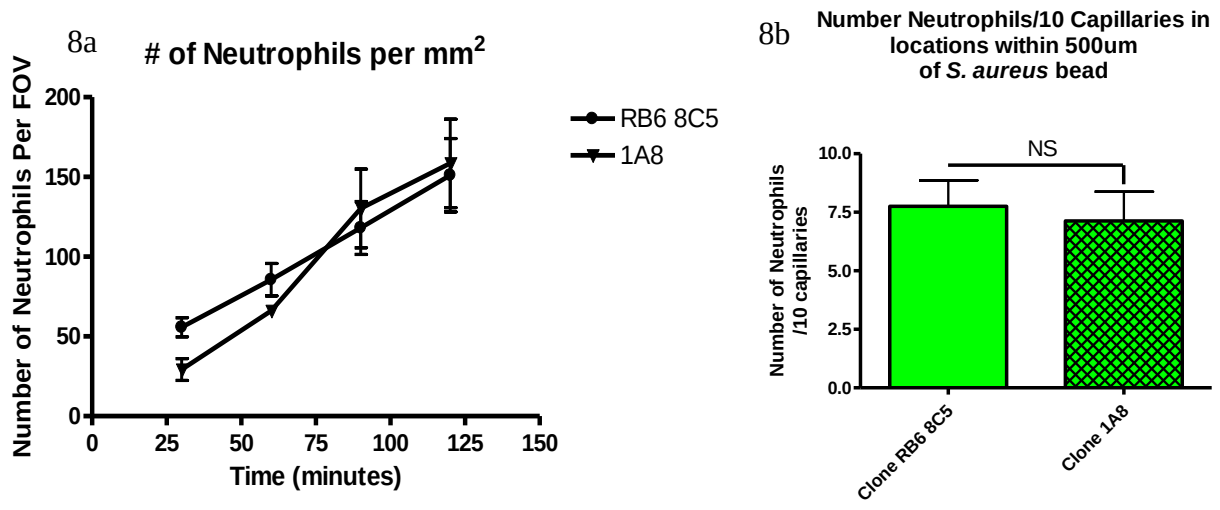

Figure 8: Comparison of the recruitment of cells labelled by the anti-Ly6g antibody clones RB6 8C5 and 1A8.

Mice were treated with 10µl at 0.2mg/ml of either antibody conjugated to PE, as well as 10µl at 1.0mg/ml anti-CD31 conjugated to Alexa647, IV. 8a: Overall recruitment of cells labelled with either RB6 8C5 or 1A8The number of neutrophils was quantified at 30, 60, 90 and 120 minutes post-insertion of the bead into the skin tissue. The 0 timepoint was not quantified, as the amount of time needed to place the mouse on the scope varied from one experiment to the next. 8b: Overall recruitment of neutrophils to the capillaries over ten minutes after labelling with either anti-Ly6g antibody clone RB6 8C5 or anti-Ly6g antibody clone 1A8 control antibodies. Differences between the clones were non-significant at $p<0.05$, which indicates that the majority of cells being recruited to the bead and crawling in the capillaries are neutrophils, and not monocytes. N=11 independent experiments for the anti-Ly6g antibody clone RB6 8C5 and 4 independent experiments for the anti-Ly6g antibody clone 1A8. Independent experiments consisted of one 4x magnified FOV for figure 8a and four or more 10x magnified FOV's (averaged) for figure 8b. In 10x FOVs, the number of neutrophils per 10 capillaries was

averaged. Neutrophils were quantified as “recruited” if they remained in the FOV for ≥30 seconds during a ten minute 10x magnification video of the region within 500μm of the bead.

9a

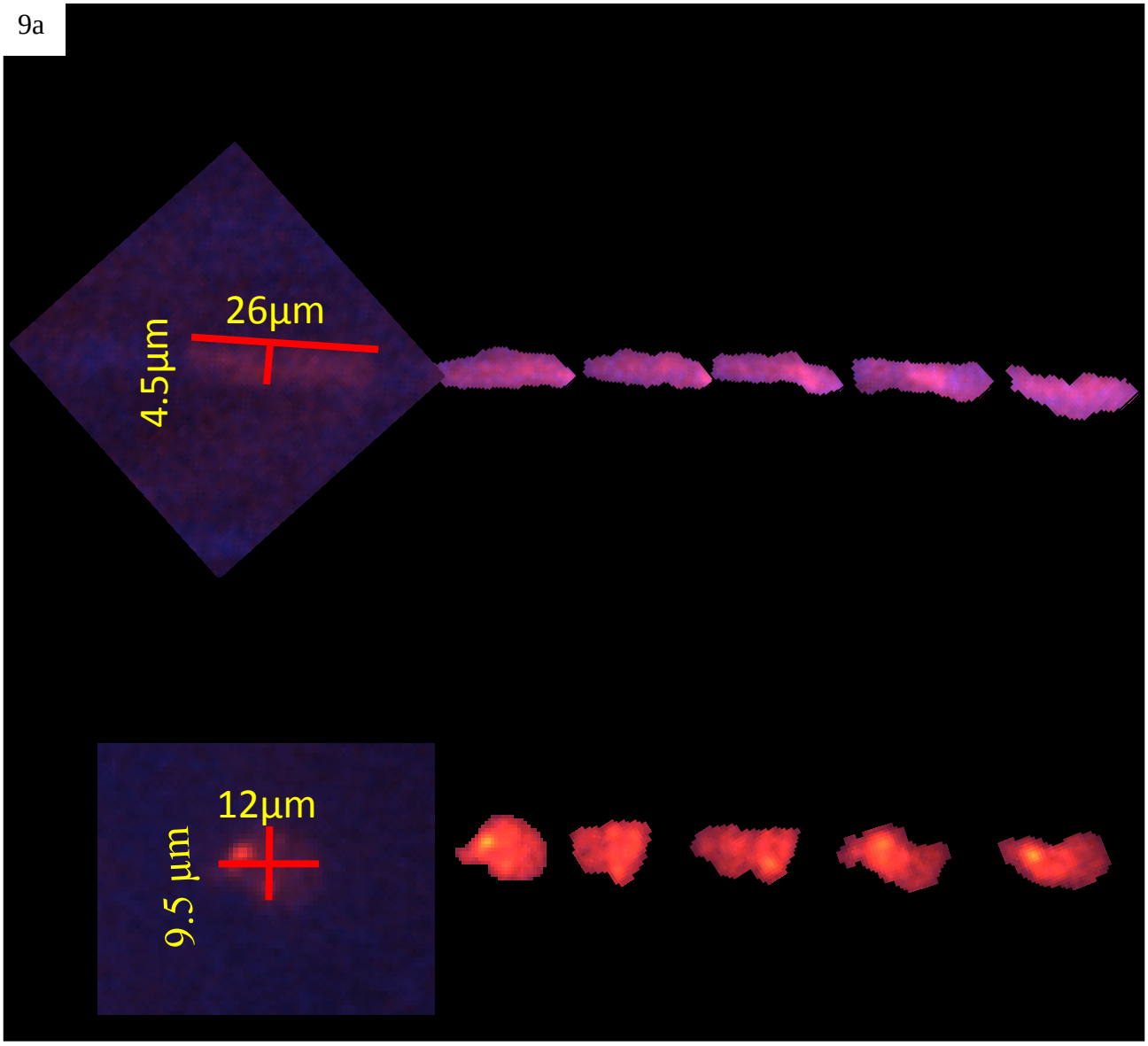
26µm
4.5µm
12µm
9.5 µm

9b

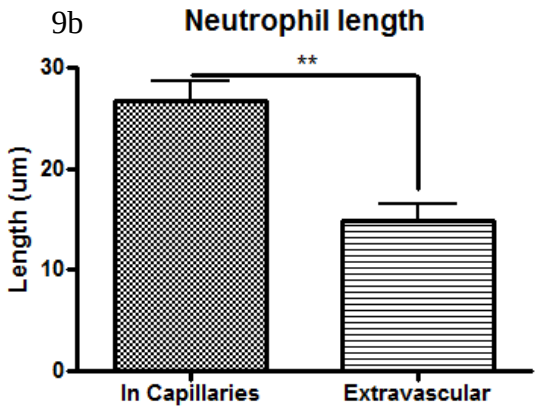
Neutrophil length
**
Length (um)
30
20
10
0
In Capillaries
Extravascular

9c

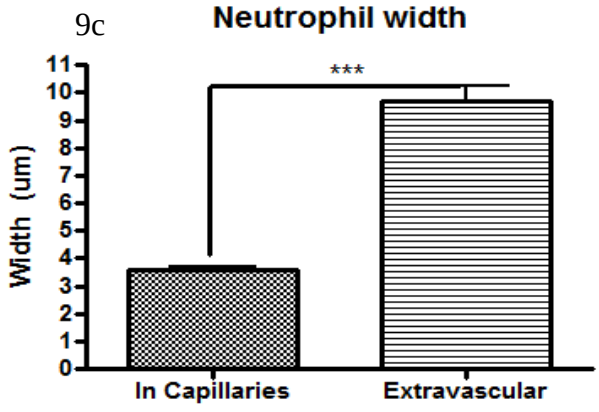
Neutrophil width
***
Width (um)
11
10
9
8
7
6
5
4
3
2
1
0
In Capillaries
Extravascular

Figure 9: Differences in neutrophil shape when in capillaries

10 minutes videos were taken at 10x magnification. Neutrophils were quantified by averaging the maximum length and width from measurements taken every 2 minutes during the 10 minute video. Approximately 10 neutrophils were quantified per independent experiment within a single 10x FOV (approximately 500μm^2). N=3 independent experiments. 9a: Images of neutrophils crawling during ten-minute videos, either outside of the vasculature or inside the capillaries. 9b: The length (in μm) of neutrophils in the capillary microvasculature or external to the vasculature. 9c: The width (in μm) of neutrophils external to the vasculature. $^{**}p<0.01$, $^{***}p<0.001$.

As neutrophils were recruited to the capillaries, we examined their behaviour. We initially sought to characterize behaviours at each step of the leukocyte recruitment cascade: rolling, adherence, crawling, and emigration. However, we saw no neutrophils in the subcutaneous capillaries of the skin rolling or emigrating from the capillaries during any experimental conditions, controls, or antibody treatments. Therefore, we focused exclusively on neutrophil adherence and crawling. There were very few neutrophils in the capillaries in basal conditions (Figure 7). In contrast, in mice that have been given *S. aureus* beads, there were significantly elevated numbers of neutrophils in the capillaries, compared with mice given sterile beads. The majority of these neutrophils within the capillaries were crawling within the vasculature (Figure 10). This observation was made using both the anti-Ly6g antibody clone RB6-8C5 and the anti-Ly6g antibody clone 1A8.

As a final control, we questioned whether these responses were specific to the USA300 strain of *S. aureus*. We tested another strain of bacteria of *S. aureus* (strain ATCC25923, Figure 11) in our model, using beads containing the bacteria as well as fluorescent microspheres used in the sterile control experiments. This strain showed no significant differences in recruitment of neutrophils to the bead per FOV, and no significant differences in recruitment of neutrophils to the capillaries from MRSA (p=0.3683), demonstrating that this response is not exclusive to the strain USA300.

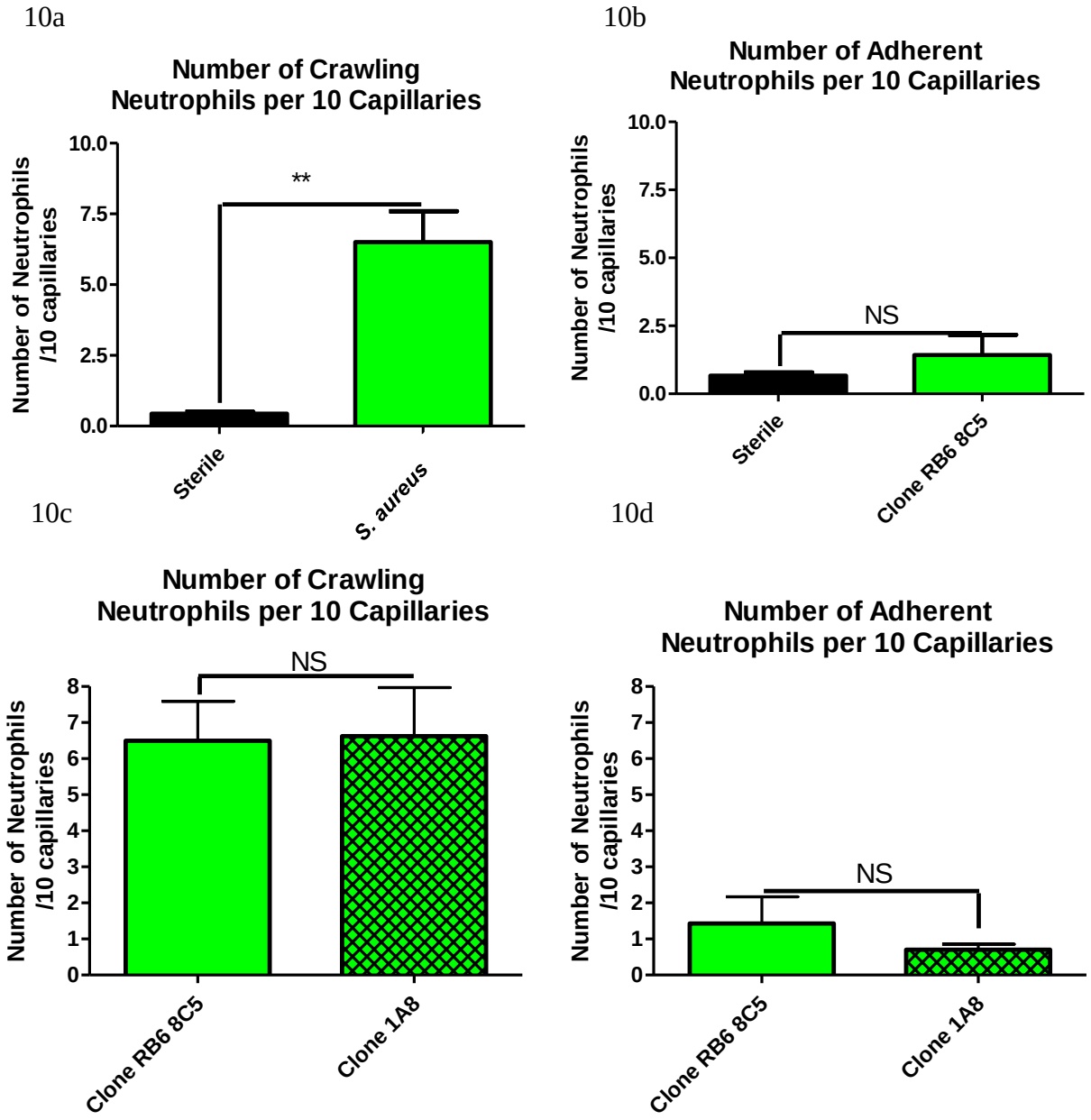

Figure 10: Behaviours of neutrophils within the capillaries

Neutrophil numbers were normalized for every 10 capillaries. The number of neutrophils was determined from approximately 4 fields of view per mouse imaged. Neutrophils were labelled with the anti-Ly6g antibody RB6 8C5 in figures 10a and 10b. 10a: Number of crawling

neutrophils. Neutrophils were determined to be crawling if they moved within the capillary microvasculature, and remained in the FOV for 30 or more seconds. 10b: Number of adherent neutrophils. Neutrophils were quantified as adherent if they stayed in a single location for 30 or more seconds, and did not move from that location during the duration of the video. N=3 independent experiments for sterile beads, 6 independent experiments for *S. aureus* beads. Each independent experiment consisted of collecting data from 4 or more 10x FOVs and averaging the results. 10c: Comparison of the number of crawling cells identified using the anti-Ly6g antibody clone RB6 8C5 and the anti-Ly6g antibody clone 1A8. 10d: Comparison of the number of adherent cells identified using the anti-Ly6g antibody clone RB6 8C5 and the anti-Ly6g antibody clone 1A8. Differences between the clones were non-significant at $p<0.05$, which indicates that the majority of cells being recruited to the bead and crawling in the capillaries are neutrophils, and not monocytes. N=6 independent experiments for the anti-Ly6g antibody clone RB6 8C5 and 4 independent experiments for the anti-Ly6g antibody clone 1A8. ** $p<0.01$

11a

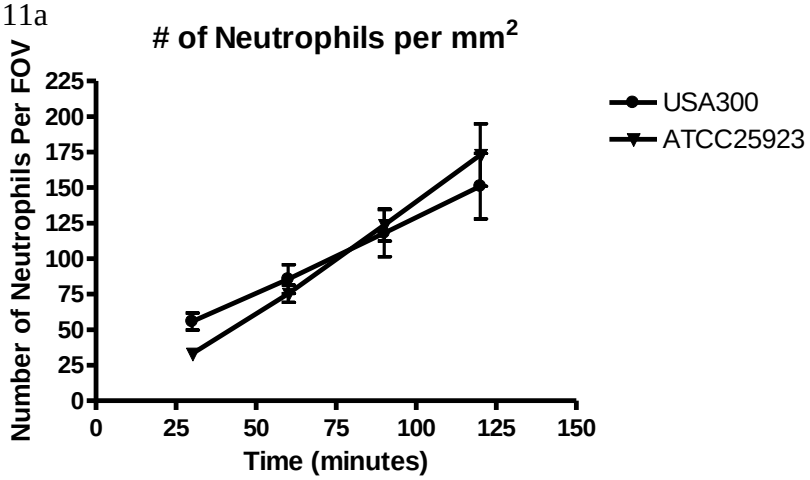

11b

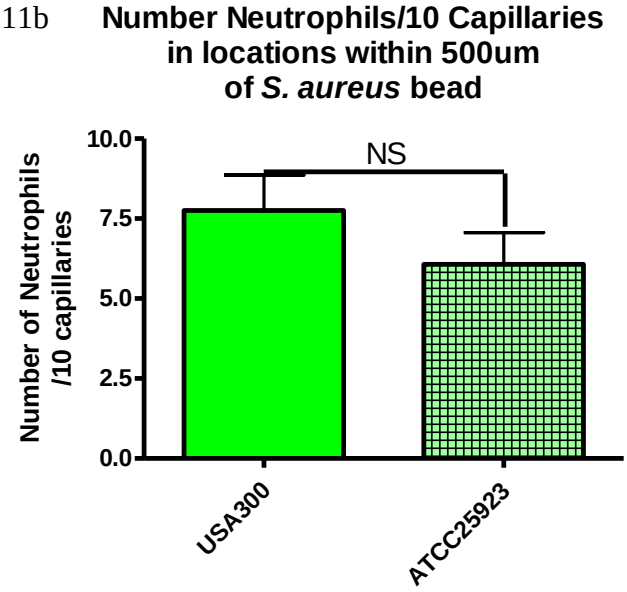

Figure 11: Recruitment of neutrophils to a bead containing *S. aureus* of either the strain, USA300 or the strain ATCC25923

11a: The number of neutrophils per FOV at a 4x magnification was quantified at the 30, 60, 90 and 120 minute time points for both the strain USA300 and the strain ATCC25923. N=11 for USA300 and N=3 for ATCC25923. 11b: The number of neutrophils quantified at 10x FOV and

then normalized per 10 capillaries. Only neutrophils that remained in the FOV for 30 seconds or more were quantified. N=5 independent experiments for USA300 and 3 independent experiments for ATCC25923. Each individual experiment consisted of collecting data from one 4x FOV of view, and collecting data from 4 or more 10x FOVs and averaging the results.

To summarize, we designed and tested a model for recruiting neutrophils to a nidus of *S. aureus* infection. We determined the number of CFUs being used in this infection model, and then began to investigate the behaviour of the neutrophils in this model. We saw an increase of neutrophil recruitment in response to the *S. aureus* infection, and also saw an increase in neutrophil recruitment to the capillaries near the bead, when compared with sterile beads. We then examined the capillary neutrophils in more depth, showing changes in the shape of these neutrophils, as well as the performance of specific components of the leukocyte recruitment cascade, namely crawling and adhesion, but not rolling or emigration. Finally, we also determined that this behaviour was not specific for the strain in use, USA300, as another strain of *S. aureus* (ATCC25923) could also induce this behaviour in neutrophils.

Chapter Four: Molecular Mechanisms of Neutrophil Recruitment to the Capillaries

4.1 Introduction: integrins and their role in neutrophil adhesion and crawling

As neutrophils within the capillaries underwent only two of the steps of the leukocyte recruitment cascade (crawling and adhesion), we decided to investigate what molecules could be involved in this behaviour in greater detail. Given that firm adhesion and crawling of neutrophils are mediated by integrins in the venules (71), we postulated that integrins are important in the recruitment of neutrophils to the capillaries of the skin.

4.1.1 Integrin function: overview

Integrins are heterodimeric transmembrane molecules consisting of α and β subunits, which can bind molecules found either in the extracellular milieu or on other cells. They are involved in a wide range of biological processes, ranging from tissue morphogenesis (130) to immunocyte recruitment (64, 75). Integrins are particularly important for cell-to-cell and cell-to-extracellular matrix component binding and are often found in an inactive state, in which the α and β subunits are bound together by a salt bridge. This interaction prevents exposure of the extracellular binding region, thus preventing interactions with ligand receptors (130). During leukocyte recruitment, cellular interactions with chemokines or selectins alter this inactive state, triggering integrins to assume their active conformation (67, 131). Cytokines induce selectin-based neutrophil rolling that leads to the recruitment of important intermediates, such as Talin1 and kindlin-3, which alter the structure of the integrin to a high affinity active form, exposing the binding region to the extracellular milieu (67, 69, 70). The now-active integrin interacts with extracellular ligand receptors, such as the ICAMs or fibronectin, resulting in downstream cellular

signalling that is necessary for firm adhesion and actin rearrangement within the cell (131). In neutrophils, this "outside in" signalling also induces ROS production and degranulation (131).

There are at least 24 distinct integrin heterodimers described in the literature (132). We focused our studies on integrins specific to neutrophils that play roles in adhesion and crawling. We targeted the β_2 integrins lymphocyte function antigen 1 (LFA-1) and macrophage 1 antigen (Mac-1) as well as the β_1 integrin, very late leukocyte antigen 4 (VLA-4).

4.1.2 Lymphocyte function-associated antigen (LFA-1)

Firm adhesion of neutrophils in the peripheral venules is mediated by the integrin LFA-1(71). This integrin can be found in an inactive, active, or intermediate activity state, whereby the integrin is extended but the headpiece of the molecule containing the ligand receptor binding region is not fully exposed to the external environment (67). LFA-1 binds to the ICAMs to mediate cell-cell adhesion (131). Following activation, LFA-1 induces downstream signalling through the Src family kinases (133), which are important for ROS production and degranulation in neutrophils (134, 135).

4.1.3 Macrophage 1 antigen (Mac-1)

Although the signalling pathways of Mac-1 are similar to those involved in LFA-1, Mac-1 plays a different role in neutrophils. Mac-1 is primarily involved in the intravascular crawling of neutrophils during recruitment (71). This integrin is critical for crawling; when Mac-1 is blocked, neutrophils do not crawl within the peripheral post-capillary venules (71). Crawling can occur either with or against blood flow, and allows for neutrophils to migrate to regions

where they may emigrate more easily. Interaction of Mac1 with a ligand receptor results in activation and can lead to actin reorganization. In addition to ICAM-1 and ICAM-2, Mac1 can bind to many other molecules, such as fibronectin, the coagulation cascade factor X and complement cascade factor C3b (131). Mac-1 can also interact with virulence factors from *S. aureus* such as LukAB (136).

It is difficult to distinguish differences between LFA1 and Mac-1 in terms of downstream signalling following "outside in" signalling. Many molecules, such as the Src family kinases, have been found to be activated downstream of both integrins (135). This suggests that common pathways found for LFA-1 are also important in Mac-1 integrin interactions, possibly because Mac1 shares a common β subunit with LFA-1 and has common ligand receptors, such as ICAM-1 and ICAM-2 (131). However, some studies have demonstrated differences in activation of these two β_2 integrins; for instance, Li et al found that Mac 1 and LFA1 had different binding affinities for ICAM-1, particularly at intermediate activations states (137), and Jakob et al. found that the molecule hematopoietic progenitor kinase 1 (HPK1) was important for LFA-1 activation and function, but not for Mac-1 (138). It is likely that these integrins are activated through overlapping but not entirely homologous pathways, due to the different but closely related roles these molecules play during the neutrophil recruitment cascade. Due to the complex roles that LFA-1 and Mac-1 play in neutrophil recruitment from the post-capillary venules, we decided to block these molecules individually (via antibodies targeting the differing α subunits of these integrins) as well as together (via antibodies targeting the common β subunit).

4.1.4 Very late antigen-4 (VLA-4)

Another integrin we decided to investigate was VLA-4. VLA-4, or $\alpha_4\beta_1$, is believed to have a distinct signalling pathway from both LFA-1 and Mac1. This may be partly due to the structural differences of this integrin when compared to LFA-1 and Mac-1; VLA-4 possesses both a different α and β subunit than either of the latter integrins, and therefore belongs to a different family of integrins (the β_1 family rather than the β_2 group to which LFA-1 and Mac-1 belong) (131). Many parts of the VLA-4 signalling pathway are not well described. It is known that VLA-4 plays a role in neutrophil recruitment to specific tissues, such as the lung (72). It is also known that VLA-4 may play a role in some types of infections, such as sepsis (73). VLA-4 may also be constitutively expressed on murine neutrophils (139), though this is controversial. There are several ligand receptors that VLA-4 can bind to, such as vascular cell adhesion molecule (or VCAM-1), fibronectin and junctional adhesion molecule B (or JAM-B) (140). The result of this molecular binding involves activation and respiratory burst, mediated by Src family kinases such as fgr, lyn and hck (139). Since $\alpha_4\beta_1$ is involved in neutrophil activation and may play important roles in some infections, we decided to examine its role in the vascular bed during *S. aureus* infection.

4.2 Blocking recruitment of neutrophils to the capillaries

4.2.1 Blocking molecules on the neutrophil

As neutrophils were either adhering or crawling within the capillaries (Figure 9, Chapter 3), we decided to focus our preliminary experiments on the integrins described above. All

experiments conducted in this chapter involve blocking antibodies administered two hours post infection. This ensured that preliminary recruitment of neutrophils occurred normally and we would only be influencing the behaviour of the neutrophils after they had been recruited, and would thus limit the effects the blocking antibodies had on the initial recruitment of neutrophils to the *S. aureus* bead.

Initially, we blocked the function of both LFA-1 and Mac-1 using an antibody targeting the β_2 subunit (CD18) found in both of these integrins, two hours after infection. When we administered the anti-CD18 antibody, we observed a significant reduction in the number of neutrophils recruited to the capillaries, compared with administration of an IgG1isotype control (Figure 12a). The majority of the remaining neutrophils that were visible within the capillaries were crawling (Figure 12b), with no change in the number of adherent neutrophils (Figure 12c).

Having established that the β_2 integrins play significant roles in neutrophil crawling in the capillaries, we examined whether blocking specifically Mac-1 or LFA-1, two important β_2 integrins found on the neutrophil, could significantly change the recruitment or behaviour of the neutrophils. Initially we targeted Mac-1, as the majority of the neutrophils seen in the capillary microvasculature were crawling. Since Mac-1 is important in venular crawling, we targeted it to reduce neutrophil recruitment to the capillary microvasculature. Surprisingly, there were no significant changes in neutrophil recruitment to this vascular bed with administration of anti-CD11b antibodies (p=0.6249 when compared with isotype controls), which block Mac-1 binding (Figure 13a). There were also no significant changes in behaviour, either in terms of crawling or adhesion (p=0.8401, Figure 13b, and p=0.1425, Figure 13c, respectively), of neutrophils treated with Mac-1 blocking antibodies, when compared with isotype controls.

12a

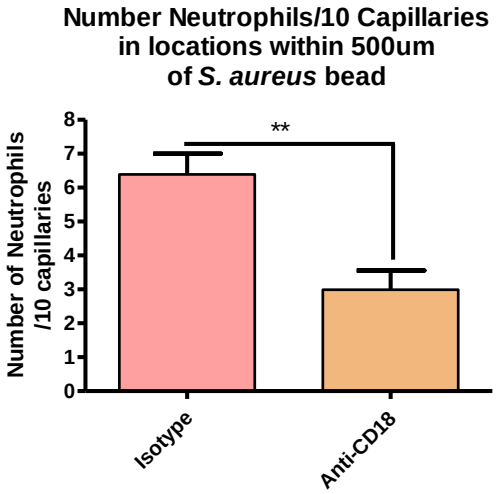

12b

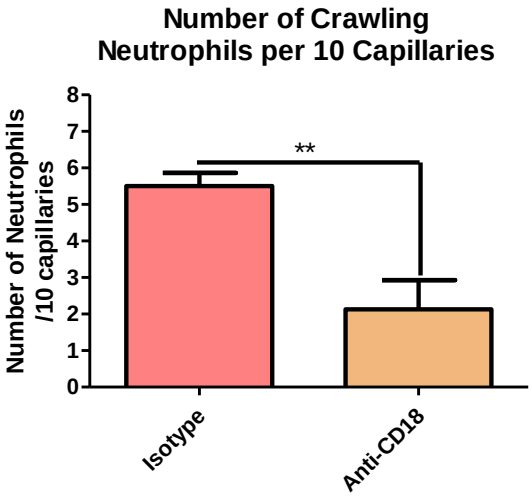

12c

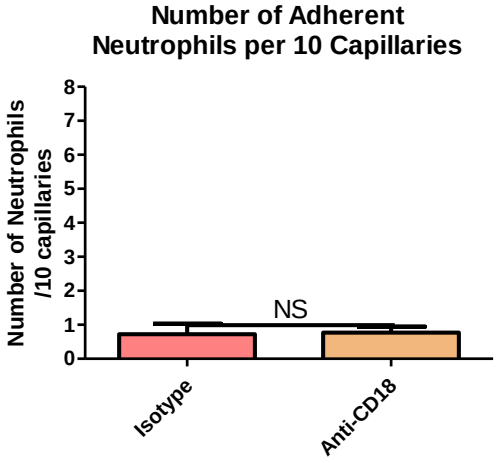

Figure 12: The role of CD18 in mediating neutrophil recruitment in the capillaries

Two hours after the bead had been inserted into the subcutaneous dorsal skin of C5BL6 mice, 30 µg of monoclonal IgG1 anti-CD18 blocking antibodies, or isotype control antibodies were injected intravenously. Multiple videos per mouse were imaged for 10 minutes at 10x magnification, and the number of neutrophils as well as their behaviours within the capillaries was quantified 12a: Overall recruitment of neutrophils to the capillaries over ten minutes after treatment with either anti-CD18 antibodies or isotype control antibodies. Multiple 10x FOVs

were then imaged per mouse for 10 minutes, and the total number of neutrophils within the capillaries was quantified. 12b: Number of crawling neutrophil in the capillaries. 12c: Number of adherent neutrophils in the capillaries. A neutrophil was identified as adherent if it remained in the same location for 30 seconds, and was quantified as crawling if it moved, but remained within the FOV for 30 seconds or more. N=3 independent experiments for mice given anti-CD18 antibodies, and 4 independent experiments for mice given isotype control antibodies. Each experiment consisted of collecting data from 4 or more 10x FOVs from a single mouse and averaging the results. ** $p<0.01$.

13a

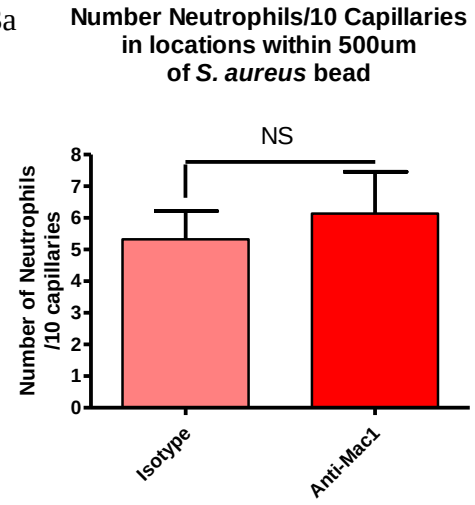

13b

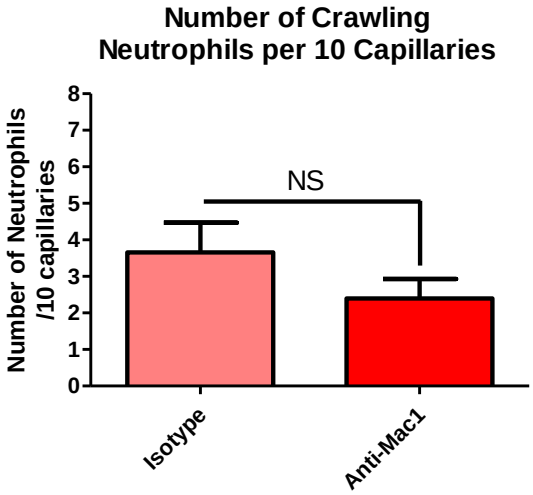

13c

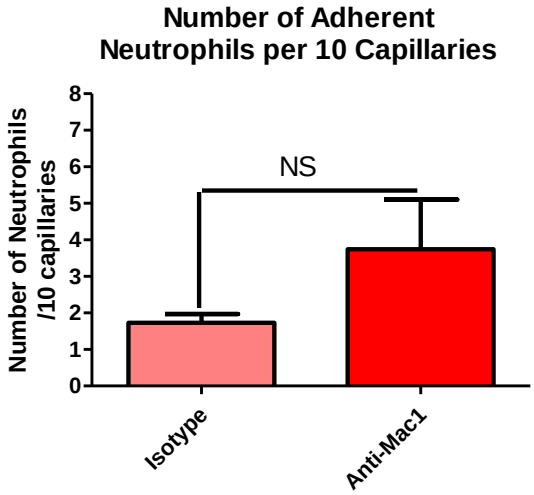

Figure 13: Neutrophil behaviour following treatment of mice with anti-CD11b blocking antibodies

Mice were treated with 30μg of blocking antibodies or IgG2b isotype controls 2 hours following infection. Multiple videos per mouse were imaged for 10minutes at 10x magnification, and the number of neutrophils as well as their behaviours within the capillaries was quantified. 13a: Overall recruitment of neutrophils to the capillaries over ten minutes after treatment with either anti-Mac 1 antibodies or isotype control antibodies. 13b: Number of crawling cells recruited to the capillaries following treatment with anti-Mac-1 antibodies or isotype control antibodies. 13c:

Number of adherent cells following treatment with anti-Mac-1 antibodies or isotype control antibodies. N=5 independent experiments for Mac-1 and for isotype control experiments. Each experiment consisted of collecting data from 4 or more 10x FOVs from a single mouse and averaging the results.

We then targeted LFA-1. Administration of blocking antibodies targeted towards LFA-1 resulted in no reduction in neutrophil recruitment ($p = 0.10$, Figure 14a). Nonetheless, administration of antibodies blocking LFA-1 caused significant changes in neutrophil behaviour, drastically decreasing the number of neutrophils that were crawling within the capillaries ($p<0.001$, Figure 14b), although there was no significant change in the number of adherent cells ($p=0.1859$, Figure 14c).

The drop in recruitment we observed following the blocking of CD18 did not result in a complete absence of neutrophils being recruited to the capillaries. While there was a significant reduction in neutrophil recruitment, there were still neutrophils recruited to the capillaries when anti-CD18 antibodies were administered. The reduction in neutrophil recruitment was approximately 50% of the neutrophil recruitment seen with isotype controls. This suggested that another molecule may have been involved. We therefore set out to examine other integrins that might be involved in this behaviour. We targeted the integrin VLA-4, by administering anti-α_4 blocking antibodies into the system 2 hours following infection. This resulted in a significant drop in neutrophil recruitment to the capillaries (Figure 15a). This recruitment was roughly equivalent to the drop in neutrophil recruitment seen in the administration of anti-CD18 antibodies, approximately 50% ($p=0.0341$). It is important to note that this behaviour did not correspond to any differences in the number of crawling cells ($p=0.1807$, Figure 15b), but did correspond with a significantly reduced number of adhering cells ($p=0.0210$, Figure 15c) in the capillary microvasculature.

14a

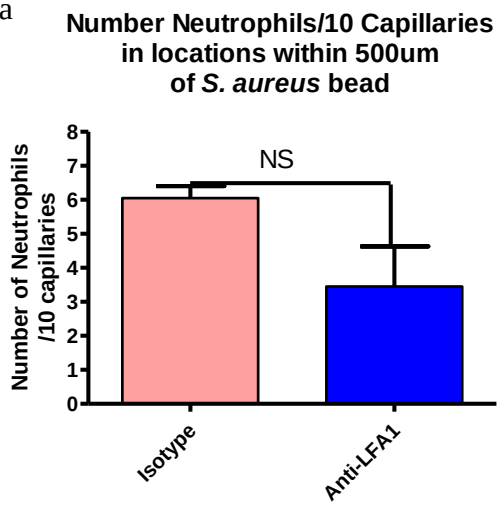

14b

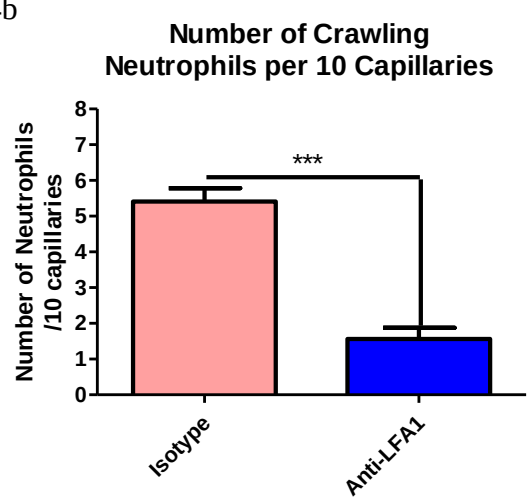

14c

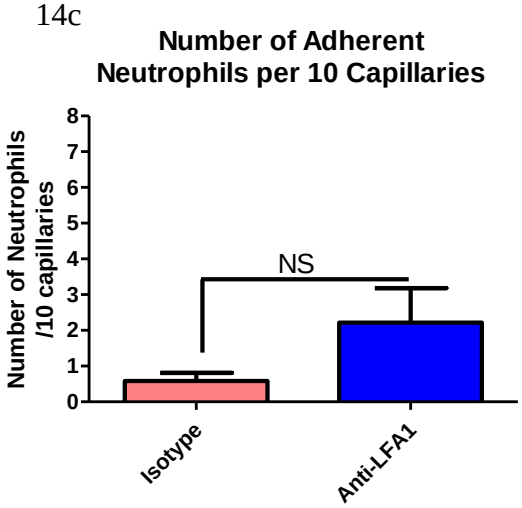

Figure 14: Neutrophil behaviour following treatment of mice with anti-CD11a blocking antibodies

Mice were treated with 30µg of blocking antibodies or IgG2a isotype controls 2 hours following infection. Multiple videos per mouse were imaged for 10 minutes at 10x magnification, and the number of neutrophils as well as their behaviours within the capillaries was quantified. 14a: overall recruitment of neutrophils to the capillaries over ten minutes after treatment with either anti-LFA1 antibodies or isotype control antibodies. 14b: number of crawling cells recruited to the capillaries following treatment with anti-LFA-1 antibodies or

isotype control antibodies. 14c: number of adherent cells following treatment with anti-LFA-1 antibodies or isotype control antibodies. N=5 independent experiments for mice treated with LFA-1 blocking antibodies and 4 independent experiments for isotype controls. Each experiment consisted of collecting data from 4 or more 10x FOVs from a single mouse and averaging the results. *** $p<0.001$

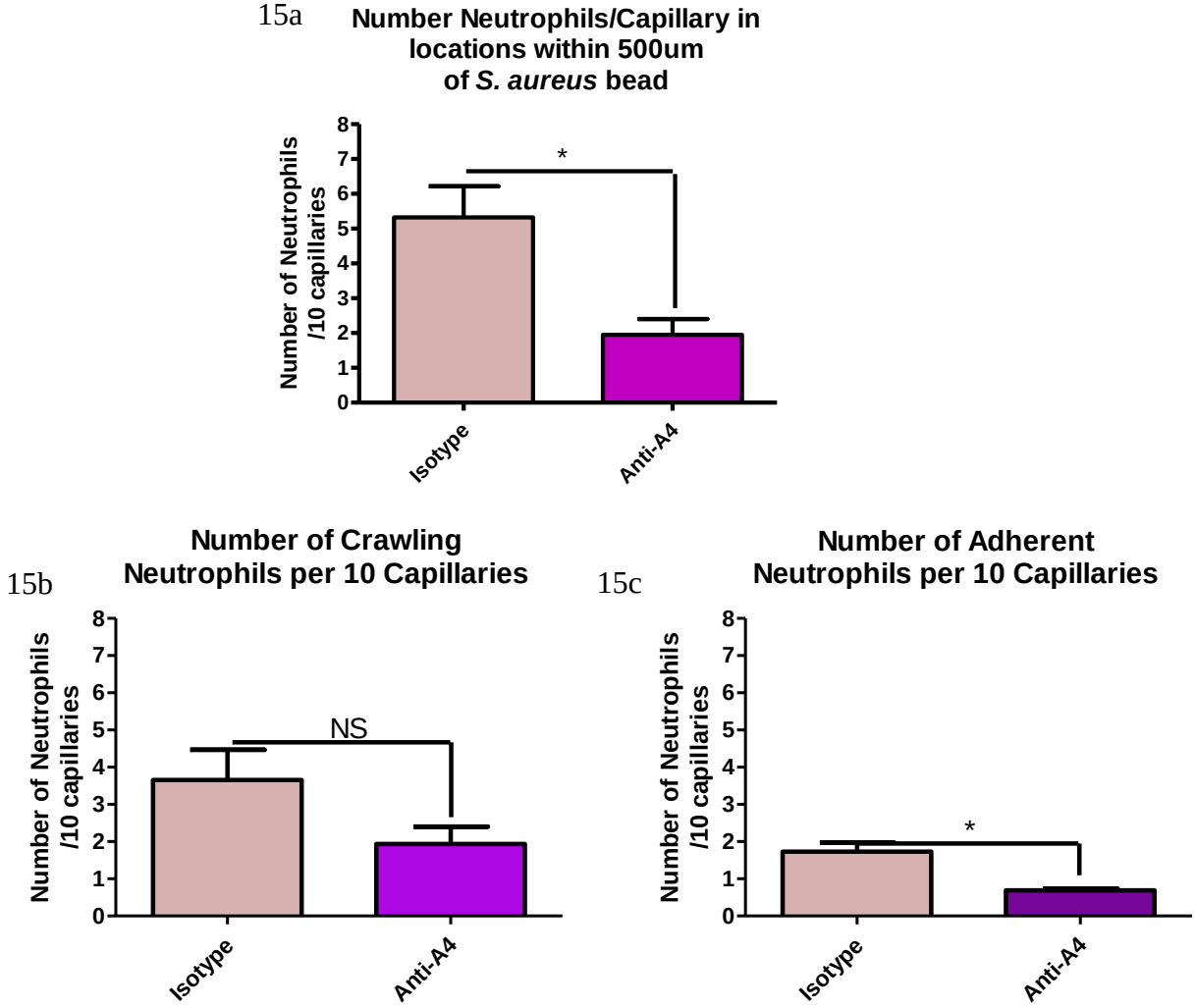

Figure 15: Neutrophil behaviour following treatment of mice with anti-α_4 blocking antibodies

Mice were treated with 50 µg of blocking antibodies or IgG2b isotype control antibodies 2 hours following infection. Multiple videos per mouse were imaged for 10minutes at 10x magnification, and the number of neutrophils as well as their behaviours within the capillaries was quantified. 15a: Overall recruitment of neutrophils to the capillaries over ten minutes after treatment with either anti-α_4 antibodies or isotype control antibodies. 15b: Number of crawling cells recruited to the capillaries following treatment with anti-α_4 antibodies or isotype control

antibodies. 15c: Number of adherent cells following treatment with anti- α_4 antibodies or isotype control antibodies. N=3 independent experiments for α_4 blocking antibodies, and 5 independent experiments for isotype control treatment. Each experiment consisted of collecting data from 4 or more 10x FOVs from a single mouse and averaging the results. * $p<0.05$.

Our next goal was to examine whether blocking both VLA-4 (via anti-α_4 antibodies) and the β_2 integrins (via anti-CD18 antibodies) had additive effects on the recruitment of neutrophils to the capillaries. We administered both anti-CD18 antibodies and anti-α_4 antibodies together. Interestingly, we saw a complete absence of neutrophil recruitment to the capillaries (Figure 16a). This complete absence corresponded to significant reductions in crawling when compared with CD18 isotype antibodies ($p<0.0001$, Figure 16b), and significant reduction in the number of both crawling and adhering neutrophils when compared with isotype control antibodies for anti-α_4 ($p=0.0183$ for crawling, Figure 16b, and $p=0.0218$ for adherence, Figure 16c).

4.2.2 *Blocking molecules on the endothelium*

We then sought to determine which ligand receptors these integrins were binding to in the capillaries. As described above, there are many potential ligand receptors that can bind to both Mac-1 and LFA-1. VLA-4 also has several ligand receptors that it can bind to in order to induce activation. However, we decided to focus on molecules that have been shown in the literature to be expressed in some skin endothelial cells following stimulation. Our primary targets were the molecules ICAM-1 and VCAM-1. We focus on these molecules because they are known to be expressed on endothelial cells, and have been shown to be upregulated on endothelial cells *in vitro* after stimulation with components of the *S. aureus* cell wall (141). Furthermore, VCAM-1 expression has been shown to occur in the deep vascular plexus, a layer of vessels which drains into the SC (142). We conducted preliminary experiments to determine whether ICAM-1 was expressed on the endothelium in the capillaries, showing that both ICAM-1 and VCAM-1 were expressed in the capillaries 2 hours after infection (Figures 17 and 18).

16a

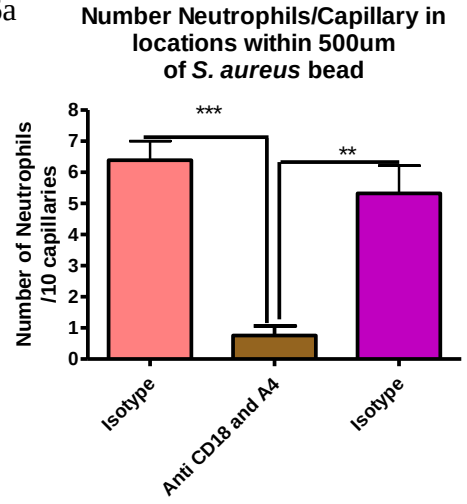

16b

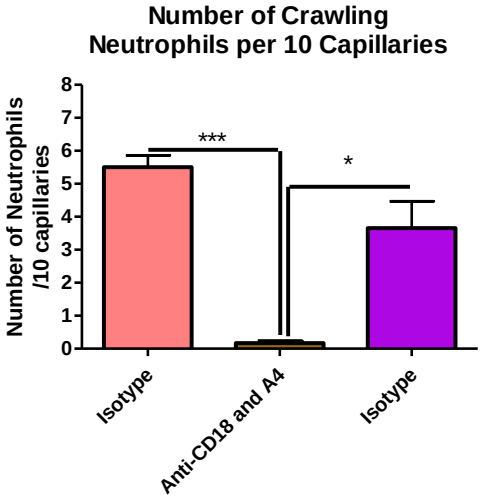

16c

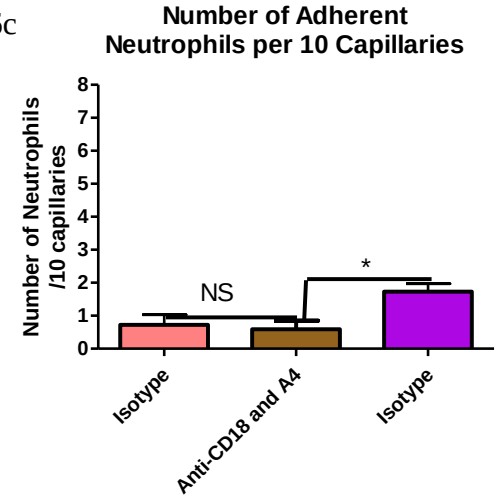

Figure 16: Neutrophil behaviour following treatment of mice with anti CD18 and anti-α_4 blocking antibodies

Mice were treated with blocking antibodies or a cocktail of IgG1 and IgG2b isotype controls 2 hours following infection. Multiple videos per mouse were imaged for 10minutes at 10x magnification, and the number of neutrophils as well as their behaviours within the capillaries was quantified. 16a: Overall recruitment of neutrophils to the capillaries over ten minutes after treatment with either CD18 and anti-α_4 antibodies or isotype control antibodies for both of those

conditions. 16b: Number of crawling cells recruited to the capillaries following treatment with anti CD18 and anti-α_4 antibodies or isotype control antibodies. 16c: Number of adherent cells following treatment with anti-CD18 and anti- α_4 antibodies or isotype control antibodies. N=3 independent experiments for dual block and 4 for the isotype controls. Each experiment consisted of collecting data from 4 or more 10x FOVs from a single mouse and averaging the results. ** $p<0.01$, *** $p<0.001$.

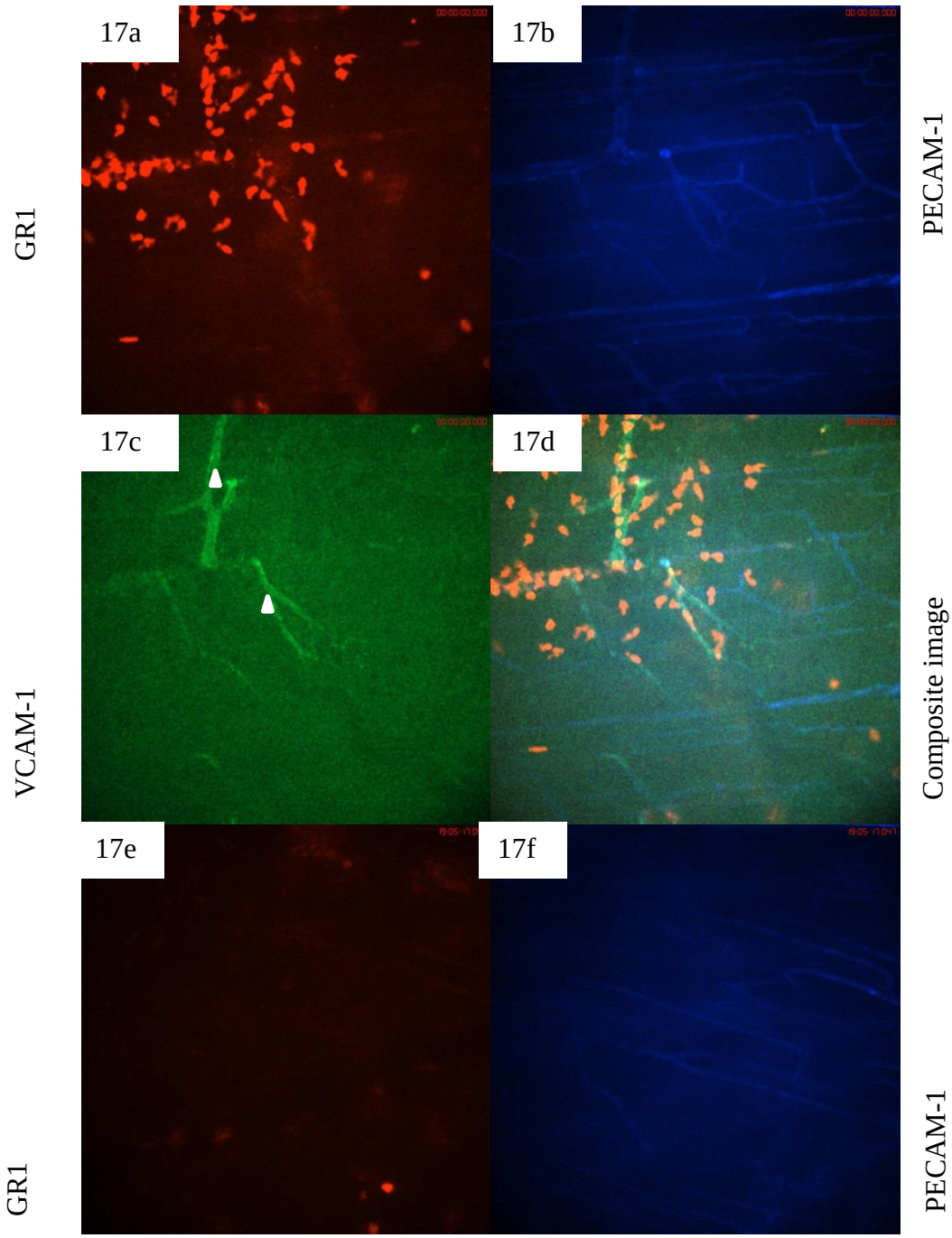
17a
17b
17c
17d
17e
17f
GR1
PECAM-1
VCAM-1
Composite image
GR1
PECAM-1

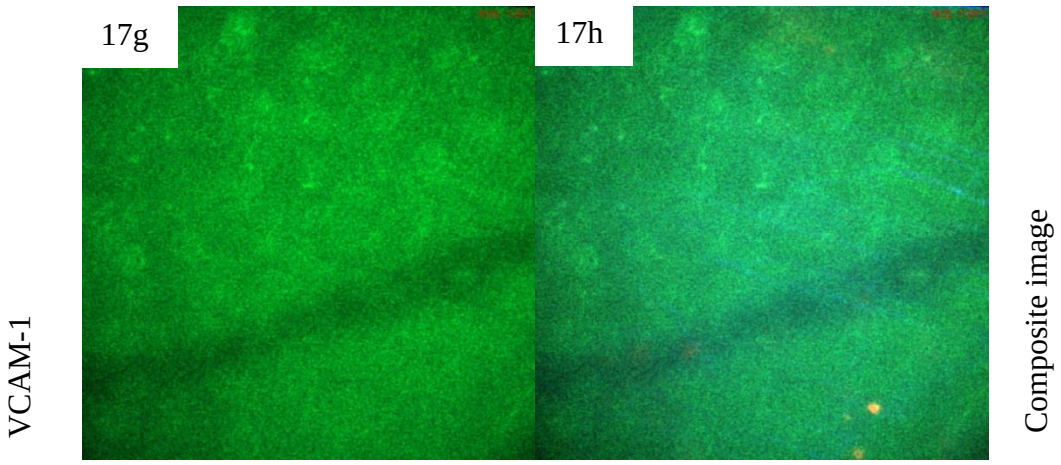

Figure 17: Expression of VCAM-1 in the microvasculature 2-3 hours post bead infection

Mice were infected with a GFP-expressing *S. aureus* bead and treated with 10µl at 0.2mg/ml anti-Ly6g (clone 1A8) conjugated to PE as well as 10µl 1.0mg/ml CD31 conjugated to Alexa647 IV. After ~2.5 hours of imaging, mice were also treated with 20µl of anti-VCAM-1 at 0.5 mg/ml conjugated to FITC. Additionally, control experiments were also performed, where mice were anesthetized and treated with control microsphere containing beads as well as 10µl at 0.2mg/ml anti-Ly6g (clone 1A8) conjugated to PE and 10µl 1.0mg/ml CD31 conjugated to Alexa647 IV. The skin tissue was then exteriorized, and images of the tissue where taken. 17a: Neutrophil recruitment to the microvasculature at 10x magnification within 500µm of a *S. aureus* bead. 17b: Expression of CD31 on the microvasculature. 17c: Expression of VCAM-1 on the microvasculature. VCAM-1 expressing vessels are denoted by white arrowheads 17d: Composite image. Images 17a-17d are representative of 3 independent experiments. Figure 17e: Neutrophil recruitment in the microvasculature within 500µm of the sterile bead. 17f: expression of CD31 on the microvasculature of a mouse given sterile beads. Figure 17g: expression of VCAM-1 in the sterile bead treated mouse. Figure 17h: composite image. The

uniform staining is indicative of an absence of VCAM-1, as auto contrast was used in all experiments. Images 17e-17h are representative of 2 independent experiments.

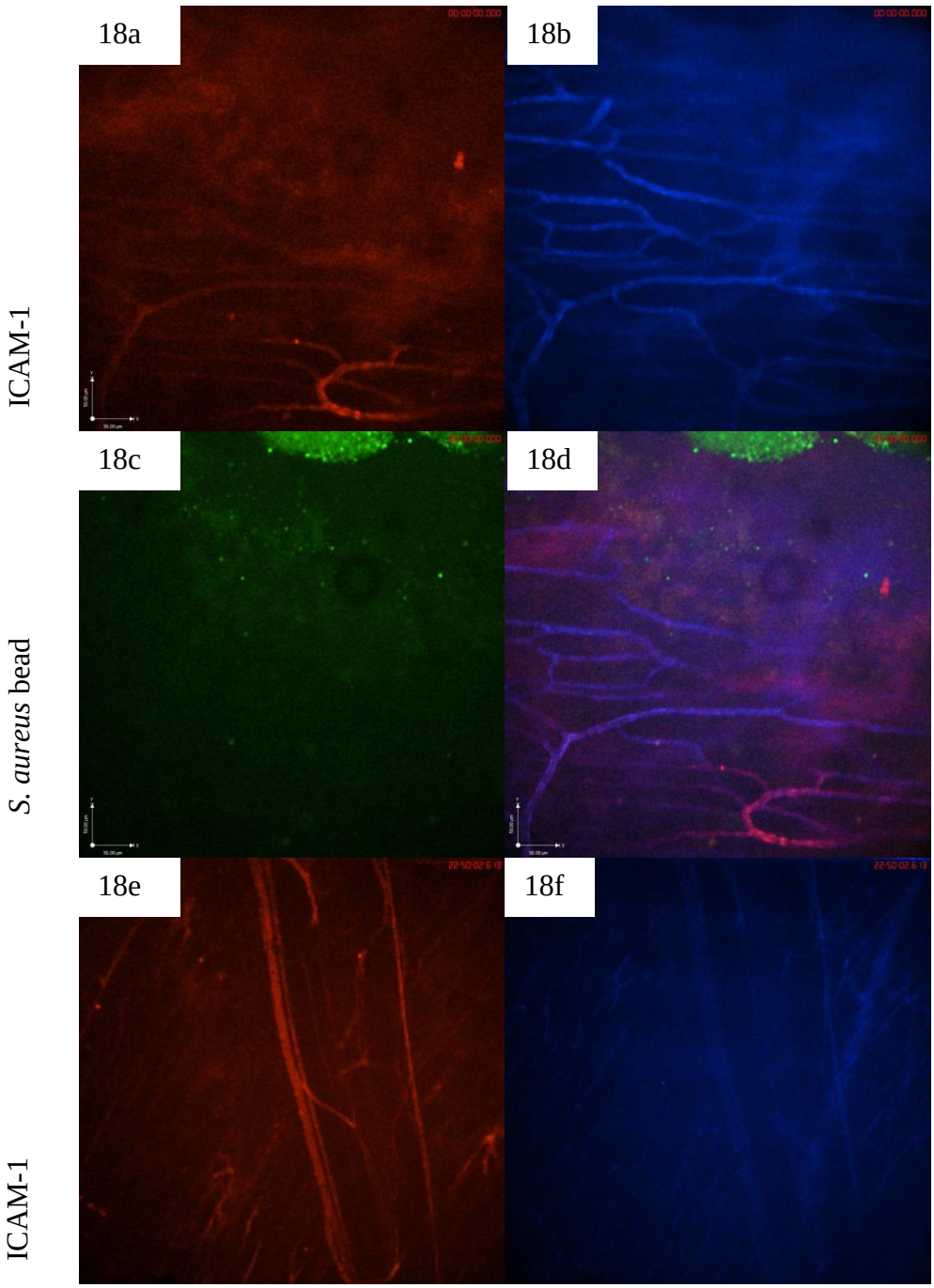
18a
18b
18c
18d
18e
18f
ICAM-1
PECAM-1
S. aureus bead
Composite image
ICAM-1
PECAM-1

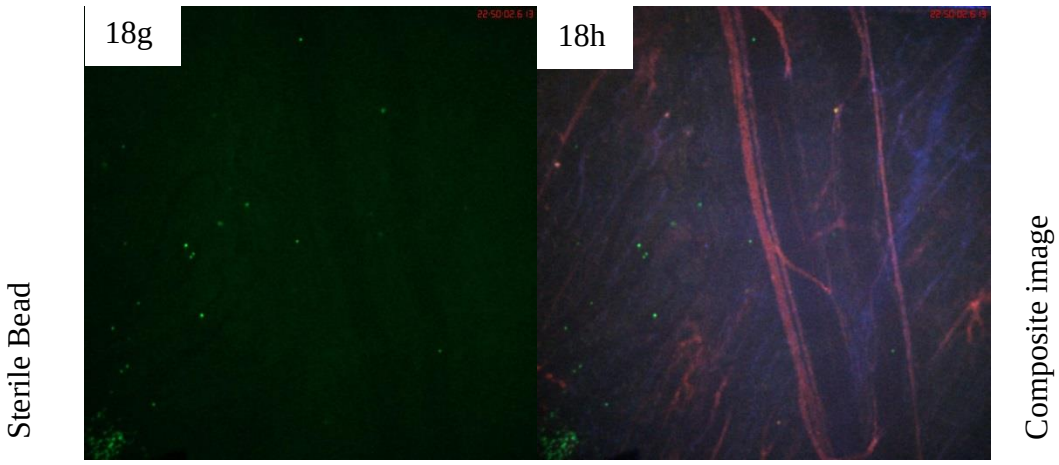

Figure 18: Expression of ICAM-1 in the microvasculature 2-3 hours post bead infection

Mice were infected with a GFP-expressing *S. aureus* bead and treated with 10µl 1.0mg/ml CD31 conjugated to Alexa647 IV. After ~2.5 hours of imaging, mice were also treated with 10µl of anti-ICAM-1 at 1.0mg/ml conjugated to PE. Additionally, control experiments were also performed, where mice were anesthetized and treated with sterile beads as well as 10µl 1.0mg/ml CD31 conjugated to Alexa647 IV. 18a: ICAM-1 expression in the microvasculature at 10x magnification within 500µm of a *S. aureus* bead near the *S. aureus* bead. 18b: Expression of CD31 on the microvasculature. 18c: The fluorescent *S. aureus* bead. 18d: Composite image. Images 18a-18d are representative of 3 independent experiments. Figure 18e: expression of ICAM-1 on the microvasculature of a mouse given a sterile bead. Figure 18f: expression of CD31 on the microvasculature of a mouse given a sterile bead. Figure 18g: the fluorescent microspheres in the image associated with the sterile bead (bead is located below and to the left of the image. Figure 18h: composite image. Images 18e-18h are representative of 2 independent experiments.

Blocking ICAM-1 via anti-ICAM-1 antibodies resulted in a significant reduction in the number of neutrophils recruited to the capillaries, when compared with IgG2b isotype controls (p=0.0246, Figure 19a). However, there was no significant change in crawling (p=0.1437, Figure 19b) or adherent neutrophils (p=0.6022, Figure 19c) when ICAM-1 was blocked. When VCAM-1 was blocked, there was a significant decrease in the number of recruited neutrophils (p=0.0087), as well as in the number of crawling neutrophils in the capillaries (p=0.0030), with no change in the number of adherent neutrophils (p=0.3097, Figure 20). Finally, blocking both VCAM-1 and ICAM-1 resulted in no significant differences in recruitment or behaviour compared with either ICAM-1 or VCAM-1 alone (p=0.4815 and p=0.2446, Figure 21). Blocking these ICAM-1 and VCAM-1 then did not have an additive effect comparable to what was seen by blocking of CD18 and α_4 integrin.

4.3 Effect of blocking antibodies on recruitment in the venules

As we observed that the β_2 integrins and VLA-4 prevented neutrophil recruitment to the capillaries, we tested the effect of these blocking antibodies on the venules in the bead model. Blocking CD18 and α_4 resulted in significantly reduced adhesion compared to isotype controls (Figure 22a, p=0.0004 for CD18 isotype controls and p<0.0001 for α_4 isotype controls). This treatment also significantly altered emigration compared to CD18 isotype controls (Figure 22b, p=0.0008). There was decreased neutrophil adhesion and emigration following treatment with anti-CD18 and anti-α_4 antibodies.

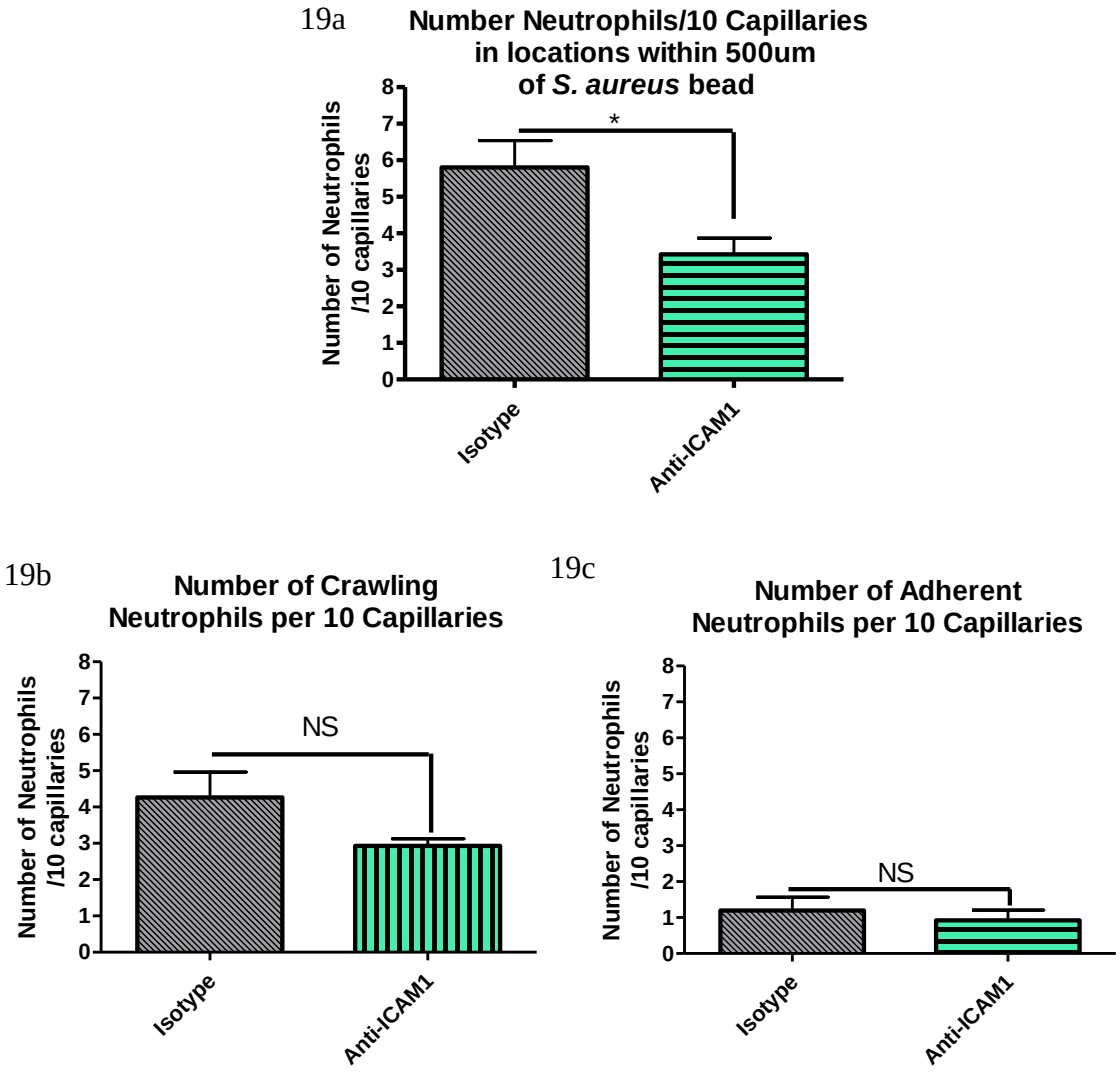

Figure 19: Neutrophil behaviour following treatment of mice with ICAM-1 blocking antibodies

Mice were treated with 100µg of blocking antibodies or IgG2b isotype controls 2 hours following infection. Multiple videos per mouse were imaged for 10minutes at 10x magnifications, and the number of neutrophils as well as their behaviours within the capillaries was quantified. 19a: Overall recruitment of neutrophils to the capillaries over ten minutes after

treatment with ICAM-1 antibodies or isotype control antibodies. N=4 independent experiments for ICAM-1 and isotype controls. Each experiment consisted of collecting data from 4 or more 10x FOVs from a single mouse and averaging the results. 19b: Number of crawling cells recruited to the capillaries following treatment with anti ICAM-1 antibodies or isotype control antibodies. 19c: Number of adherent cells following treatment with anti-VCAM-1 antibodies or isotype control antibodies. $*p<0.05$.

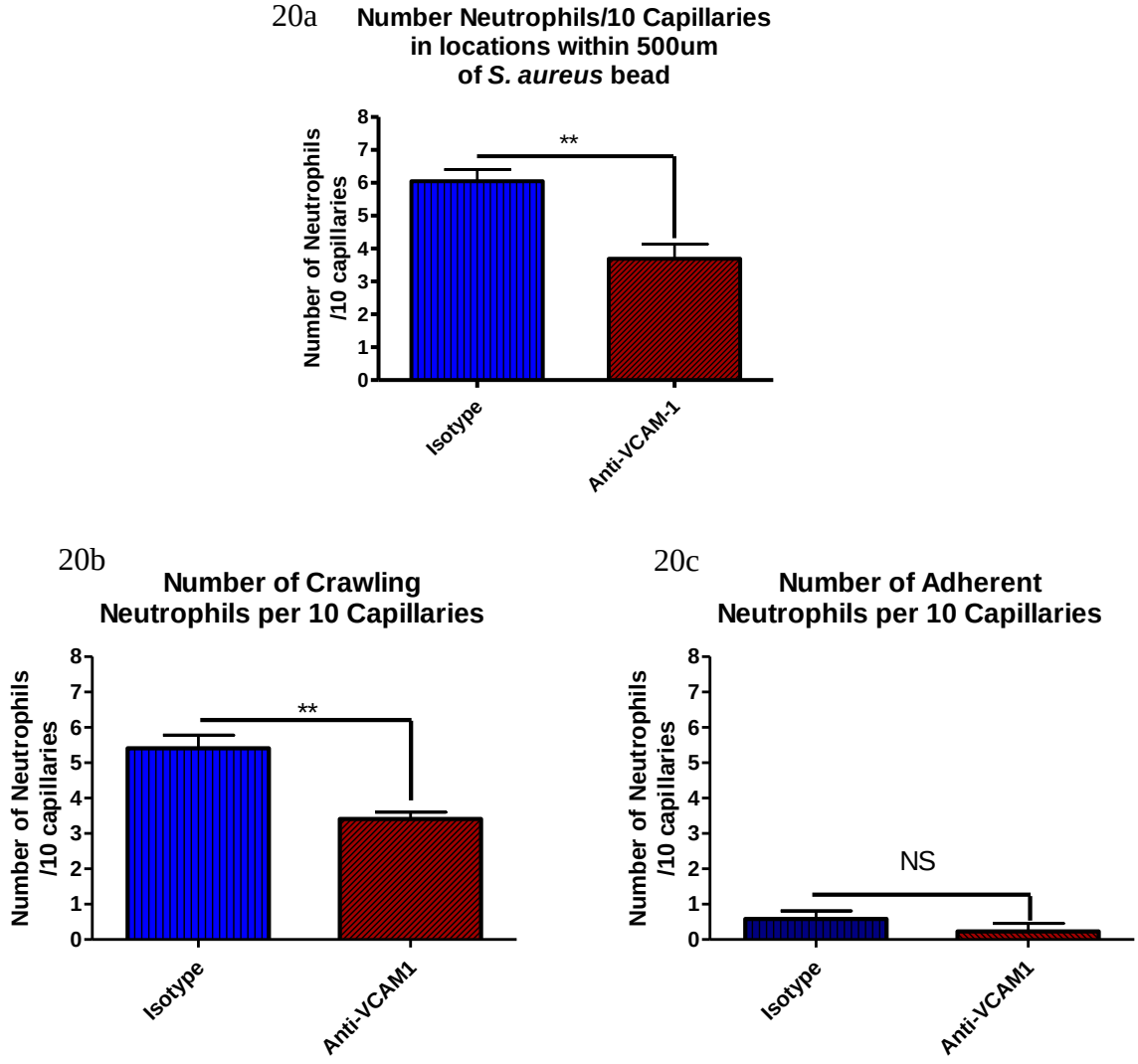

Figure 20: Neutrophil behaviour following treatment of mice with VCAM-1 blocking antibodies.

Mice were treated with 50µg of blocking antibodies or IgG2a isotype controls 2 hours following infection. Multiple videos per mouse were imaged for 10minutes at 10 x magnifications, and the number of neutrophils as well as their behaviours within the capillaries was quantified. 20a: Overall recruitment of neutrophils to the capillaries over ten minutes after treatment with VCAM-1 antibodies or isotype control antibodies. N=4 independent experiments for both

VCAM-1 and isotypes. Each experiment consisted of collecting data from 4 or more 10x FOVs from a single mouse and averaging the results. 20b: Number of crawling cells recruited to the capillaries following treatment with anti VCAM-1 antibodies or isotype control antibodies. 20c: Number of adherent cells following treatment with anti-VCAM-1 or isotype control antibodies. ** $p<0.01$

21a

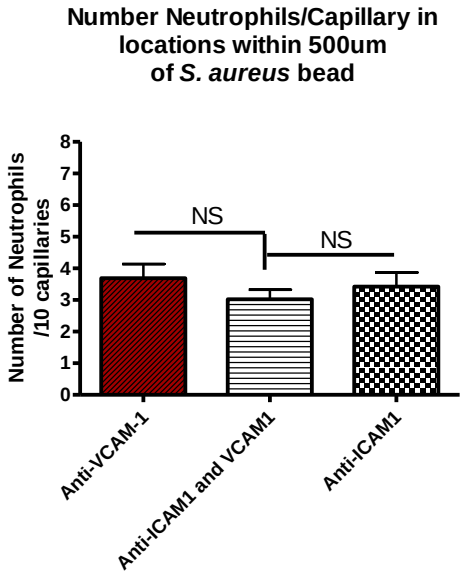

21b

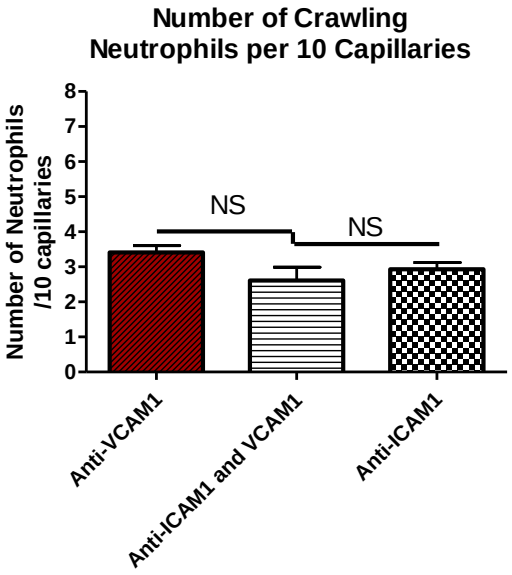

21c

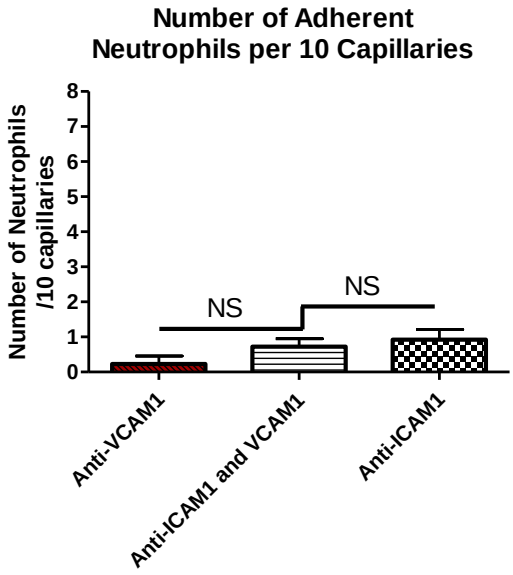

Figure 21: Neutrophil behaviour following treatment of mice with VCAM-1 and ICAM-1 blocking antibodies

Mice were treated with either 50µg of anti-VCAM-1 blocking antibodies, 100µg of anti-ICAM-1 antibodies, or both treatments 2 hours following infection. Multiple videos per mouse were imaged for 10 minutes at 10 x magnifications, and the number of neutrophils as well as their

behaviours within the capillaries was quantified. 21a: Overall recruitment of neutrophils to the capillaries over ten minutes after treatment with anti-ICAM-1, anti-VCAM-1, or both blocking antibodies. N=4 independent experiments for VCAM-1, 5 independent experiments for ICAM-1, and 5 independent experiments for ICAM-1+VCAM-1. Each independent experiment consisted of collecting data from 4 or more 10x FOVs from a single mouse and averaging the results. 21b: Number of crawling cells recruited to the capillaries following treatment with anti-ICAM-1 antibodies, anti-VCAM-1 antibodies, or both blocking antibodies. 21c: Number of adherent cells following treatment with anti-ICAM-1 antibodies, anti-VCAM-1 antibodies, or both blocking antibodies.

22a

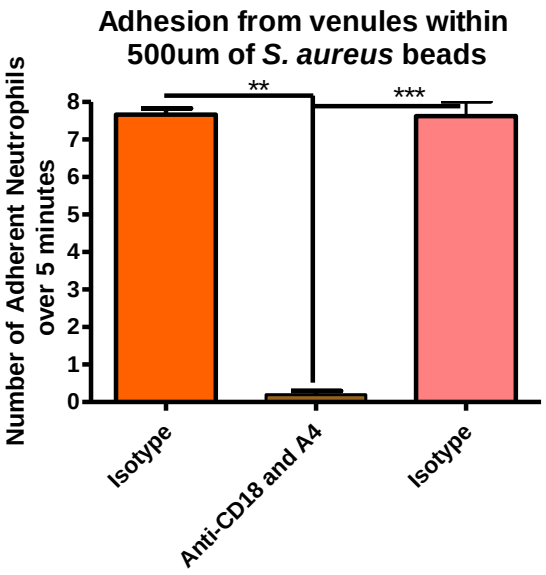

22b

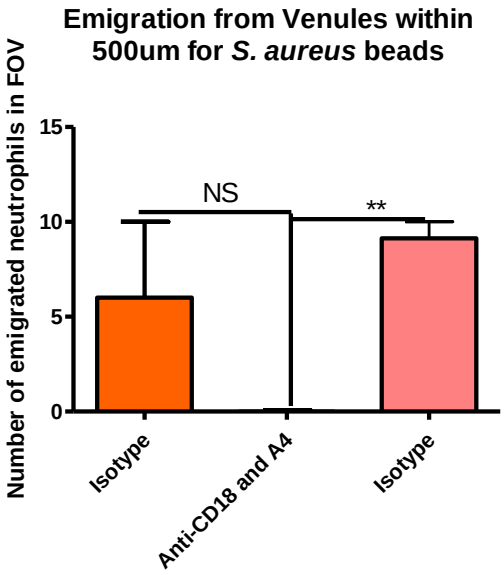

Figure 22: Effect of CD18 and α_4 blocking antibodies on venular recruitment

The numbers of adherent and emigrated neutrophils from venules were measured over 5 minutes in multiple FOVs near the *S. aureus* bead. 22a: the number of adherent neutrophils in a 100µm stretch of 20-40µm venule was measured over 5 minutes. Neutrophils were considered adherent if they remained stationary for more than 30 seconds. 22b: the number of emigrated neutrophils in the FOV was determined over the 5-minute period. Any neutrophil outside of the vasculature was determined to be emigrated. N=3 independent experiments. Each independent experiment consisted of quantification of 3 or more venules at 10x magnification. $^{**}p<0.01$, $^{***}p<0.001$.

In summary, in this chapter we have identified several molecules responsible for neutrophil recruitment into the capillaries. We have examined the molecules on the neutrophil, identifying that the β_2 integrins (Mac-1 and LFA-1) play an important role in recruitment behaviour. Notably, neither Mac-1 nor LFA-1 is individually responsible for neutrophil recruitment; blocking either alone did not significantly change the number of neutrophils recruited. However, we did see a reduction in neutrophil crawling following LFA-1 treatment. VLA-4 also appears to play an important role in mediating neutrophil recruitment, as blocking this molecule significantly reduced the number of neutrophils in the capillaries. Furthermore, blocking both CD18 and VLA-4 simultaneously led to a complete abrogation of neutrophil recruitment in the capillaries, suggesting that these molecules together are the major molecules on the neutrophil which mediate this behaviour. The ligand receptors associated with this behaviour appear to be ICAM-1 and VCAM-1, as blocking both of those molecules led to a reduction in the number of neutrophils recruited to the capillaries, though notably this did not lead to the complete abrogation of neutrophils in the capillaries as seen when using anti-CD18 antibodies and anti-α_4 antibodies simultaneously. Finally, using the anti-CD18 and anti-VLA-4 antibodies also appears to have a significant impact on the venules, completely abrogating neutrophil adhesion.

Chapter Five: Functional effects of neutrophil recruitment

5.1 Introduction: local consequences of *S. aureus* infections

Typically, MRSA soft tissue infections result in purulent cellulitis or subcutaneous abscesses (143). These abscesses are usually hypoxic regions containing necrotic cells (117), large numbers of neutrophils (61) (which are recruited rapidly following infection) and, after several days, proliferating myeloid cells (96). These cells have prolonged survival rates within the abscess, but in the case of neutrophils, this may not be to the benefit of the host (96, 144). In mouse models, the maximum amount of tissue damage or spontaneous open wound formation typically occurs between two and four days following infection (96, 116, 117), though these results are not universal (61). Abscesses and lesions containing *S. aureus* can release bacteria to disseminate, leading to secondary tissue abscess formation (145) as well as life threatening systemic complications, such as sepsis (4).

In this chapter, we examine the influence of neutrophil recruitment in the formation of abscesses, and the local physiological consequences of neutrophil recruitment. Better understanding of neutrophil function in abscess formation may direct more effective treatment of *S. aureus* infections, through modification of neutrophil behaviour. We began by investigating the recruitment of neutrophils to the capillaries, to identify whether this unexpected behaviour might have an effect upon the microvasculature or the tissue surrounding the capillary bed. Of particular interest was the question of whether neutrophils in the capillaries were occluding the microvasculature. We then examined cell death in the tissue near the bead, in order to determine whether the influx of neutrophils to the nidus of infection might induce cell death in the surrounding tissue. This led to another set of experiments in which we investigated how

neutrophil recruitment might have a gross impact on the formation and expansion of *S. aureus* induced lesions.

5.2 Microvasculature perfusion

To better understand the consequences of localized neutrophil recruitment to the capillaries, we queried whether neutrophil recruitment to these vessels occluded the microvasculature. We investigated this question using an intravenous injection of FITC-albumin. Following intravenous injection, this protein flows freely through the microvasculature, labelling it green (146, 147). However, an obstruction in the microvasculature will prevent FITC-albumin from flowing through the vessel, and thus the vasculature immediately downstream from the obstruction will not be labelled.

In our experiments, prior to the injection of FITC-albumin (green), vessels were labelled using Alexa 647 conjugated to anti-CD31 antibodies (blue). If a vessel was occluded, the vasculature did not become labelled by the FITC-albumin, but remained labelled with Alexa-647, and thus appeared blue. In this manner, we were able to clearly visualize which vessels were perfused and which were occluded. As shown by the representative image in Figure 23a, vascular occlusion of the capillary beds is apparent during *S. aureus* bead infection. Upon visual inspection, we observed that this vascular occlusion (shown in blue) was associated with neutrophils (shown in red) present in the capillary microvasculature while perfused vessels remained green and had no neutrophils (white arrowheads). When we quantified these results, we saw significantly greater occlusion of the microvasculature in *S. aureus*-treated mice than when mice were treated with sterile beads (Figure 23b). Almost all of the capillaries in mice treated with sterile beads showed perfusion, with virtually no occlusion of the microvasculature.

23a

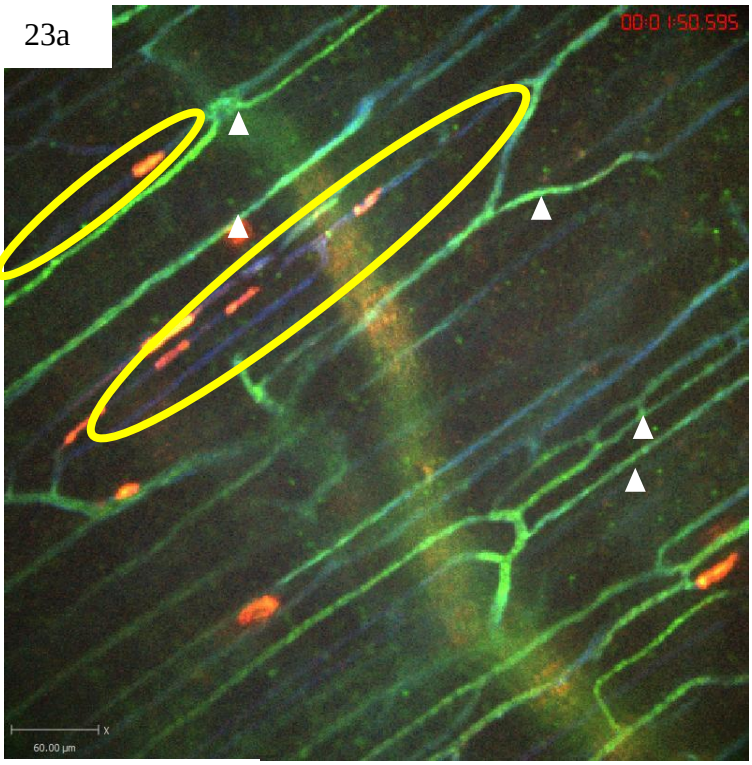

Red: Neutrophils

Blue: Vasculature

Green: FITC Albumin

23b

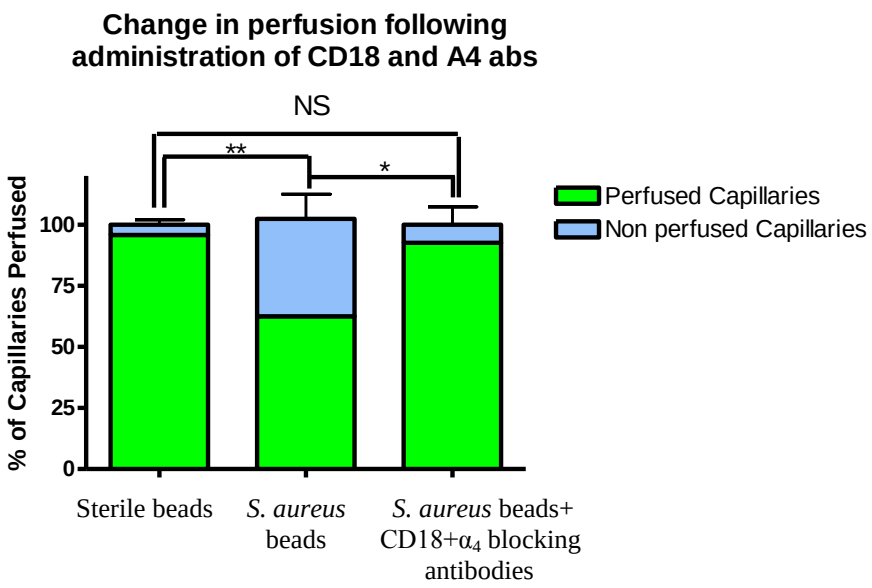

Figure 23: Occlusion of the capillary microvasculature following insertion of *S. aureus* bead

23a: Image of capillary occlusion adjacent to a *S. aureus* bead. Mice were treated with10µl at 1.0 g/ml of CD31 and 10µl of Ly6g at 0.2 g/ml conjugated to PE, as well as *S. aureus* beads, for two hours prior to image acquisition. Mice were then injected with approximately 50 µl of FITC-albumin solution after video acquisition began. Neutrophils are labelled in red, the vasculature in blue, and the flow of blood in green. The *S. aureus* containing bead is located to the right of the image, just out of view. 23b: Graphical representation of occlusion of the capillary microvasculature. Vessels were considered occluded if, 30 seconds after FITC albumin labelling became present in the FOV, the vessels were not positive for FITC albumin fluorescence. One FOV was selected randomly for quality of visual microvasculature prior to FITC albumin injection and then quantified per independent experiment. The numbers of occluded capillaries were quantified as a percentage of the total capillaries present in the FOV. Mice were given blocking antibodies (anti-CD18 and anti-α_4) 20 minutes before injection of FITC albumin. N=3 independent experiments for mice with sterile control beads, 4 independent experiments for *S. aureus* beads, and 3 independent experiments for mice given *S. aureus* beads and treated with blocking antibodies. $^{**}p<0.01$

In contrast, mice treated with *S. aureus* beads had significantly more occlusion of the microvasculature (p= 0.0042) with ~50% of the capillary microvasculature occluded.

We next decided to test whether neutrophil presence was associated with microvascular occlusion, by quantifying occlusion following treatment with antibodies that we had shown to inhibit neutrophil recruitment to the capillaries (Figure 16 from Chapter 4). When we treated *S. aureus* bead-injected mice with anti-CD18 and anti-α_4 antibodies to block neutrophil recruitment, we found that capillary occlusion was significantly reduced compared to *S. aureus* mice (p= 0.0108, Figure 21b). Capillary occlusion in the antibody-treated *S. aureus* mice was not significantly different from mice treated with the control sterile beads (p=0.4372, Figure 21b). Through this rescue experiment, we demonstrated that preventing neutrophil recruitment to the site of *S. aureus* infection was sufficient to reverse the vascular occlusion phenotype and restore perfusion to baseline conditions.

5.3 Cell death

Neutrophil recruitment during infection is not entirely beneficial to the surrounding tissue. Neutrophils are potent antimicrobial cells, but many of the molecules that neutrophils use to kill microbes, such as ROS and NETs, are also toxic to mammalian cells (88). We investigated the degree of cell death that occurred during *S. aureus* investigations using propidium iodide, and determined whether this cell death was associated with neutrophil recruitment. Propidium iodide is a fluorescent cell marker for death; when applied, it intercalates with DNA and increases its fluorescence. Propidium iodide is membrane-impermeable, and thus only stains cells with disrupted plasma membranes, or extracellular DNA. We used propidium iodide to investigate the degree of cell death both with and without

neutrophil recruitment, by using the antibodies blocking CD18 and α_4 integrins, which we had previously shown to abrogate neutrophil recruitment (Figure 15). We treated mice with these blocking antibodies before *S. aureus* treatment, to better understand the role of neutrophil recruitment in causing cell death.

Before using our blocking antibodies, we tested several controls to ensure that we were not quantifying any artefacts caused by the surgery involved in preparing the exteriorized skin or any constitutive cell death that may normally occur in skin and cause background noise (Figure 24). We first tested if there was increased cell death near the *S. aureus* bead, compared to cell death in other areas of skin (minimum 2000μm away from the bead, Figure 24). This confirmed that there was increased cell death near the *S. aureus* bead, as compared to farther away, suggesting that the presence of the *S. aureus* bead was responsible for the increased cell death, above and beyond baseline cell death in the exteriorized skin. We then quantified the differences in cell death when beads containing sterile microspheres were inserted as compared to *S. aureus* beads and confirmed significant increases in cell death with the *S. aureus* beads (Figure 25a, p=0.0258), as compared to the beads with sterile microspheres. Finally, we treated with either blocking antibodies (anti-CD18 and anti-α) or isotype control antibodies, and observed a significant (Figure 25b, p=0.0247) reduction in the number of dead cells when mice were given the blocking antibodies before *S. aureus* bead insertion. These cells did not appear to be neutrophils; we did not see evidence of colocalization between Ly6g labelled cells and propidium iodide (Figure 26).

24a

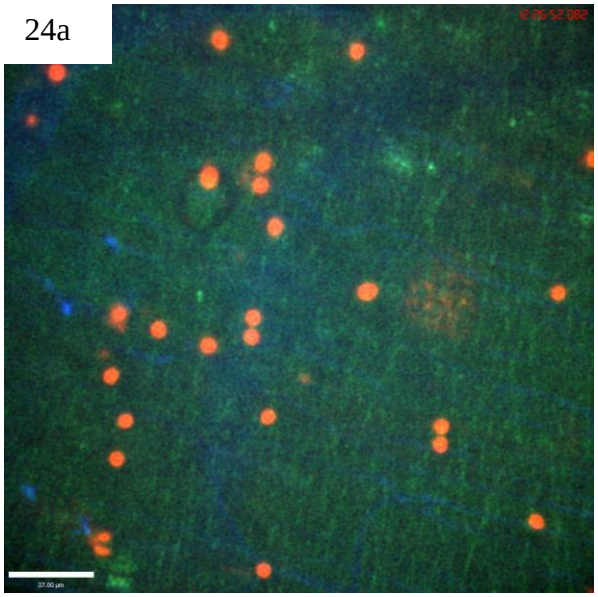

24b

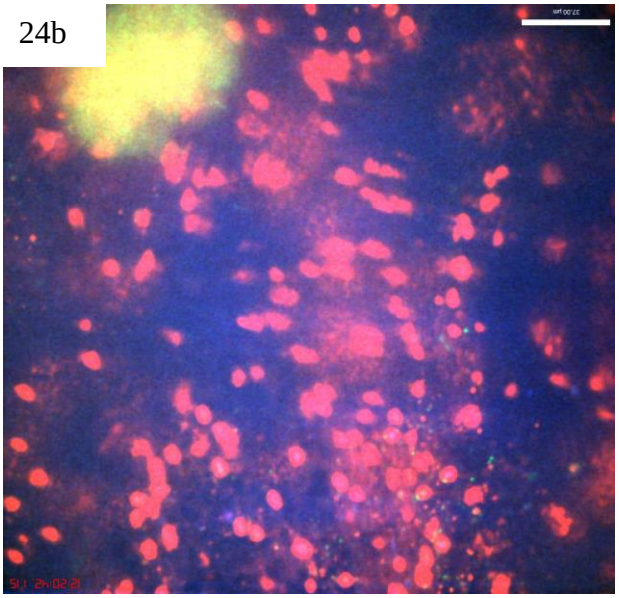

Away from Bead

Near Bead

24c

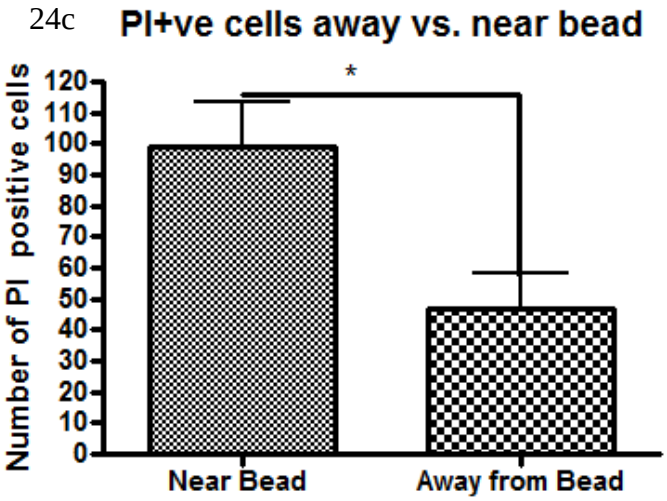

Figure 24: Effect of *S. aureus* bead on cell death

Multiple 10x magnification FOVs in mice were quantified to compare the amount of cell death which occurs near versus away from the bead. Mice were treated with 50µl of 2 µg/ml propidium iodide superfused over the tissue. Away from the bead was defined as a minimum of 2000µm from a *S. aureus* bead. 24a: A FOV away from a *S. aureus* bead. Propidium iodide positive cells are in red, the vasculature is in blue, and the neutrophils are in bright blue. 24b: A

FOV near a *S. aureus* bead. Propidium iodide positive cells are in red and the GFP-*S. aureus* bead is in green. 24c: Graphical analysis of the number of propidium iodide positive cells ~2000 µm away from the bead versus adjacent (within 500µm) of the bead. N=3 independent experiments. Each independent experiment consisted of collecting data from 3 different 10x FOVs. *$p<0.05$.

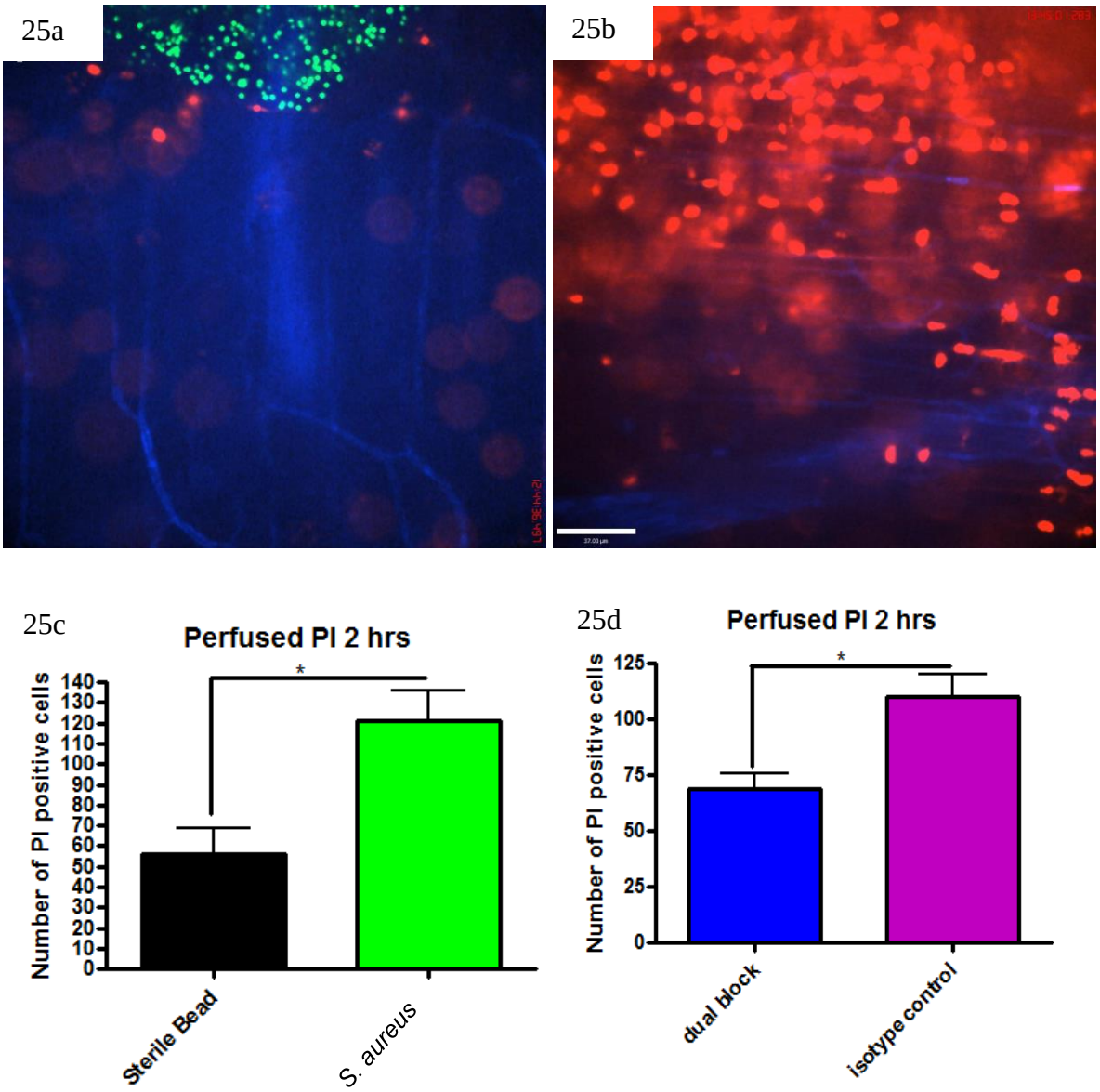

Figure 25: Quantification of cell death induced by beads

25a: Image of a sterile bead and nearby propidium iodide positive cells. Propidium iodide positive cells are in red, the vasculature is labelled blue, and the bead is labelled green. 25b: Image adjacent to a GFP-*S. aureus* bead. Propidium iodide positive cells are in red, the vasculature is in blue, and the neutrophils are in bright blue. The bead is located just above the FOV. 25c: The number of propidium iodide positive cells found in 10x magnification FOVs

near a bead when comparing sterile and *S. aureus* beads. Data is from multiple fields of view per mouse. N=3 independent experiments for sterile beads and 5 independent experiments for *S. aureus* beads. 25d: The number of propidium iodide positive cells found in 10x magnification FOVs near an *S. aureus* bead when comparing mice treated with anti-CD18 and anti α_4 antibodies, and isotype controls. Mice were treated with antibodies at the same time as insertion of *S. aureus* beads. N=3 for isotype control treatment, N=4 for the dual block treatment. *$p<0.05$

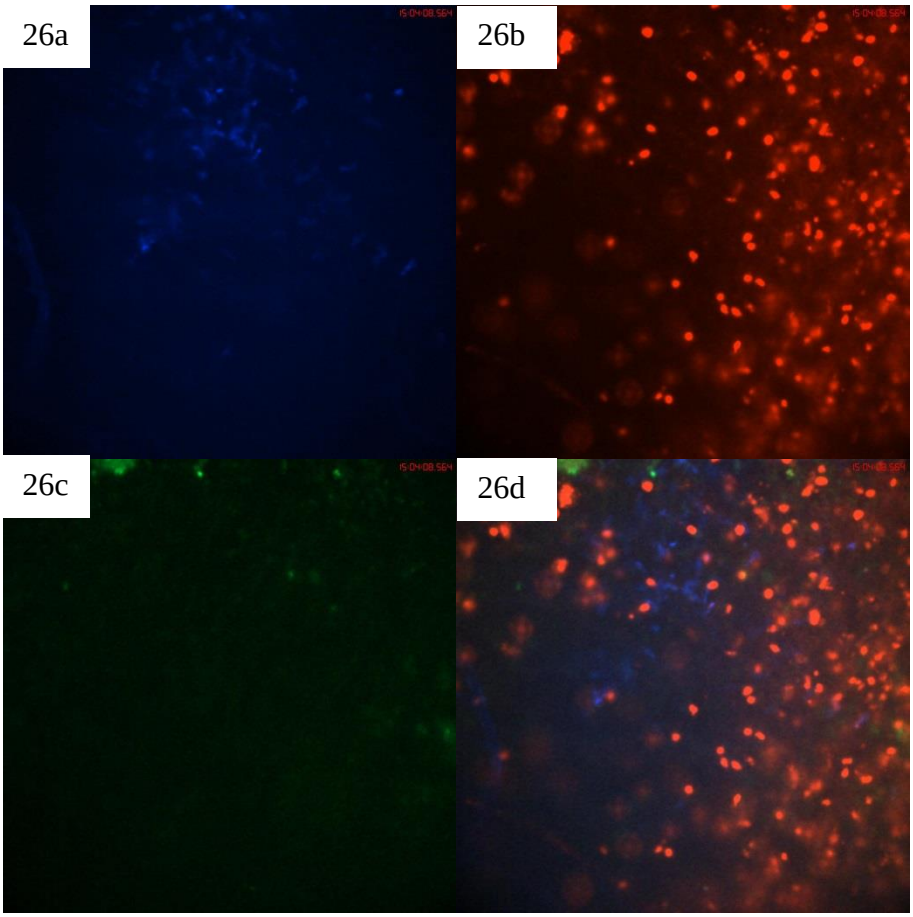

Figure 26: 10x magnification of propidium iodide positive cells and Ly6g positive cells. Mice were treated with 10µl at 0.2mg/ml of anti-Ly6g (clone RB6-8C5, in blue) at the time of bead insertion (in green), as well as 10 µl at 1.0mg/ml anti-CD31 (also in blue). Mice were treated with 50µl of 2 µg/ml propidium iodide (red) superfused over the tissue two hours after infection. Bead is located adjacent to the FOV, above the image. 26a: Ly6g (RB6 8C5) and CD31 expressing cells within 500µm of the bead. 26b: propidium iodide positive cells within 500µm of the bead. 26c: edge of the GFP-SA bead (located north of the bead). 26d: Composite image. Image is representative of 4 independent experiments examining single FOVs at 4x magnification.

5.4 Lesion size

We then examined whether preventing neutrophil recruitment could significantly alter the size of the lesion caused by a *S. aureus* bead 48 hours after infection. We administered blocking antibodies, either two hours before or after the injection of *S. aureus* beads containing $5x10^5$ CFU, and then examined the size of the lesion 48 hours after infection. We found that blocking neutrophil recruitment two hours after infection resulted in reduced lesion size at 48 hours (Figure 27a). Paradoxically, we found that blocking neutrophil recruitment two hours before infection resulted in increased lesion size (Figure 27b). Furthermore, the only group of mice which had recoverable CFU's of *S. aureus* in the blood at the time of tissue harvest were those treated with blocking antibodies two hours before infection (Figure 27c and d), suggesting that the reduced lesion size seen in mice given anti-CD18 and anti-α_4 integrin after infection did not result in *S. aureus* escaping the abscess and causing bacteremia, which would be detrimental to the health of the host.

In conclusion, in this chapter we have examined the functional consequences of neutrophil recruitment to a *S. aureus* infection, both immediately surrounding the bead and in the nearby capillaries. In the capillaries, we saw increased vascular occlusion with *S. aureus* infections. This occlusion could be reduced by blocking the recruitment of neutrophils to the capillary microvasculature. When we examined recruitment to the beads, we saw increased cell death with *S. aureus* beads as compared to sterile controls, which could be prevented by inhibiting neutrophil recruitment at the early stages of infection. Furthermore, blocking neutrophil recruitment at a specific timepoint (2 hours after infection) decreased lesion size. In contrast, preventing neutrophil recruitment 2 hours before infection caused larger lesions sizes,

27a

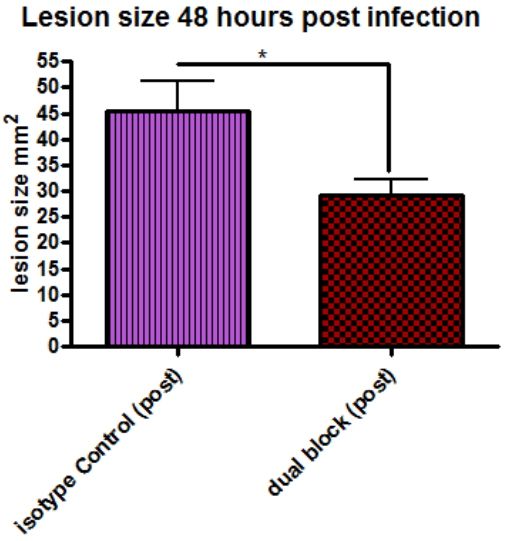

27b

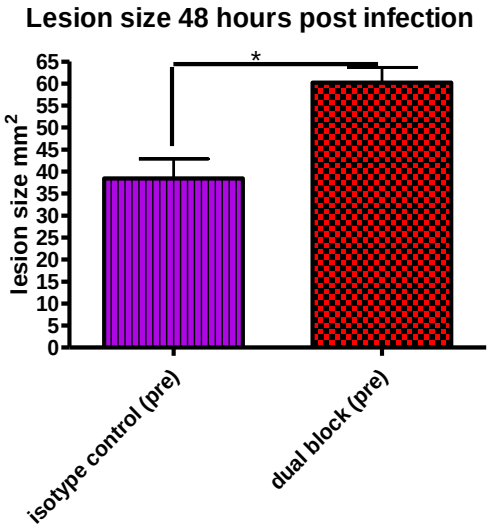

27c

Presence or Absence of *S. aureus* in the blood of mice 48 hours after infection

Time point of injection	2 hours before bead injection		2 hours after bead injection	
Treatment	Isotype control	Dual Block	Isotype control	Dual block
Replicate 1	Yes	Yes	No	No
Replicate 2	No	Yes	No	No
Replicate 3	No	No	No	No
Replicate 4	No	No	No	N/A

27d

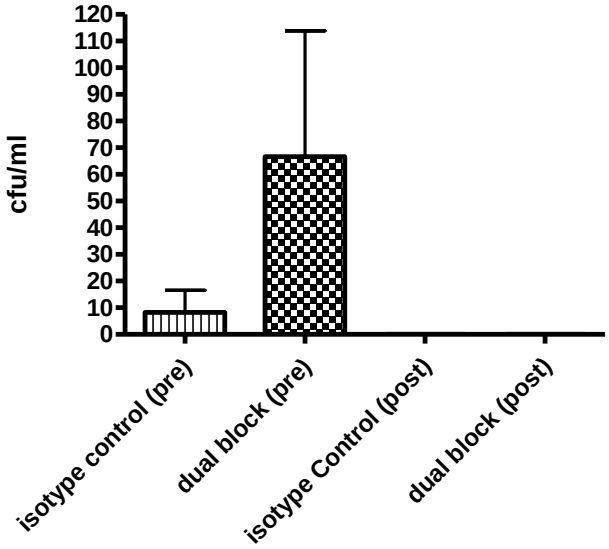

Figure 27: Effect of blocking antibodies on lesion formation 48 hours after bead injection.

Beads (approximately 10^5 CFU) were injected SC into mice. Mice were treated with a cocktail of either isotype control IgG1 and IgG2b antibodies or anti-CD18 and anti-α_4 antibodies (via tail vein injection) either two hours before or two hours after injection of beads. Tissue was excised 48 hours following infection, and then the lesion was photographed and analyzed using ImageJ software to identify the size in mm^2. 27a: Effect of blocking antibodies administered two hours after infection by injection of *S. aureus* beads. N=4 independent experiments for isotype control treatment, and 4 independent experiments for dual blocking treatment. Each independent experiment consisted of analysis of a single lesion. 27b: Effect of blocking antibodies injected two hours before infection. N=4 independent experiments for isotype control treatment and3 independent experiments for dual block two hours before infection. Each independent experiment consisted of analysis of a single lesion. 27c: Presence or absence of CFUs in blood of mice harvested 48 hours after infection. Blood was harvested via cardiac puncture and plated to determine absence or presence of CFUs. "Yes" indicates the presence of *S. aureus* CFUs in the blood, "no" indicates the absence of *S. aureus* CFUs. 27d: CFUs/ml of blood found in mice following treatment with blocking antibodies or isotype controls either two hours before or after infection. Blood was plated on BHI agarose with 20µg/ml chloramphenicol.

suggesting that neutrophil recruitment is important during the early stages of infection, but may also cause additional bystander tissue damage.

Chapter Six: Discussion

6.1 Summary and significance of this study

S. aureus is a serious pathogen, responsible for the majority of soft tissue infections (3) and approximately 18,500 deaths per year in the United States (2). It can cause significant complications following infection, such as necrotizing fasciitis and sepsis (4), which are potentially fatal. *S. aureus* remains a serious clinical challenge due to its capacity to rapidly adapt and mitigate the effect of many types of antibiotics, including beta-lactams, vancomycin, and daptomicin (13, 15, 16). A more sophisticated understanding of this pathogen's behaviour at the molecular level is of utmost importance, in order to combat it and prevent mortality in infected patients.

Recent research has focused on the complex and often paradoxical role that the innate immune system plays in *S. aureus* infection. In particular, neutrophil recruitment to *S. aureus* during infection has been well-documented in the literature (2, 83). This recruitment is considered critically important to control *S. aureus* infections, since deficiencies in neutrophil function can impair the host's ability to combat *S. aureus* infections, as demonstrated in both patients and experimental mouse models (44, 109). However, neutrophil recruitment is not entirely to the host's benefit, as neutrophils are also highly cytotoxic. As suicidal pro-inflammatory "foot soldiers" of the innate immune system, they can cause substantial bystander tissue damage in the process of controlling infections (88, 110). In this study, we probed the complex role that neutrophils play during *S. aureus* skin infections *in vivo* using spinning disk confocal microscopy. We developed and validated a novel *in vivo* model of localized *S. aureus* skin infection, and used this model to characterize neutrophil behaviour in real time, in order to better understand the role of these cells in *S. aureus* infections.

6.2 Analysis of model development

In Chapter 3, we developed a model that used viable *S. aureus* immobilized on an agarose bead. This model generated significant recruitment of neutrophils towards *S. aureus* infection sites (Figures 5 and 6), which occurred in spite of the many virulence factors (such as CHIPs and SSL5) that *S. aureus* secretes that can inhibit neutrophil recruitment *in vitro* (98, 148). In our model, neutrophils are recruited swiftly and en masse to the site of *S. aureus* infection, recapitulating the results of similar studies by multiple other groups (2, 83). Is it to the advantage of the host or the pathogen to have large numbers of neutrophils recruited to the infection site? Despite the crucial role neutrophils play in containing *S. aureus* infection, the capacity of neutrophils to cause bystander tissue damage suggests that their presence may not be entirely beneficial. Many studies (102, 149-151) have shown that *S. aureus* is capable of surviving neutrophil phagocytosis, and furthermore, that *S. aureus* possesses the ability to lyse neutrophils and contribute to infection after phagocytosis. Some have even speculated that neutrophils may act as a "Trojan horse" for *S. aureus*, allowing the pathogen to disseminate more easily throughout the body and cause secondary infections via migration of infected neutrophils (114). This suggests that, paradoxically, neutrophil recruitment may be of benefit to the pathogen (facilitating bacterial dissemination) and to the host (facilitating bacterial clearance), whilst simultaneously being detrimental to the pathogen (via ROS-mediated bacterial killing and trapping with NETs, for example) and to the host (via bystander tissue damage). Although this study did not attempt to conclusively resolve this complex paradoxical relationship, our goal was to further elucidate the neutrophil-*S. aureus* interaction through an in-depth characterization of neutrophil behaviour at the localized site of *S. aureus* infection *in vivo*.

To approach this challenge, we adapted a previously established agarose bead model of infection. In the cystic fibrosis literature, the agarose bead approach was used to immobilize *P. aeruginosa* in the lung (127). We developed a similar agarose bead model of *S. aureus* for a number of reasons. Firstly, immobilization simplified the bacterial infection in our experiments, allowing us to concentrate on examining the leukocyte behaviours to a nidus of infection using real-time imaging with spinning disk confocal microscopy. The bead model also focused on a specific region (the areas within 500 to 1000μm of the bead) rather than dealing with variable concentrations of bacteria that can be found when *S. aureus* is injected subcutaneously. Importantly, we believe this method of *S. aureus* inoculation also recapitulates an important clinical scenario in patients: the bead represents a physical vector that carries the bacteria underneath the cutaneous layers of the skin, which we consider to be equivalent to a wooden splinter or fragment of broken glass. This is relevant to a clinical infection with *S. aureus*, where infection is not typically caused by fluid being injected underneath the skin (the method used in our preliminary studies and elsewhere in the literature (24, 25, 117). Furthermore, introducing beads into the skin creates a mixing of *S. aureus* with a foreign particle, which has been shown to enhance pathogenicity compared to *S. aureus* in saline alone (121, 124). It is possible the increased pathogenicity caused by *S. aureus* with foreign particles may be because this mixture "confuses" the immune system, reducing its ability to detect the severity of a *S. aureus* infection and respond appropriately, and may help to explain why *S. aureus* does not need large CFUs to induce soft tissue infections in patients. Alternatively, foreign particles may allow for *S. aureus* biofilm formation, which can enhance virulence (152).

We used male C57B6 mice in this model for several reasons. There are many knockouts available on this genetic background of mice (for example, mice deficient in the β_2 integrins

LFA1 and Mac1 (153, 154), which could be relevant to this project). When we selected the strain of mice, we were uncertain whether to use knockouts or blocking antibodies, and were considering the use of LysmGFP mice (which we have on a C57B6 background) to label neutrophils. We ultimately decided against this option because of the bacterial strains used in our experiments. The brightest USA300 fluorescent strain we had was GFP-expressing. While we also had access to red fluorescent protein (RFP) expressing USA300, these bacteria were not bright enough to consistently identify beads. Using LysmeGFP mice in conjugation with GFP expressing *S. aureus* would have made differentiation of neutrophils and bacteria difficult; therefore, we decided to use PE-conjugated antibodies to label the neutrophils. We used only male mice to avoid the possibility of sex-related differences confounding our experiments. As a control, future experiments could try this model in another strain of mouse (like BalbC) to determine whether the observed neutrophil behaviour varies between strains, as well as examine whether female C57B6s show similar neutrophil behaviour.

In order to get an indication of the early neutrophil responses to *S. aureus*, our preliminary data, collected following subcutaneous injection of *S. aureus*, was analyzed at one hour post infection. Others have demonstrated that neutrophil activation to *S. aureus* in the skin is a fairly rapid response, occurring within 2hrs (47), both due to the extreme sensitivity of the skin to any perturbation, as well as the fact that *S. aureus* potently stimulates innate immune responses (32).

Prior to using our model for experimentation, the bead characteristics were thoroughly analyzed and quantified. We measured the CFUs prior to bead construction in order to estimate the overall number of bacteria being used (Figure 4b) and subsequently identified the best mechanisms to measure CFUs in individual beads in later experiments, via plating of individual

beads. The CFU total better reflects the concentration of CFUs, compared with measuring individual beads, where the size of the bead must also be taken into account to determine CFUs. We also verified the length of time that *S. aureus* beads retain viability (Figure 4c), and so tailored our experiments to avoid variation in *S. aureus* numbers due to the age of the beads.

Importantly**,** our model corroborates the results of other studies (24, 31, 45, 61, 83, 117) that demonstrate that neutrophils are actively recruited to the site of *S. aureus* infection (Figures 5 and 6). Typical of neutrophil recruitment, we see neutrophils both adhering and emigrating from the venules (Figure 22). In this model of infection, neutrophils clearly exit the vasculature (Figure 22) and move through the extravascular compartment toward the nidus of infection (Figure 6). It is likely that neutrophils are being recruited by bacterial proteins, as well as chemokines released by damaged cells and other immunocytes.

Following validation of our model, we conducted an in-depth examination of neutrophil behaviour near the site of localized infection. In particular, we observed neutrophil adhesion and crawling inside the capillaries, in addition to inside the venules, during neutrophil recruitment to *S. aureus* beads, a phenomenon that has not been previously observed and described, to our knowledge. Nonetheless, it is difficult to label the capillaries specifically. Therefore, capillaries were identified as vessels that were a) $\leq 10\mu m$ in size, as described in the literature (155) and b) that transitioned into venules. We used 3D imaging (Figure 7d) to confirm that neutrophils were inside the capillaries. This disproved the alternative hypothesis that neutrophils were crawling on the surface of the capillaries, instead of within them. Further evidence supporting our assertion that neutrophils were inside the capillaries is the effect these cells had on perfusion in the capillaries (Figure 19), clearly showing that the neutrophils were associated with occlusion of the vasculature, something that they are highly unlikely to do from outside the capillary.

Thus, it was clear that neutrophil recruitment to the bead was occurring not only through the venules, but also in the capillaries, a previously undescribed behaviour in the context of *S. aureus* infections. This recruitment occurred in response to the *S. aureus* present in the bead, and not to the bead alone (Figure 5) demonstrating that this was not an artefact caused by surgical manipulation of the mouse or the insertion of the bead. It is difficult to see how this capillary recruitment could be beneficial to the host, as the neutrophils were not observed to emigrate from this vascular bed, but instead crawled in close proximity to the bead within the capillaries. It is possible that neutrophils are recruited in order to prevent any bacterial dissemination through the vasculature from the initial infection point. Activation of neutrophil host defense mechanisms such as NETs could protect against further dissemination, should the bacteria enter the capillary microvasculature. The presence of neutrophils would also allow for phagocytosis and potentially killing of netted bacteria. A method to begin testing this hypothesis *in vivo* would be to use molecules such as SYTOX green or orange as well as antibodies against neutrophil elastase and histones to label NETs, as has been used previously (54, 112). An alternative hypothesis for the capillary recruitment behaviour is that *S. aureus* promotes this neutrophil recruitment for its own benefit, increasing the tissue damage and subsequent neutrophil recruitment in order to promote dissemination of infection via neutrophils, as suggested by the literature (114). This is supported by the fact that the capillaries are occluded by the neutrophils, and this occlusion likely causes damage to those capillaries. When we labelled with propidium iodide to examine cell death, we observed that some of the propidium iodide cells appeared to co-localize with the CD31-labelled endothelial cells (Figure 23b). This could be examined in greater detail by quantifying the percentage of propidium iodide positive cells that co-localize with the capillaries, to determine if cell death is associated

with proximity to the capillaries. Another possibility is that capillary recruitment has no effect on infection, being neither beneficial nor detrimental to the host, but is a side effect of the massive neutrophil influx. As there are still far fewer neutrophils in the capillaries than the venules, these intra-capillary neutrophils may be a side effect of neutrophils being signalled to migrate to the bead site, and may not cause any physiologically significant change in cell death or local tissue damage. Unfortunately, when we inhibited neutrophil recruitment to the capillaries, we also altered neutrophil recruitment to the venules (Figure 18, chapter 4), so deciphering the precise role of neutrophil recruitment to the capillaries was not possible.

The observation of neutrophils within the capillaries as elongated cells (Figure 8) suggests that these neutrophils are capable of crawling within small vessels (5-10μm in diameter). Neutrophils within small vessels crawl independently in a dynamic fashion. This observation is supported by the data showing that integrin inhibiting antibodies were capable of inhibiting neutrophil recruitment (Figures 11, 14, 15), demonstrating that this behaviour was not mechanically mediated. In other words, neutrophils are being actively recruited rather than passively lodged in the capillary bed. The number of adherent neutrophils in the capillaries was not reduced by administration of integrin inhibiting antibodies (Figure 10a), so it is possible there were some neutrophils getting "stuck" and unable to move through the capillaries by means other than the integrins we investigated. However these numbers were exceedingly low, so even if this does occur, it likely does not play an important role in recruitment to the capillaries. This has interesting implications for other tissues where neutrophils transit through relatively small microvasculature. In the lung, for instance, some have hypothesized (156-158) that the size of lung capillaries results in a mechanical inability for activated neutrophils pass easily through this vascular bed; the neutrophils are trapped due to their size. This trapping was hypothesized to be

part of the reason why there is a delay in neutrophil transits through the lung. Furthermore, this was suggested to occur during infection or lung injury, as these insults result in cytoskeletal changes of neutrophils (156-158). Our data supports a different hypothesis: if neutrophils are capable of crawling through microvasculature such as the capillaries of the skin during infection, it is less likely that they are being mechanically trapped in the similarly sized capillaries of the lung.

This leads to another important feature: the heterogeneity of the endothelium. Endothelial cells vary both between different organs of the host, as well as between various different vascular beds within the same organ (66, 159). This coincides with different physiological pressures on different regions of the endothelium. Shear force is typically lower in the capillaries than in many other vascular bodies, but in vessels that have a diameter 10μm or less, the shear stress can be comparatively high (160). This may be why neutrophils crawl and adhere within capillary vessels of this diameter, as integrins are known to have catch bond functions and thus may prove an effective means of recruiting cells at high shear stress regions of the capillary microvasculature.

After we observed neutrophil recruitment to the capillaries, we sought to determine whether this phenomenon was unique to the strain of *S. aureus* we were using (USA300). We found no significant differences in neutrophil recruitment, either to the bead or in the capillaries, when we compared ATCC25923 with the USA300 strain. This experiment confirms that neutrophil recruitment to the capillaries is not unique to USA300. However, it does not confirm whether or not all *S. aureus* strains cause this behaviour. An important future direction would be to examine other *Staphylococcal* strains in this model, particularly non virulent ones. Strains which differ significantly in terms of virulence from the strains used here, such as a colonization

strain like M92, may not cause this effect in the capillaries. Clearly some *S. aureus* strains are capable of inducing this behaviour; this is not dependent on methicillin resistance or HA versus CA designation (ATCC25923 is a MSSA strain originally derived from a hospital infection, whereas USA300 is a CA MRSA strain). Testing closely related species, such as *Staphylococcus epidermis,* may give further insight into what distinguishes *S. aureus* from its less pathogenic cousin. Furthermore, it would be instructive to examine other common skin pathogens, like *Streptococcus pyogenes,* to see if similar behaviours occur in response to other skin pathogens.

These observations raised the question of why there was no emigration from the capillaries. It is possible that the capillary endothelium lacks some proteins or molecules necessary for neutrophil emigration, such as JAMs or VE-cadherin. There may be differences in the junctions of capillaries as compared to venules in the skin, or the signals provided by the endothelium to the neutrophil in this vascular bed may inhibit neutrophil emigration. The lack of emigration is worth further study in the future, as defining the difference between the venular and capillary endothelium and the possible reasons why this behaviour occurs may provide further insight into whether this behaviour contributes to *S. aureus* virulence. To examine differences in capillary endothelium, future experiments could stain for molecules such as JAMC VE-cadherin, or Claudin 5, which are typically found at endothelial junctions and involved in emigration from the venules. Claudin 5, in particular, has been found at the tight junctions between both murine dermal endothelial cells and in human dermal capillary endothelial cells (161, 162). This, combined with 3D imaging, might allow us to assess whether or not these proteins are present, and thus determine whether the inability to emigrate from the capillaries is based on the protein surface expression of the endothelium. Another possibility is that the vasculature here is less permeable to larger molecules, so there is no signal (such as an

extravascular chemokine gradient) that can be recognize to induce emigration out of the vasculature.

6.3 Analysis of the molecular components of capillary recruitment

In Chapter 4 of this study, we interrogated the role of integrins in neutrophil recruitment to the capillaries, and demonstrated that the β_2 integrins and the α_4 integrin VLA4 are important in mediating this phenomenon.

We chose to investigate the role of the β_2 integrins with blocking antibodies, rather than using mouse knock-outs. We found previously that neutrophil recruitment to the capillaries occurred consistently at ~2 hours (Figure 5) and wanted to investigate the importance of various molecules in mediating neutrophil recruitment at this timepoint. Using mice deficient in these integrins would not give us the ability to conduct time-specific blocking of neutrophil recruitment. We also wanted to avoid any side effects of blocking neutrophils for the first two hours. Additionally, $CD18^{-/-}$ mice have significantly more circulating neutrophils than wild type mice (163)**,** and, to our knowledge, there is no α_4 integrin knockout mouse. If we prevented the gross neutrophil recruitment at earlier timepoints, this reduction in neutrophil numbers could alter the recruitment of neutrophils in the capillaries by preventing the production of chemoattractants (such as LTB4) by emigrated neutrophils. Thus we could be causing indirect effects on capillary recruitment, rather than directly changing behaviour within them. Furthermore, it is possible for mice deficient in integrins to develop mechanisms for compensating for these deficiencies, whereas mice treated with antibodies do not typically suffer from this limitation, due to the rapid nature of the blocking effect. However, antibody treatment does introduce the risk of non-specific binding. The antibodies can then alter the behaviour of

cells by crosslinking with Fc receptors found on the surface of many immunocytes. This can change the behaviour of the cells in question, through mechanisms unrelated to the direct blocking of the molecule being targeted. Additionally, the blocking antibody could bind and alter the function of the cell where non-specific binding is occurring, and could induce cell-cell interactions that are again not related to the molecule being targeted. In order to address some of these limitations, we treated with isotype control antibodies, and in most analyses, we observed significant differences between the blocking antibodies and their isotype controls.

The importance of the β_2 integrins in this system was confirmed. It has been previously shown that the β_2 integrins play important roles in leukocyte recruitment in the peripheral tissues, such as skin and cremasteric vein (71, 164). The fact that removing CD18 significantly reduced the number of crawling cells, but not the number of adherent cells, suggests that adherent cells are not heavily influenced by the β_2 integrin in this vascular bed. An important corollary, mentioned earlier, is that there were very low levels of adherent neutrophils to begin with; thus neutrophil adhesion may be caused by factors other than adhesion molecules (i.e. mechanical stresses on the cells or an inability to crawl for other reasons), and did not play an important role in the behaviour of the neutrophils.

Of note, blocking either Mac1 or LFA-1 alone did not have significant effects on neutrophil recruitment within the capillaries (although blocking LFA1 did alter neutrophil behaviour, see Figure 14). This suggests that these integrins perform different roles in the capillaries, as compared to the venules. This is supported by the fact that blocking LFA 1 reduced neutrophil crawling (Figure 14), whereas blocking Mac1 had no effect on neutrophil behaviour (Figure 13). This implies that the neutrophils are capable of adhering via either LFA1 or Mac1 in the capillaries (possibly due to the differing structure of these vessels as compared to

the venules), but require LFA1 in order to move through the capillary microvasculature. This data also suggests that Mac 1 and LFA1 play overlapping roles in the capillaries, and both must be blocked in order to prevent neutrophil recruitment to the capillaries. While it is possible that another β_2 integrin is responsible for these behaviours, we feel this is unlikely. Mac1 and LFA1 are expressed at high levels constitutively in neutrophils, and are thought to be the primary molecules involved in crawling and adhesion (71, 75, 82, 165). Other α subunits of the β_2 integrins are probably not involved in this behaviour. For example, CD11d is primarily expressed on monocytes and macrophages, not neutrophils (166). In contrast, CD11c may be expressed on neutrophils, but is not expressed in large amounts and has never been assigned any function (167, 168).

The role that α_4 integrin played in this model warrants discussion. The presence of α_4 integrin on neutrophils is controversial, with some authors suggesting that neutrophils do not express this integrin (169). Others have suggested that this molecule only plays a role in specific tissue beds in the body, such as the lung (72), or in cases of infection, such as sepsis (73). It is possible that this molecule is externalized on the cell surface of neutrophils during infections, and thus the reason why we saw α_4 integrin playing a role in the capillaries (Figure 14) and venules (Figure 18) was due to infectious stimuli (the *S. aureus* in our model). Future studies could use a sterile model of inflammation in the skin, which is similar in function to the bead (possibly filter paper or another mechanical structure that releases chemoattractants like MIP2, FMLPs or LTB_4), and analyze different behaviours. Such studies, combined with treatment of blocking antibodies of α_4 integrin, might address the importance of this integrin on the neutrophil. Further validation experiments, such as colocalization of the β_2 and α_4 integrins and the neutrophil marker Ly6g (specifically with the 1A8 antibody to label neutrophils

exclusively), should also be performed *in vivo* to ensure that the integrins are localized on the expected cell types. Such experiments would also provide insight into which other cell types, if any, are being inhibited by these antibodies.

We also used blocking antibodies to examine the potential ligand receptors involved in neutrophil recruitment in the bead model, and found a role for ICAM-1. ICAM-1 is known to bind to both LFA-1 and Mac1, and is upregulated on endothelial cells during infection (170, 171). Indeed, we saw expression of ICAM-1 on the endothelium at the two hour timepoint in both infected and control mice (Figure 18), and blocking ICAM-1 resulted in reduced neutrophil recruitment to the capillaries (Figure 19).

We also used blocking antibodies to examine VCAM-1, which is well known to be an important ligand receptor for α_4. This molecule is expressed at low levels constitutively in murine skin endothelium (172). Furthermore, expression on endothelial cells is increased by 2 hours following an inflammatory stimulus (173). In line with these data, we could see expression of VCAM-1 in specific regions of the capillaries within 2-3 hours of treatment with *S. aureus* beads, though not in mice treated with control beads (Figure 17). Furthermore, blocking VCAM-1 yielded a significant reduction in the number of neutrophils in the capillaries (Figure 20), suggesting that VCAM-1 is an important molecule for neutrophil crawling in the capillaries. With this in mind, we decided to block VCAM-1 and ICAM-1 together, to see if blocking both of them could abrogate neutrophil recruitment, similar to effect seen by blocking α_4 and CD18(figure 15).

VCAM-1 and ICAM-1 together did not result in an additive effect (Figure 21), suggesting that these molecules are not the only important ligand receptors for neutrophil recruitment, and that another ligand receptor can mediate neutrophil recruitment to the

capillaries. It is possible that α_4 is binding to another molecule, such as fibronectin (another potential binding partner for this molecule (174) in the capillaries, and inducing changes in neutrophil recruitment through indirect binding to endothelial cells. It would be interesting to investigate further whether other ligand receptors of α_4 might be responsible for this change in behaviour. Another future experiment would be to investigate the co-localization of VCAM-1 and the crawling neutrophils seen in the capillary microvasculature, to further interrogate if VCAM-1 expression is directly associated with the crawling of neutrophils in the capillaries. Furthermore, one could stimulate the endothelium with IL-4 prior to infection with a *S. aureus* bead (which is known to increase expression of VCAM-1 (174), and examine if there are increased numbers of neutrophils in the capillaries, again interrogating the role for VCAM-1 in this model in greater depth.

Additionally, the structure of the endothelium varies with the size of the vessel, the type of vessel, and the depth of the vessel within the skin tissue (142). Thus VCAM-1 and ICAM-1 expression may not be heterogeneous throughout the skin capillaries, but rather may vary depending on depth. Therefore, the roles of these integrin ligand receptors which we saw on the vasculature may not be uniform. Other integrin ligand receptors may play roles at different depth or even different sizes of the capillary vasculature.

6.4 Functional consequences of infection analysis

In Chapter 5 of this investigation, we examined the local consequences of neutrophil recruitment in the capillaries, and investigated some of the broader consequences of inhibiting total neutrophil recruitment.

The absence of perfusion (Figure 23) further confirms that neutrophils are within the capillaries, rather than outside them. We analyzed the images 30 seconds after FITC albumin became visible within the capillaries to allow for blood flow to pass through the microvasculature. Analyzing at later times following FITC administration would have allowed for passive diffusion of the FITC into vessels that were occluded, and thus limited our ability to determine the occlusion of the microvasculature. Additionally, we did not test the effect in the capillaries with isotype controls. This was because the purpose of these antibodies in this assay was to inhibit neutrophil recruitment, and we already tested their ability to perform this action against isotype control treatments in Chapter 4 (Figure 15). FITC albumin is useful for vascular perfusion and flow, but is less useful in measuring microvascular permeability in the periphery, due its large size (66Kda). Future permeability experiments could be performed with other tools such as nanoparticles, like the ones used to label the sterile control beads. These molecules not only can be varied in size (yielding different optical properties), but are also very bright.

We next examined cell death, via propidium iodide staining, to determine the influence of *S. aureus*, and the associated neutrophil recruitment, on cell death in the skin. We saw increased numbers of propidium iodide positive cells within 500μm of the bacteria stimulus, as compared to regions without bacteria. This was found when comparing regions without *S. aureus* in the same mouse (Figure 24c) or comparing mice given *S. aureus* with those given sterile beads (Figure 25c). We also saw a reduction in the number of propidium iodide positive cells when mice were treated with blocking antibodies against CD18 and α_4 with the introduction of the *S. aureus* beads. Thus, neutrophil recruitment results in cell death, as measured by propidium iodide. This was at two hours following infection. One would assume if an infection progressed without neutrophils being recruited, the lack of inflammatory response to the bacteria would

allow for bacterial replication and increase the number of toxins being produced, leading to an increase in the number of dead cells at later timepoints. Many studies have demonstrated that either neutrophil depletion or defects in neutrophil functionality can result in increased tissue damage and increased severity of *S. aureus* infections (83, 109). This demonstrates the central paradox involved in neutrophil recruitment to a *S. aureus* infection site. Obviously neutrophils are important for controlling the infection. However, it may be that the bacteria adapt to neutrophil recruitment, and thus an excess of neutrophils do not lead to effective control of the infection but rather increased bystander tissue damage.

It is possible that some of the dead cells we observed were neutrophils. However, not all neutrophils appear to be dying in response to the *S. aureus* stimuli (Figure 25b, blue cells within the capillaries). The majority of the cells in the FOVs that we examined did not co-stain with the Ly6g neutrophil marker (Figure 26), suggesting that some other cell type is dying due to neutrophil influx. This could be a resident immune cell population in the skin, like γδ T-cells, or tissue resident macrophages. This is particularly interesting given that γδ T-cells are thought to be important in the neutrophil recruitment to sites of *S. aureus* infection in the skin (46). These dead cells could also be resident skin cells, such as keratinocytes. It is likely that more than one type of cell is dying in this model, given that both the neutrophils and the *S. aureus* are capable of releasing widely cytotoxic molecules (2, 31, 60, 88). Future studies could focus on distinguishing what type of cells we are seeing in this model during cell death, by labelling with different cell markers. Furthermore, as propidium iodide is a general cell death marker, it would be interesting to use alternate methods to examine the type of cell death, such as immunofluorescence for caspase-1 cleavage to identify pyroptosis or caspase 3/7 cleavage to identify apoptosis (175). One could also examine whether dead cells co-localize with

neutrophil NETs. NETs are produced in the skin following *S. aureus* infection (54) and are known to cause bystander tissue damage (88). Thus, it is possible that NETs may be contributing to some of the cell death we observed.

After identifying a critical role for neutrophils in cell death, we next examined the effect of neutrophil recruitment on lesion formation 48 hours after introduction of a bead into the mouse skin. We saw that blocking neutrophil recruitment 2 hours after infection caused a significant reduction in lesion size at 48 hours, suggesting that excessive neutrophil recruitment may exacerbate the damage caused by *S. aureus* to the host. One possibility is that the reduced lesion size was caused by the dissemination of the bacteria away from the lesion site and into the bloodstream. To address this, we observed that there were no *S. aureus* CFUs in blood at the 48 hour timepoint, suggesting that the reduction in lesion size did not correspond with bacteria "escaping" the infection site and causing more serious systemic infections (Figure 27c and 27d). Nonetheless, it is worth noting that blood borne bacteria often cause secondary infections in different tissues, and are often rapidly cleared from the bloodstream. It is thus often easier to isolate bacterial CFUs from other organs rather than the blood. Recent work in the Kubes and Zhang labs has suggested that the liver and lungs of mice become infected with *S. aureus* following systemic infection with these bacteria. Therefore, an important future direction would be to harvest these tissues to examine CFUs at the 48 hour timepoint, to better identify whether this infection is remaining localized following treatment with antibodies blocking neutrophil recruitment two hours following infection.

By contrast, treatment with anti-CD18 and anti-α_4 antibodies two hours before infection increased the size of the lesion, suggesting that entirely preventing neutrophil recruitment is detrimental for the host. With too few neutrophils recruited to a *S. aureus* infection site, the

bacteria can replicate and cause increased infection, as the bacteria are not being properly controlled by the host immune system. It is possible that an excess of neutrophils at the infection site is also detrimental, allowing the bacteria to escape, possibly via disruption of neutrophil-mediated bacterial killing following phagocytosis (83, 102, 150). From the host's perspective, it is logical that a massive and immediate response to an infection with *S. aureus* or another skin pathogen would be evolutionarily conserved.

One interesting feature of the *S. aureus* bead model is that it induced less tissue damage, at a later timepoint, when compared with SC injection of *S. aureus* in saline into the skin. This is not unexpected; the CFU for our bead injections was several orders of magnitude less than that used in the *S. aureus*-saline injections. Bacteria in the beads are also not introduced to the host during log phase; they are less metabolically active (having been placed in a bead at 4^{o}C for up to six days) as compared to bacteria injected in saline and thus may not secrete as many toxins at this stage. Furthermore, our model involved injecting a solid bead, which allows for less bacterial spread than the *S. aureus*-saline injection model. Experiments performed within our lab have recently shown that the injection of several beads can cause large open wounds (Surewaard and Kubes, unpublished data), suggesting that this bead model may be able to potently induce tissue damage in subcutaneous infections, given an increase in CFUs to levels comparable to the 10^{8} CFUs used in the subcutaneous injections in saline.

Given the relatively moderate severity of infections induced by the bead model, it is possible that this model could be adapted to generate a longer lasting infection model, compared with saline injections. This is a possibility, especially given that this model was adapted from a cystic fibrosis *P. aeruginosa* infection model that induces lasting infections in rat lungs (127). Therefore, a future direction would be to examine the bead at later timepoints, from several days

to several weeks. This would determine whether this bead model can establish a persistent *S. aureus* infection, as well as identifying further complications at later timepoints.

The capacity of *S. aureus* to manipulate and alter neutrophil behaviours (83, 114), combined with the data demonstrating the detrimental nature of neutrophil recruitment (after the first two hours) on lesion size for the host (Figure 27b) suggests that *S. aureus*-neutrophil interactions may be a means by which this pathogen has evolved to survive and reproduce, to the detriment of the host, in the subcutaneous microenvironment. *S. aureus* appears to be able to survive phagocytosis by neutrophils, disrupting both the phagocytic pathway and manipulating neutrophil cell death following phagocytosis (83, 102, 149, 150). *S. aureus* may also be able to thrive in the subcutaneous region of the skin, in part as a response to being a skin and nasal commensal. Although some commensal bacteria typically evolve to downregulate inflammation and cell death in the host, *S. aureus* strains also incorporate genes that enhance bacterial survival while being actively targeted by the host immune system (30, 102, 150). Thus, commensalism may allow for the evolution of effective anti-immune strategies by this pathogen**.**

6.5 Limitations

There are several limitations of this model. The time required to construct beads means that the bacteria are not in log phase when they are inserted into the skin, but are more likely to be in stationary phase. Log phase bacteria are ideal for infection, as they are metabolically active and secrete exotoxins more readily. However, this also means that our infection model is more likely to recapitulate an infection in a patient, as it is unlikely that patients are infected by *S. aureus* while they are in log phase. The bead component is also a limitation. The agarose used may encourage the overproduction of specific virulence factors. For example, the CCY

media used by Lipinska et al. encourages the production of PVL (25, 29). Therefore, the use of TSA agar may encourage the production of specific virulence factors. Future experiments could involve characterizing the bacterial response to bead generation with different types of agar. This could allow us to refine our model further and enhance the production of various virulence factors in order to better study them. Also, since this model involves exteriorization of the skin, there is a limit to the amount of time that the animal can be imaged, making other endpoints (such as survival, bacterial dissemination, or lesion size) difficult to accommodate. For these reasons, the model has been adjusted when necessary in this study to accommodate later endpoints. We selected individual beads, and injected them in a large bore needle (the same size as used to create the beads originally, to prevent breakup of the bead). These beads were injected in 100μl of saline SC, in order to generate a model similar to our imaging model that could be followed for several days.

We also used the Ly6g antibody clone RB6-8C5 to label neutrophils. It is well known that this specific antibody does not bind only to Ly6g, but also to Ly6c, and thus recognizes not only neutrophils, but also other cells types such as monocytes (129, 176). Therefore, one could argue that our data could be representative of monocytes crawling in the capillaries, rather than neutrophils. In fact, monocytes are known to patrol within the vasculature (177), thus the "neutrophil" population that was recruited to the capillaries during *S. aureus* infection could actually be monocytes. To examine this possibility, we used the anti-Ly6g monoclonal antibody 1A8 (Appendix Figure 3), a clone that is known to target neutrophils exclusively (129). We observed no statistical differences in overall neutrophil recruitment per FOV or numbers of neutrophils in the capillaries, when compared with mice given the Ly6g antibody clone RB6-

8C5. Thus we can conclude that the cells being labelled by the Ly6g antibody clone RB6-8C5 that crawl within the capillaries are likely neutrophils.

Another limitation of this model is the influence that the dual blocking antibodies, anti-CD18 and anti-α_4, have on the venules in the subcutaneous soft tissue. For the cell death assay (Figure 25) and changes in lesion sizes (Figure 27), the observed effects of decreased cell death and decreased lesion size may be due to changes in neutrophil recruitment within the capillaries, within the venules, or within some combination of the two. Our ability to individually study the effect of behaviours in the capillaries or venules separately from one another is thus limited. Nonetheless, these experiments provide important information about the physiological effects of total neutrophil recruitment.

Another limitation is that in both the FITC albumin experiments and the propidium iodide experiments, there is the potential that CD18 and α_4 blocking antibody are inducing changes in other, unlabelled cell types present in the vasculature. CD18 and α_4 are not found only on neutrophils, but are rather found on a wide variety of other blood borne immunocytes, such as monocytes (169, 178) and T-cells (72). Thus other cell types may be involved in the blockage of capillaries, and might be responsible for the change in perfusion.

The latter limitation also applies to the lesion experiments. Injecting anti-α_4 and anti-CD18 antibodies systemically likely had effects on cells that were not neutrophils. This may be of less importance at a 2 hour timepoint, when both the imaging and the infection were focused on a short timeframe. It is less likely that the anti-CD18 and α_4 antibodies would have an effect on other immunocytes leading to changes in neutrophil recruitment and cell death at this timeframe, as within two hours neutrophils are the predominant immunocyte recruited to *S. aureus* infections. However, with the 48 hour lesion studies, this may be of more concern. As

many other cells have these integrins, including other myeloid and lymphoid cells, like monocytes and T-cells (72, 169, 178), they will be affected by the treatment with blocking antibodies. A simple future direction to address this concern would be to deplete neutrophils and then examine whether the treatment with the blocking antibodies had any effect on the lesion size, when compared with neutrophil-depleted mice treated with isotype control antibodies.

One common limitation is that many mouse models do not effectively reproduce inflammatory changes found in humans (179). In the *S. aureus* literature in particular, much of the controversy concerning PVL has been due to the fact that neutrophils from different mammals appear to have different susceptibilities to PVL (24, 25). It is possible that neutrophil crawling within the capillaries does not occur in humans. However, examining this possibility is problematic, due to the difficulties in imaging humans. Using an *in vitro* model of human tissue may also prove problematic, as many of the observations we have made occur in the microvasculature of the capillary beds. An *in vitro* model would have to generate vessels that are $\leq$10 µM in diameter and would need to use endothelium that was cultured in order to reflect capillary conditions, as it is possible that these behaviours occur due to functional heterogeneity between capillary and venular endothelial cells. A possible future direction to address the limitation of this behaviour would be to examine neutrophils *in vivo* in another mammalian species, to assess whether or not crawling within the capillaries, and the effect of blocking neutrophils at different timepoints on lesion formation, is a mouse-specific phenomenon. Alternatively, a humanized mouse where human skin is placed on a SCID mouse, as was performed by Ho et al. (180) could be performed.

It would also be interesting to investigate whether other cell types are interacting in the capillaries, either directly with adherent and crawling neutrophils or as a downstream effect of

neutrophil occlusion of the capillary microvasculature. Typically, when capillaries are occluded, other cells are unable to move through the capillary vasculature. Platelets, which have recently been shown to play anti-microbial functions in the liver (181) and can be activated and form thrombi following damage to endothelial cells (182), may not be able to pass by these occluding neutrophils. Furthermore, platelets and neutrophils have been shown to interact in deep vein thrombosis, which results in intravenous thrombosis in the microvasculature (183, 184). Do platelets become activated and form thrombi in the capillary microvasculature following neutrophil occlusion of the capillaries, further inhibiting perfusion? Investigating this could further aid in determining whether these neutrophils perform a beneficial or detrimental role to the host; if there are thrombi forming in the capillaries, one could hypothesize that these are either the beginnings of abscess formation to protect the host, or alternately, are another method by which bystander tissue damage occurs.

6.6 Significance and final Conclusions

To conclude, in this study we have examined the role of neutrophils in *S. aureus* subcutaneous infections. Using spinning disk confocal microscopy, we have developed a new model for examining neutrophil recruitment using an agarose bead containing *S. aureus* and have characterized the behaviour of neutrophils recruited to this bead. We found that neutrophils are not only recruited in the venules surrounding the bead site, but also are recruited in the capillaries surrounding the bead, which is a novel observation in the *S. aureus* literature. We determined that the molecules responsible for this behaviour were the β_2 and α_4 integrins, binding with ICAM-1 and VCAM-1, and causing occlusion of the capillary microvasculature. Blocking neutrophil recruitment reduces cell death, and if performed ~2hrs after the initial stages

of neutrophil recruitment, will reduce lesion size several days after infection with the bead. Future investigations will aim to elucidate whether this model can be translated into a persistent infection, as well as further interrogate the potential detriments to reducing neutrophil recruitment to a *S. aureus* infection site, and the effects of variable neutrophil recruitment on other cell types, such as platelets. These future investigations will hopefully lead to the development of clinically translatable strategies to modulate pathogen-host interactions in *S. aureus* infections.

References

1. Wertheim HF, Melles DC, Vos MC, van Leeuwen W, van Belkum A, Verbrugh HA, et al. The role of nasal carriage in staphylococcus aureus infections. The Lancet Infectious Diseases. 2005 12;5(12):751-62.

2. Miller LS, Cho JS. Immunity against staphylococcus aureus cutaneous infections. Nat Rev Immunol. 2011 07/01;advance online publication.

3. Moran GJ, Krishnadasan A, Gorwitz RJ, Fosheim GE, McDougal LK, Carey RB, et al. Methicillin-resistant S. aureus infections among patients in the emergency department. N Engl J Med. 2006 08/17;355(7):666-74.

4. Yamamoto T, Nishiyama A, Takano T, Yabe S, Higuchi W, Razvina O, et al. Community-acquired methicillin-resistant staphylococcus aureus: Community transmission, pathogenesis, and drug resistance. Journal of Infection and Chemotherapy. 2010 08/01;16(4):225-54.

5. Kirby WMM. Extraction of a highly potent penicillin inactivator from penicillin resistant staphylococci. Science. 1944;99(2579):452.

6. M. Patricia Jevons. "Celbenin" - resistant staphylococci. BMJ. 1961 BMJ Publishing Group Ltd;1(5219):124-5.

7. Shore AC, Coleman DC. Staphylococcal cassette chromosome mec: Recent advances and new insights. International Journal of Medical Microbiology. 2013;303(4).

8. Hartman B, Tomasz A. Low-affinity penicillin-binding protein associated with beta-lactam resistance in staphylococcus aureus. Journal of Bacteriology. 1984;158(2):513-6.

9. International Working Group on the Classification of Staphylococcal Cassette Chromosome Elements (IWG-SCC). Classification of staphylococcal cassette chromosome mec (SCCmec): Guidelines for reporting novel SCCmec elements. Antimicrobial Agents and Chemotherapy. 2009 December 01;53(12):4961-7.

10. Baba T, Takeuchi F, Kuroda M, Yuzawa H, Aoki K, Oguchi A, et al. Genome and virulence determinants of high virulence community-acquired MRSA. The Lancet. 2002 5/25;359(9320):1819-27.

11. Ala'Aldeen D. A non-multiresistant community MRSA exposes its genome. The Lancet. 2002 5/25;359(9320):1791-2.

12. Diep BA, Stone GG, Basuino L, Graber CJ, Miller A, des Etages S, et al. The arginine catabolic mobile element and staphylococcal chromosomal cassette mec linkage: Convergence of

virulence and resistance in the USA300 clone of methicillin-resistant staphylococcus aureus. Journal of Infectious Diseases. 2008 June 01;197(11):1523-30.

13. Sievert DM, Rudrik JT, Patel JB, McDonald LC, Wilkins MJ, Hageman JC. Vancomycin-resistant staphylococcus aureus in the united states, 2002–2006. Clinical Infectious Diseases. 2008 March 01;46(5):668-74.

14. Reynolds PE. Structure, biochemistry and mechanism of action of glycopeptide antibiotics. . 1989;8(11):943-950.

15. Mwangi MM, Wu SW, Zhou Y, Sieradzki K, de Lencastre H, Richardson P, et al. Tracking the in vivo evolution of multidrug resistance in staphylococcus aureus by whole-genome sequencing. Proceedings of the National Academy of Sciences. 2007 May 29;104(22):9451-6.

16. Tenover FC, Goering RV. Methicillin-resistant staphylococcus aureus strain USA300: Origin and epidemiology. Journal of Antimicrobial Chemotherapy. 2009 September 01;64(3):441-6.

17. Harris TL, Worthington RJ, Melander C. Potent small-molecule suppression of oxacillin resistance in methicillin-resistant staphylococcus aureus. Angew Chem Int Ed. 2012 11/05;51(45):11254-7.

18. King MD, Humphrey BJ, Wang YF, Kourbatova EV, Ray SM, Blumberg HM. Emergence of community-acquired methicillin-resistant staphylococcus aureus USA 300 clone as the predominant cause of skin and soft-tissue infections. Ann Intern Med. 2006 03/07;144(5):309-17.

19. Wu K, Conly J, McClure J-, Elsayed S, Louie T, Zhang K. Caenorhabditis elegans as a host model for community-associated methicillin-resistant staphylococcus aureus. Clinical Microbiology and Infection. 2010;16(3):245-54.

20. Al-Rawahi GN, Reynolds S, Porter SD, Forrester L, Kishi L, Chong T, et al. Community-associated CMRSA-10 (USA-300) is the predominant strain among methicillin-resistant staphylococcus aureus strains causing skin and soft tissue infections in patients presenting to the emergency department of a canadian tertiary care hospital. J Emerg Med. 2010 1;38(1):6-11.

21. Andrew E, Simor M, Nicolas L., Gilbert M, Denise Gravel M, Michael R, Mulvey P, Elizabeth Bryce M, Mark Loeb M, et al. Methicillin Resistant staphylococcus aureus colonization or infection in canada: National surveillance and changing epidemiology, 1995-2007. Infection Control and Hospital Epidemiology. 2010 04/01;31(4):348-56.

22. Wilmer A, M.D., Lloyd-Smith E, Romney M, M.D., Hoang L, M.D., Hull M, M.D., Champagne S, M.D. Methicillin-resistant staphylococcus aureus strain USA300 is prevalent among hospital-onset cases in an urban canadian setting. Infection Control and Hospital Epidemiology. 2011 12/01;32(12):1227-9.

23. Thurlow L, Joshi G, Clark J, Spontak J, Neely C, Maile R, et al. Functional modularity of the arginine catabolic mobile element contributes to the success of USA300 methicillin-resistant staphylococcus aureus. Cell Host & Microbe. 2013 /1/16/;13(1):100-7.

24. Kobayashi SD, Malachowa N, Whitney AR, Braughton KR, Gardner DJ, Long D, et al. Comparative analysis of USA300 virulence determinants in a rabbit model of skin and soft tissue infection. Journal of Infectious Diseases. 2011 September 15;204(6):937-41.

25. Lipinska U, Hermans K, Meulemans L, Dumitrescu O, Badiou C, Duchateau L, et al. Panton-valentine leukocidin does play a role in the early stage of*Staphylococcus aureus*Skin infections: A rabbit model. PLoS ONE. 2011 08/05;6(8):e22864.

26. Loffler B, Hussain M, Grundmeier M, Bruck M, Holzinger D, Varga G, et al. *Staphylococcus aureus*Panton-valentine leukocidin is a very potent cytotoxic factor for human neutrophils. PLoS Pathog. 2010 01/08;6(1):e1000715 EP -.

27. Li M, Cheung G, Hu J, Wang D, Joo HS, DeLeo F , et al. Comparative analysis of virulence and toxin expression of global community associated methicillin • Resistant staphylococcus aureus strains. J Infect Dis. 2010 12/15;202(12):1866-76.

28. Spaan A, Henry T, van Rooijen WM, Perret M, Badiou C, Aerts P, et al. The staphylococcal toxin panton-valentine leukocidin targets human C5a receptors. Cell Host & Microbe. 2013 5/15;13(5):584-94.

29. Woodin A. Fractionation of a leucocidin from staphylococcus aureus. Biochemical Journal. 1959;73:225-37.

30. Li M, Diep BA, Villaruz AE, Braughton KR, Jiang X, DeLeo FR, et al. Evolution of virulence in epidemic community-associated methicillin-resistant staphylococcus aureus. Proceedings of the National Academy of Sciences. 2009 04/07;106(14):5883-8.

31. Wang R, Braughton KR, Kretschmer D, Bach TL, Queck SY, Li M, et al. Identification of novel cytolytic peptides as key virulence determinants for community-associated MRSA. Nat Med. 2007 print;13(12):1510-4.

32. Krishna S, Miller L. Innate and adaptive immune responses against staphylococcus aureus skin infections. . 2012;34(2):261-280.

33. Haugwitz U, Bobkiewicz W, Han S, Beckmann E, Veerachato G, Shaid S, et al. Pore-forming staphylococcus aureus Î±-toxin triggers epidermal growth factor receptor-dependent proliferation. Cell Microbiol. 2006 10/01;8(10):1591-600.

34. Afshar M, Gallo RL. Innate immune defense system of the skin. Vet Dermatol. 2013 02/01;24(1):32-e9.

35. Harder J, Gläser R, Schröder J. Review: Human antimicrobial proteins — effectors of innate immunity. Journal of Endotoxin Research. 2007 December 01;13(6):317-38.

36. Kisich KO, Howell MD, Boguniewicz M, Heizer HR, Watson NU, Leung DY. The constitutive capacity of human keratinocytes to kill staphylococcus aureus is dependent on [beta]-defensin 3. J Invest Dermatol. 2007;127(10):2368-80.

37. Zanger P, Holzer J, Schleucher R, Scherbaum H, Schittek B, Gabrysch S. Severity of staphylococcus aureus infection of the skin is associated with inducibility of human β-defensin 3 but not human β-defensin 2. Infection and Immunity. 2010 July 01;78(7):3112-7.

38. Lai Y, Cogen A, Radek K, Park HJ, MacLeod D, Leichtle A, et al. Activation of TLR2 by a small molecule produced by staphylococcus epidermidis increases antimicrobial defense against bacterial skin infections. J Invest Dermatol. 2010;130(9):2211-21.

39. Cogen A, Yamasaki K, Sanchez K, Dorschner R, Lai Y, MacLeod D, et al. Selective antimicrobial action is provided by phenol-soluble modulins derived from staphylococcus epidermidis, a normal resident of the skin. J Invest Dermatol. 2009;130(1):192-200.

40. Prabhakara R, Foreman O, De Pascalis R, Lee GM, Plaut RD, Kim SY, et al. Epicutaneous model of community-acquired staphylococcus aureus skin infections. Infection and Immunity. 2013 April 01;81(4):1306-15.

41. Kugelberg E, Norström T, Petersen TK, Duvold T, Andersson DI, Hughes D. Establishment of a superficial skin infection model in mice by using staphylococcus aureus and streptococcus pyogenes. Antimicrobial Agents and Chemotherapy. 2005 August 01;49(8):3435-41.

42. Begier EM, Frenette K, Barrett NL, Mshar P, Petit S, Boxrud DJ, et al. A high-morbidity outbreak of methicillin-resistant staphylococcus aureus among players on a college football team, facilitated by cosmetic body shaving and turf burns. Clinical Infectious Diseases. 2004 November 15;39(10):1446-53.

43. Hruz P, Zinkernagel AS, Jenikova G, Botwin GJ, Hugot J, Karin M, et al. NOD2 contributes to cutaneous defense against staphylococcus aureus through α-toxin-dependent innate immune activation. Proceedings of the National Academy of Sciences. 2009 August 04;106(31):12873-8.

44. Miller LS, Pietras EM, Uricchio LH, Hirano K, Rao S, Lin H, et al. Inflammasome-mediated production of IL-1β is required for neutrophil recruitment against staphylococcus aureus in vivo. The Journal of Immunology. 2007 November 15;179(10):6933-42.

45. Miller LS, O'Connell RM, Gutierrez MA, Pietras EM, Shahangian A, Gross CE, et al. MyD88 mediates neutrophil recruitment initiated by IL-1R but not TLR2 activation in immunity against staphylococcus aureus. Immunity. 2006 1;24(1):79-91.

46. Cho JS, Pietras EM, Garcia NC, Ramos RI, Farzam DM, Monroe HR, et al. IL-17 is essential for host defense against cutaneous staphylococcus aureus infection in mice. J Clin Invest. 2010 05/03;120(5):1762-73.

47. Liese J, Rooijakkers SHM, van Strijp, Jos A. G., Novick RP, Dustin ML. Intravital two-photon microscopy of hostâ€“pathogen interactions in a mouse model of staphylococcus aureus skin abscess formation. Cell Microbiol. 2013 01/01:n/a,n/a.

48. Cho JS, Guo Y, Ramos RI, Hebroni F, Plaisier SB, Xuan C, et al. Neutrophil-derived IL-1B is sufficent for abscess formation in immunity against*Staphylococcus aureus* in mice. PLoS Pathog. 2012;11(8).

49. Nippe N, Varga G, Holzinger D, Loffler B, Medina E, Becker K, et al. Subcutaneous infection with S. aureus in mice reveals association of resistance with influx of neutrophils and Th2 response. J Invest Dermatol. 2011 print;131(1):125-32.

50. Gillrie MR, Zbytnuik L, McAvoy E, Kapadia R, Lee K, Waterhouse CCM, et al. Divergent roles of toll-like receptor 2 in response to lipoteichoic acid and staphylococcus aureus in vivo. Eur J Immunol. 2010;40(6):1639-50.

51. Takeuchi O, Hoshino K, Kawai T, Sanjo H, Takada H, Ogawa T, et al. Differential roles of TLR2 and TLR4 in recognition of gram-negative and gram-positive bacterial cell wall components. Immunity. 1999 10/1;11(4):443-51.

52. Takeuchi O, Hoshino K, Akira S. Cutting edge: TLR2-deficient and MyD88-deficient mice are highly susceptible to staphylococcus aureus infection. The Journal of Immunology. 2000 November 15;165(10):5392-6.

53. Jann NJ, Schmaler M, Ferracin F, Landmann R. TLR2 enhances NADPH oxidase activity and killing of staphylococcus aureus by PMN. Immunol Lett. 2011 3/30;135(1-2):17-23.

54. Yipp BG, Petri B, Salina D, Jenne CN, Scott BN, Zbytnuik LD, et al. Infection-induced NETosis is a dynamic process involving neutrophil multitasking*in vivo*. Nat Med. 2012 2012/09;18(9):1386-93.

55. Clarke SR, Mohamed R, Bian L, Routh AF, Kokai-Kun JF, Mond JJ, et al. The staphylococcus aureus surface protein IsdA mediates resistance to innate defenses of human skin. Cell Host & Microbe. 2007 5/17;1(3):199-212.

56. Sieprawska-Lupa M, Mydel P, Krawczyk K, Wójcik K, Puklo M, Lupa B, et al. Degradation of human antimicrobial peptide LL-37 by staphylococcus aureus-derived proteinases. Antimicrobial Agents and Chemotherapy. 2004 December 01;48(12):4673-9.

57. Liu C, Liu GY, Song Y, Yin F, Hensler ME, Jeng W, et al. A cholesterol biosynthesis inhibitor blocks staphylococcus aureus virulence. Science. 2008 March 07;319(5868):1391-4.

58. Simanski M, Glaser R, Katen B, Meyer-Hoffert U, Wanner S, Weidenmaier C, et al. Staphylococcus aureus subverts cutaneous defense by d-alanylation of teichoic acids. Exp Dermatol. 2013 04/01;22(4):294-6.

59. Soong G, Chun J, Parker D, Prince A. Staphylococcus aureus activation of caspase 1/calpain signaling mediates invasion through human keratinocytes. Journal of Infectious Diseases. 2012 May 15;205(10):1571-9.

60. Valeva A, Walev I, Pinkernell M, Walker B, Bayley H, Palmer M, et al. Transmembrane β-barrel of staphylococcal α-toxin forms in sensitive but not in resistant cells. Proceedings of the National Academy of Sciences. 1997 October 14;94(21):11607-11.

61. Molne L, Verdrengh M, Tarkowski A. Role of neutrophil leukocytes in cutaneous infection caused by staphylococcus aureus. Infect Immun. 2000 November 1;68(11):6162-7.

62. Schmidt S, Moser M, Sperandio M. The molecular basis of leukocyte recruitment and its deficiencies. Mol Immunol. 2013 8;55(1):49-58.

63. Hidalgo A, Peired AJ, Wild MK, Vestweber D, Frenette PS. Complete identification of E-selectin ligands on neutrophils reveals distinct functions of PSGL-1, ESL-1, and CD44. Immunity. 2007 4/27;26(4):477-89.

64. Ley K, Laudanna C, Cybulsky MI, Nourshargh S. Getting to the site of inflammation: The leukocyte adhesion cascade updated. Nat Rev Immunol. 2007 print;7(9):678-89.

65. Hwang JM, Yamanouchi J, Santamaria P, Kubes P. A critical temporal window for selectin-dependent CD4+ lymphocyte homing and initiation of late-phase inflammation in contact sensitivity. J Exp Med. 2004 05/03;199(9):1223-34.

66. Petri B, Phillipson M, Kubes P. The physiology of leukocyte recruitment: An in vivo perspective. The Journal of Immunology. 2008 05/15;180(10):6439-46.

67. Lefort CT, Ley K. Neutrophil arrest by LFA-1 activation. Frontiers in Immunology. 2012;3.

68. Dixit N, Kim M, Rossaint J, Yamayoshi I, Zarbock A, Simon SI. Leukocyte function antigen-1, kindlin-3, and calcium flux orchestrate neutrophil recruitment during inflammation. The Journal of Immunology. 2012 December 15;189(12):5954-64.

69. Lim J, Hotchin NA. Signalling mechanisms of the leukocyte integrin Î±MÎ²2: Current and future perspectives. Biology of the Cell. 2012 11/01;104(11):631-40.

70. Moser M, Legate KR, Zent R, Fässler R. The tail of integrins, talin, and kindlins. Science. 2009 May 15;324(5929):895-9.

71. Phillipson M, Heit B, Colarusso P, Liu L, Ballantyne CM, Kubes P. Intraluminal crawling of neutrophils to emigration sites: A molecularly distinct process from adhesion in the recruitment cascade. The Journal of Experimental Medicine. 2006 November 27;203(12):2569-75.

72. Kadioglu A, De Filippo K, Bangert M, Fernandes VE, Richards L, Jones K, et al. The integrins mac-1 and α4β1 perform crucial roles in neutrophil and T cell recruitment to lungs during streptococcus pneumoniae infection. The Journal of Immunology. 2011 May 15;186(10):5907-15.

73. Ibbotson GC, Doig C, Kaur J, Gill V, Ostrovsky L, Fairhead T, et al. Functional (alpha)4-integrin: A newly identified pathway of neutrophil recruiment in critically ill septic patients. Nat Med. 2001;7(4):465-70.

74. Phillipson M, Kaur J, Colarusso P, Ballantyne CM, Kubes P. Endothelial domes encapsulate adherent neutrophils and minimize increases in vascular permeability in paracellular and transcellular emigration. PLoS ONE. 2008 02/20;3(2):e1649.

75. Kolaczkowska E, Kubes P. Neutrophil recruitment and function in health and inflammation. Nat Rev Immunol. 2013;13(3):159-75.

76. Sumagin R, Sarelius IH. Intercellular adhesion molecule-1 enrichment near tricellular endothelial junctions is preferentially associated with leukocyte transmigration and signals for reorganization of these junctions to accommodate leukocyte passage. The Journal of Immunology. 2010 05/01;184(9):5242-52.

77. Petri B, Kaur J, Long EM, Li H, Parsons SA, Butz S, et al. Endothelial LSP1 is involved in endothelial dome formation, minimizing vascular permeability changes during neutrophil transmigration in vivo. Blood. 2011 January 20;117(3):942-52.

78. Stark K, Eckart A, Haidari S, Tirniceriu A, Lorenz M, von Bruehl M, et al. Capillary and arteriolar percityes attract innate leukocytes exiting through venules and 'instruct' them with pattern-recognition and motility programs. Nat Immunol. 2013 2013/01//print;14(1):41-51.

79. Heit B, Tavener S, Raharjo E, Kubes P. An intracellular signaling hierarchy determines direction of migration in opposing chemotactic gradients. The Journal of Cell Biology. 2002 October 14;159(1):91-102.

80. McDonald B, Pittman K, Menezes GB, Hirota SA, Slaba I, Waterhouse CCM, et al. Intravascular danger signals guide neutrophils to sites of sterile inflammation. Science. 2010 10/15;330(6002):362-6.

81. Wong CHY, Heit B, Kubes P. Molecular regulators of leucocyte chemotaxis during inflammation. Cardiovasc Res. 2010 05/01;86(2):183-91.

82. Phillipson M, Kubes P. The neutrophil in vascular inflammation. Nat Med. 2011;17(11):1381-90.

83. Rigby K, DeLeo F. Neutrophils in innate host defense against staphylococcus aureus infections. Seminars in Immunopathology. 2012 03/01;34(2):237-59.

84. Segal A. How neutrophils kill microbes. Annu Rev Immunol. 2005;23:197-223.

85. Brinkmann V, Reichard U, Goosmann C, Fauler B, Uhlemann Y, Weiss DS, et al. Neutrophil extracellular traps kill bacteria. Science. 2004 03/05;303(5663):1532-5.

86. Jenne C, Wong CY, Zemp F, McDonald B, Rahman M, Forsyth P, et al. Neutrophils recruited to sites of infection protect from virus challenge by releasing neutrophil extracellular traps. Cell Host & Microbe. 2013 2/13;13(2):169-80.

87. Menegazzi R, Decleva E, Dri P. Killing by neutrophil extracellular traps: Fact or folklore? Blood. 2012 February 02;119(5):1214-6.

88. Clark SR, Ma AC, Tavener SA, McDonald B, Goodarzi Z, Kelly MM, et al. Platelet TLR4 activates neutrophil extracellular traps to ensnare bacteria in septic blood. Nat Med. 2007 print;13(4):463-9.

89. Pilsczek FH, Salina D, Poon KKH, Fahey C, Yipp BG, Sibley CD, et al. A novel mechanism of rapid nuclear neutrophil extracellular trap formation in response to staphylococcus aureus. The Journal of Immunology. 2010 12/15;185(12):7413-25.

90. Darr MC, Kristian SA, Otto M, Matteoli G, Margolis PS, Trias J, et al. Neutrophil chemotaxis by pathogen-associated molecular patterns: formylated peptides are crucial but not the sole neutrophil attractants produced by staphylococcus aureus. Cell Microbiol. 2006;8(2):207-17.

91. Mantovani A, Cassatella MA, Costantini C, Jaillon S. Neutrophils in the activation and regulation of innate and adaptive immunity. Nat Rev Immunol. 2011 print;11(8):519-31.

92. Netea MG, Simon A, van dV, Kullberg B, Van dM, Joosten LAB. IL-1Î² processing in host defense: Beyond the inflammasomes. PLoS Pathog. 2010 02/26;6(2):e1000661.

93. Mankan AK, Dau T, Jenne D, Hornung V. The NLRP3/ASC/caspase-1 axis regulates IL-1β processing in neutrophils. Eur J Immunol. (3):710.

94. Jaillon S, Galdiero MR, Prete D, Cassatella MA, Garlanda C, Mantovani A. Neutrophils in innate and adaptive immunity. Seminars in Immunopathology. 2013 07/01;35(4):377-94.

95. Peters-Golden M, Henderson WR. Leukotrienes. N Engl J Med. 2007 11/01; 2013/05;357(18):1841-54.

96. Kim M, Granick JL, Kwok C, Walker NJ, Borjesson DL, Curry FE, et al. Neutrophil survival and c-kit+-progenitor proliferation in staphylococcus aureusâ€“infected skin wounds promote resolution. Blood. 2011 03/24;117(12):3343-52.

97. de Haas CJC, Veldkamp KE, Peschel A, Weerkamp F, Van Wamel WJB, Heezius ECJM, et al. Chemotaxis inhibitory protein of staphylococcus aureus, a bacterial antiinflammatory agent. The Journal of Experimental Medicine. 2004 March 01;199(5):687-95.

98. Postma B, Poppelier MJ, van Galen JC, Prossnitz ER, van Strijp JAG, de Haas CJC, et al. Chemotaxis inhibitory protein of staphylococcus aureus binds specifically to the C5a and formylated peptide receptor. The Journal of Immunology. 2004 June 01;172(11):6994-7001.

99. Higgins J, Loughman A, Van Kessel KPM, Van Strijp JAG, Foster TJ. Clumping factor A of staphylococcus aureus inhibits phagocytosis by human polymorphonuclear leucocytes. FEMS Microbiol Lett. 2006;258(2):290-6.

100. Bartlett AH, Foster TJ, Hayashida A, Park PW. A-toxin facilitates the generation of CXC chemokine gradients and stimulates neutrophil homing in staphylococcus aureus pneumonia. Journal of Infectious Diseases. 2008 November 15;198(10):1529-35.

101. Forsman H, Christenson K, Bylund J, Dahlgren C. Receptor-dependent and -independent immunomodulatory effects of phenol-soluble modulin peptides from staphylococcus aureus on human neutrophils are abrogated through peptide inactivation by reactive oxygen species. Infection and Immunity. 2012 June 01;80(6):1987-95.

102. Pang YY, Schwartz J, Thoendel M, Ackermann LW, Horswill AR, Nauseef WM. Agr-dependent interactions of staphylococcus aureus USA300 with human polymorphonuclear neutrophils. J Innate Immun. 2010;2(6):546-59.

103. Muñoz-Planillo R, Franchi L, Miller LS, Núñez G. A critical role for hemolysins and bacterial lipoproteins in staphylococcus aureus-induced activation of the Nlrp3 inflammasome. The Journal of Immunology. 2009 September 15;183(6):3942-8.

104. Craven RR, Gao X, Allen IC, Gris D, Wardenburg JB, McElvania-TeKippe E, et al. *Staphylococcus aureus*Î±-hemolysin activates the NLRP3-inflammasome in human and mouse monocytic cells. PLoS ONE. 2009 10/14;4(10):e7446.

105. Suttorp N, Seeger W, Zucker-Reimann J, Roka L, Bhakdi S. Mechanism of leukotriene generation in polymorphonuclear leukocytes by staphylococcal alpha-toxin. Infection and Immunity. 1987 January 01;55(1):104-10.

106. Carnes E, Lopez D, Donegan N, Cheung A, Gresham H, Timmins G, et al. Confinement-induced quorum sensing of individual staphylococcus aureus bacteria. Nat Chem Biol. 2010;6(1):41-5.

107. Thammavongsa V, Kern JW, Missiakas DM, Schneewind O. Staphylococcus aureus synthesizes adenosine to escape host immune responses. The Journal of Experimental Medicine. 2009 October 26;206(11):2417-27.

108. Cronstein BN, Haskó G. Regulation of inflammation by adenosine. Frontiers in Immunology. 2013;4.

109. Robertson CM, Perrone EE, McConnell KW, Dunne WM, Boody B, Brahmbhatt T, et al. Neutrophil depletion causes a fatal defect in murine pulmonary staphylococcus aureus clearance. J Surg Res. 2008 12;150(2):278-85.

110. Hoffmann MH, Bruns H, Bäckdahl L, Neregård P, Niederreiter B, Herrmann M, et al. The cathelicidins LL-37 and rCRAMP are associated with pathogenic events of arthritis in humans and rats. Annals of the Rheumatic Diseases. 2012 November 21.

111. Moraes T, Zurawska J, Downey G. Neutrophil granule contents in the pathogenesis of lung injury. Curr Op, Hema. 2006;13(1):21-7.

112. McDonald B, Urrutia R, Yipp B, Jenne C, Kubes P. Intravascular neutrophil extracellular traps capture bacteria from the bloodstream during sepsis. Cell Host & Microbe. 2012 9/13;12(3):324-33.

113. Gresham HD, Lowrance JH, Caver TE, Wilson BS, Cheung AL, Lindberg FP. Survival of staphylococcus aureus inside neutrophils contributes to infection. The Journal of Immunology. 2000 April 01;164(7):3713-22.

114. Thwaites GE, Gant V. Are bloodstream leukocytes trojan horses for the metastasis of staphylococcus aureus? Nat Rev Micro. 2011 print;9(3):215-22.

115. van Sorge NM, Beasley FC, Gusarov I, Gonzalez DJ, von Köckritz-Blickwede M, Anik S, et al. Methicillin-resistant staphylococcus aureus bacterial nitric-oxide synthase affects antibiotic sensitivity and skin abscess development. Journal of Biological Chemistry. 2013 March 01;288(9):6417-26.

116. Bubeck Wardenburg J, Palazzolo-Ballance AM, Otto M, Schneewind O, DeLeo FR. Panton-valentine leukocidin is not a virulence determinant in murine models of community-associated methicillin-resistant staphylococcus aureus disease. Journal of Infectious Diseases. 2008 October 15;198(8):1166-70.

117. Kennedy AD, Wardenburg JB, Gardner DJ, Long D, Whitney AR, Braughton KR, et al. Targeting of alpha-hemolysin by active or passive immunization decreases severity of USA300 skin infection in a mouse model. Journal of Infectious Diseases. 2010 October 01;202(7):1050-8.

118. Brubaker AL, Rendon JL, Ramirez L, Choudhry MA, Kovacs EJ. Reduced neutrophil chemotaxis and infiltration contributes to delayed resolution of cutaneous wound infection with advanced age. The Journal of Immunology. 2013 February 15;190(4):1746-57.

119. Cho JS, Zussman J, Donegan N, Ramos RI, Garcia NC, Uslan D, et al. Noninvasive in vivo imaging to evaluate immune responses and antimicrobial therapy against staphylococcus aureus and USA300 MRSA skin infections. J Invest Dermatol. 2011;131(4):907-15.

120. Levenson SM, Kan-Gruber D, Gruber C, Molnar J, Seifter,E. Wound healing accelerated by staphylococcus aureus. Archives of Surgery. 1983 03/01;118(3):310-20.

121. Noble WC. The production of subcutaneous staphylococcal skin lesions in mice. Br J Exp Pathol. 1965;46(3):254-62.

122. James RC, MacLeod CJ. Induction of staphyloccal infections in mice with small inocula introduced on sutures. Br J Exp Pathol. 1961;42(3):266-77.

123. Yoong P, Pier GB. Antibody-mediated enhancement of community-acquired methicillin-resistant staphylococcus aureus infection. Proceedings of the National Academy of Sciences. 2010 February 02;107(5):2241-6.

124. Ford CW, Hamel JC, Stapert D, Yancey RJ. Establishment of an experimental model of a staphylococcus aureus abscess in mice by use of dextran and gelatin microcarriers. Journal of Medical Microbiology. 1989 April 01;28(4):259-66.

125. Graf R, Rietdorf J, Zimmermann T. Live cell spinning disk microscopy. In: Rietdorf J, editor. Springer Berlin Heidelberg; 2005. p. 57-75.

126. Shimozawa T, Yamagata K, Kondo T, Hayashi S, Shitamukai A, Konno D, et al. Improving spinning disk confocal microscopy by preventing pinhole cross-talk for intravital imaging. Proceedings of the National Academy of Sciences. 2013 February 26;110(9):3399-404.

127. Guilbault C, Martin P, Houle D, Boghdady M, Guiot M, Marion D, et al. Cystic fibrosis lung disease following infection with pseudomonas aeruginosa in cftr knockout mice using novel non-invasive direct pulmonary infection technique. Laboratory Animals. 2005 July 01;39(3):336-52.

128. Cash HA, Woods DE, McCullough B, Johanson WGJ, Bass JA.
A rat model of chronic respiratory infection with Pseudomonas aeruginosa**.** Am Rev Respir Dis. 1979;3(119):453-9.

129. Daley JM, Thomay AA, Connolly MD, Reichner JS, Albina JE. Use of Ly6G-specific monoclonal antibody to deplete neutrophils in mice. Journal of Leukocyte Biology. 2008 January 01;83(1):64-70.

130. Wolfenson H, Lavelin I, Geiger B. Dynamic regulation of the structure and functions of integrin adhesions. Developmental Cell. 2013 3/11;24(5):447-58.

131. Abram CL, Lowell CA. The ins and outs of leukocyte integrin signaling. Annu Rev Immunol. 2009 04/01; 2013/07;27(1):339-62.

132. Luo B, Carman CV, Springer TA. Structural basis of integrin regulation and signaling. Annu Rev Immunol. 2007 04/01; 2013/07;25(1):619-47.

133. Hogg N, Patzak I, Willenbrock F. The insider's guide to leukocyte integrin signalling and function. Nat Rev Immunol. 2011;11(6):416-26.

134. Mocsai A, Ligeti E, Lowell CA, Berton G. Adhesion-dependent degranulation of neutrophils requires the src family kinases fgr and hck. The Journal of Immunology. 1999 01/15;162(2):1120-6.

135. Zarbock A, Ley K. Protein tyrosine kinases in neutrophil activation and recruitment. Arch Biochem Biophys. 2011 6/15;510(2):112-9.

136. DuMont AL, Yoong P, Day CJ, Alonzo F, McDonald WH, Jennings MP, et al. Staphylococcus aureus LukAB cytotoxin kills human neutrophils by targeting the CD11b subunit of the integrin mac-1. Proceedings of the National Academy of Sciences. 2013 June 25;110(26):10794-9.

137. Li N, Mao D, LÃ¼ S, Tong C, Zhang Y, Long M. Distinct binding affinities of mac-1 and LFA-1 in neutrophil activation. The Journal of Immunology. 2013 04/15;190(8):4371-81.

138. Jakob SM, Pick R, Brechtefeld D, Nussbaum C, Kiefer F, Sperandio M, et al. Hematopoietic progenitor kinase 1 (HPK1) is required for LFA-1–mediated neutrophil recruitment during the acute inflammatory response. Blood. 2013 May 16;121(20):4184-94.

139. Pereira S, Zhou M, Mócsai A, Lowell C. Resting murine neutrophils express functional a4 integrins that signal through src family kinases. The Journal of Immunology. 2001 March 15;166(6):4115-23.

140. Cook-mills JM, Marchese ME, Abdala-Valencia H. Vascular cell adhesion molecule-1 expression and signalling during disease: Regulation by reactive oxygen species and antioxidants. Antioxidants and Redox Signaling. 2011;15(6):1607-38.

141. Mattsson E, Heying R, Gevel VD, Hartung T, Beekhuizen H. Staphylococcal peptidoglycan initiates an inflammatory response and procoagulant activity in human vascular endothelial cells: A comparison with highly purified lipoteichoic acid and TSST-1. FEMS Immunology & Medical Microbiology. 2008 01/01;52(1):110-7.

142. Petzelbauer P, Bender JR, Wilson J, Pober JS. Heterogeneity of dermal microvascular endothelial cell antigen expression and cytokine responsiveness in situ and in cell culture. The Journal of Immunology. 1993 11/01;151(9):5062-72.

143. DeLeo FR, Otto M, Kreiswirth BN, Chambers HF. Community-associated meticillin-resistant staphylococcus aureus. The Lancet. 2010 5/1–7;375(9725):1557-68.

144. McLoughlin RM, Lee JC, Kasper DL, Tzianabos AO. IFN-γ regulated chemokine production determines the outcome of staphylococcus aureus infection. The Journal of Immunology. 2008 July 15;181(2):1323-32.

145. Cheng AG, DeDent AC, Schneewind O, Missiakas D. A play in four acts: Staphylococcus aureus abscess formation. Trends Microbiol. 2011 5;19(5):225-32.

146. Uddin MN, McLean LB, Hunter FA, Horvat D, Severson J, Tharakan B, et al. Vascular leak in a rat model of preeclampsia. Am J Nephrol. 2009;30(1):26-33.

147. Krueger M, HÃ¤rtig W, Reichenbach A, Bechmann I, Michalski D. Blood-brain barrier breakdown after embolic stroke in rats occurs without ultrastructural evidence for disrupting tight junctions. PLoS ONE. 2013 02/26;8(2):e56419.

148. Bestebroer J, Poppelier MJJG, Ulfman LH, Lenting PJ, Denis CV, van Kessel KPM, et al. Staphylococcal superantigen-like 5 binds PSGL-1 and inhibits P-selectin–mediated neutrophil rolling. Blood. 2007 April 01;109(7):2936-43.

149. Surewaard BGJ, de Haas, C. J. C., Vervoort F, Rigby KM, DeLeo FR, Otto M, et al. Staphylococcal alpha-phenol soluble modulins contribute to neutrophil lysis after phagocytosis. Cell Microbiol. 2013 08/01;15(8):1427-37.

150. Kobayashi SD, Braughton KR, Palazzolo-Ballance A, Kennedy AD, Sampaio E, Kristosturyan E, et al. Rapid neutrophil destruction following phagocytosis of staphylococcus aureus. J Innate Immun. 2010;2(6):560-75.

151. Gresham HD, Lowrance JH, Caver TE, Wilson BS, Cheung AL, Lindberg FP. Survival of staphylococcus aureus inside neutrophils contributes to infection. The Journal of Immunology. 2000 04/01;164(7):3713-22.

152. Otto M. Staphylococcal biofilms. In: Romeo T, editor. Springer Berlin Heidelberg; 2008. p. 207-28.

153. Berlin-Rufenach C, Otto F, Mathies M, Westermann J, Owen MJ, Hamann A, et al. Lymphocyte migration in lymphocyte function-associated antigen (LFA)-1–deficient mice. The Journal of Experimental Medicine. 1999 May 03;189(9):1467-78.

154. Lu H, Smith CW, Perrard J, Bullard D, Tang L, Shappell SB, et al. LFA-1 is sufficient in mediating neutrophil emigration in mac-1-deficient mice. J Clin Invest. 1997 03/15;99(6):1340-50.

155. Brehmer-Andersson E. The dermal blood vasculature. In: Springer Berlin Heidelberg; 2006. p. 4-8.

156. Eguchi T, Hamanaka K, Kondo R, Saito G, Shiina T, Koizumi T, et al. Lung re-expansion following one-lung ventilation induces neutrophil cytoskeletal rearrangements in rats. Annals of Thoracic and Cardiovascular Surgery. 2013;advpub.

157. Saito H, Lai J, Rogers R, Doerschuk CM. Mechanical properties of rat bone marrow and circulating neutrophils and their responses to inflammatory mediators. Blood. 2002(6):2207.

158. Palani K, Rahman M, Hasan Z, Zhang S, Qi Z, Jeppsson B, et al. Rho-kinase regulates adhesive and mechanical mechanisms of pulmonary recruitment of neutrophils in abdominal sepsis. Eur J Pharmacol. 2012 5/5;682(1–3):181-7.

159. Aird WC. Phenotypic heterogeneity of the endothelium: I. structure, function, and mechanisms. Circ Res. 2007 /2/2;100(2):158-73.

160. Koutsiaris AG, Tachmitzi SV, Batis N, Kotoula MG, Karabatsas CH, Tsironi E, et al. Volume flow and wall shear stress quantification in the human conjunctival capillaries and post-capillary venules in vivo. Biorheology. 2007 01/01;44(5):375-86.

161. Morita K, Sasaki H, Furuse K, Furuse M, Tsukita S, Miyachi Y. Expression of claudin-5 in dermal vascular endothelia. Exp Dermatol. 2003 06/01;12(3):289-95.

162. Kluger MS, Clark PR, Tellides G, Gerke V, Pober JS. Claudin-5 controls intercellular barriers of human dermal microvascular but not human umbilical vein endothelial cells. Arterioscler Thromb Vasc Biol. 2013 03/01;33(3):489-500.

163. Wilson RW, Ballantyne CM, Smith CW, Montgomery C, Bradley A, O'Brien WE, et al. Gene targeting yields a CD18-mutant mouse for study of inflammation. The Journal of Immunology. 1993 August 01;151(3):1571-8.

164. Mizgerd JP, Kubo H, Kutkoski GJ, Bhagwan SD, Scharffetter-Kochanek K, Beaudet AL, et al. Neutrophil emigration in the skin, lungs, and peritoneum: Different requirements for CD11/CD18 revealed by CD18-deficient mice. The Journal of Experimental Medicine. 1997 October 20;186(8):1357-64.

165. Issekutz AC, Issekutz TB. The contribution of LFA-1 (CD11A/CD18) and MAC-1 (CD11b/CD18) to the*in vivo*migration of polymorphonuclear leucocytes to inflammatory reactions in the rat. Immunology. 1992 08;76(4):655-61.

166. Noti JD, Johnson AK, Dillon JD. Structural and functional characterization of the leukocyte integrin gene CD11d : ESSENTIAL ROLE OF Sp1 AND Sp3. Journal of Biological Chemistry. 2000 March 24;275(12):8959-69.

167. Hogg N, Takacs L, Palmer DG, Selvendran Y, Allen C. The p150,95 molecule is a marker of human mononuclear phagocytes: Comparison with expression of class II molecules. Eur J Immunol. 1986(3):240.

168. Myones BL, Dalzell JG, Hogg N, Ross GD. Neutrophil and monocyte cell surface p150,95 has iC3b-receptor (CR4) activity resembling CR3. J Clin Invest. 1988 08/01;82(2):640-51.

169. Luissint A, Lutz PG, Calderwood DA, Couraud P, Bourdoulous S. JAM-l–mediated leukocyte adhesion to endothelial cells is regulated in cis by a4ß1 integrin activation. The Journal of Cell Biology. 2008 December 15;183(6):1159-73.

170. Malik AB, Lo SK. Vascular endothelial adhesion molecules and tissue inflammation. Pharmacol Rev. 1996 06/01;48(2):213-29.

171. Albelda SM, Smith CW, Ward PA. Adhesion molecules and inflammatory injury. The FASEB Journal. 1994 05/01;8(8):504-12.

172. Vallien G, Langley R, Jennings S, Specian R, Granger DN. Expression of endothelial cell adhesion molecules in neovascularized tissue. Microcirculation. 2000 08/01;7(4):249-58.

173. Henninger DD, Panés J, Eppihimer M, Russell J, Gerritsen M, Anderson DC, et al. Cytokine-induced VCAM-1 and ICAM-1 expression in different organs of the mouse. The Journal of Immunology. 1997 February 15;158(4):1825-32.

174. Weber C, Springer TA. Interaction of very late antigen-4 with VCAM-1 supports transendothelial chemotaxis of monocytes by facilitating lateral migration. The Journal of Immunology. 1998 December 15;161(12):6825-34.

175. Fink SL, Cookson BT. Apoptosis, pyroptosis, and necrosis: Mechanistic description of dead and dying eukaryotic cells. Infection and Immunity. 2005 April 01;73(4):1907-16.

176. Fleming TJ, Fleming ML, Malek TR. Selective expression of ly-6G on myeloid lineage cells in mouse bone marrow. RB6-8C5 mAb to granulocyte-differentiation antigen (gr-1) detects members of the ly-6 family. The Journal of Immunology. 1993 September 01;151(5):2399-408.

177. Auffray C, Fogg D, Garfa M, Elain G, Join-Lambert O, Kayal S, et al. Monitoring of blood vessels and tissues by a population of monocytes with patrolling behavior. Science. 2007 08/03;317(5838):666-70.

178. Sumagin R, Prizant H, Lomakina E, Waugh RE, Sarelius IH. LFA-1 and mac-1 define characteristically different intralumenal crawling and emigration patterns for monocytes and neutrophils in situ. The Journal of Immunology. 2010 12/01;185(11):7057-66.

179. Seok J, Warren HS, Cuenca AG, Mindrinos MN, Baker HV, Xu W, et al. Genomic responses in mouse models poorly mimic human inflammatory diseases. Proceedings of the National Academy of Sciences. 2013 February 26;110(9):3507-12.

180. Ho M, Hickey MJ, Murray AG, Andonegui G, Kubes P. Visualization of plasmodium falciparum–Endothelium interactions in human microvasculature: Mimicry of leukocyte recruitment. The Journal of Experimental Medicine. 2000 October 16;192(8):1205-12.

181. Wong CH, Jenne CN, Petri B, Chrobok N, Kubes P. Nucleation of platelets with blood-borne pathogens on kupffer cells precedes other innate immunity and contributes to bacterial clearance. Nat Immunol. 2013;14(8):785-92.

182. Engelmann B, Massberg S. Thrombosis as an intravascular effector of innate immunity. Nat Rev Immunol. 2013;13(1):34-45.

183. Massberg S, Grahl L, von Bruehl M, Manukyan D, Pfeiler S, Goosmann C, et al. Reciprocal coupling of coagulation and innate immunity via neutrophil serine proteases. Nat Med. 2010 print;16(8):887-96.

184. von Brühl M, Stark K, Steinhart A, Chandraratne S, Konrad I, Lorenz M, et al. Monocytes, neutrophils, and platelets cooperate to initiate and propagate venous thrombosis in mice in vivo. The Journal of Experimental Medicine. 2012 April 09;209(4):819-35.